COMPARISON OF STATIC AND DYNAMIC TEST METHODS FOR DETERMINING THE STIFFNESS PROPERTIES OF GRAPHITE/EPOXY LAMINATES

by

MICHAEL DERRYCK TURNER

B.S., University of Washington
(1977)

SUBMITTED IN PARTIAL FULFILLMENT

OF THE REQUIREMENTS FOR THE

DEGREE OF MASTER OF SCIENCE

at the

MASSACHUSETTS INSTITUTE OF TECHNOLOGY

June, 1979

Signature of Author _____
Department of Aeronautics and Astronautics
April 19, 1979

Certified by _____
Thesis Supervisor

Accepted by _____
Chairman, Departmental Graduate Committee

COMPARISON OF STATIC AND DYNAMIC TEST METHODS FOR DETERMINING THE STIFFNESS PROPERTIES OF GRAPHITE/EPOXY LAMINATES

by

Michael Derryck Turner

Submitted to the Department of

Aeronautics and Astronautics on April 19, 1979

in partial fulfillment of the requirements for

the degree of Master of Science.

ABSTRACT

Various test methods for determining the in-plane stiffness properties of composite materials are considered. These tests include tensile coupon, sandwich beam, cantilever beam, and static and dynamic flexure tests. A series of tests are carried out to determine these properties for AS1/3501-6 Graphite/Epoxy laminates. The results indicate a significantly lower longitudinal modulus is found by static and dynamic flexure tests than by the other tests used. Computer software is developed to analyze the data quickly and accurately and also produce graphical output that can be easily interpreted to evaluate each test. Results from several test methods are compared and differences analyzed.

Thesis Supervisor: James W. Mar
Title: Professor of Aeronautics
and Astronautics

ACKNOWLEDGEMENT

To all those who cooperated on this project the author would like to express deep appreciation. First to Professor J. W. Mar for his support and understanding in the area of composite materials. Also, to Professor J. Dugundji for his advice and encouragement which was so useful in carrying out the work. Thanks should go to Fred Merlis for his assistance: particularly, for all the photographs that are in this report. The author is grateful to Al Supple for his help in setting up and running the test equipment. Acknowledgement should also be given to Jerome Fanucci and Maria Bozzuto for their cooperation with the author while writing and debugging computer programs. Thanks also, to Ms. N. Ivey for typing the manuscript. Finally, the author wishes to acknowledge all the other people who cooperated in this project.

This work was supported by the U.S. Air Force Materials Laboratory under Contract No. F33615-77-C-5155: Dr. Stephen W. Tsai, technical monitor.

TABLE OF CONTENTS

LIST OF TABLES

LIST OF ILLUSTRATIONS

SECTION I

INTRODUCTION

Graphite/epoxy and other advanced composite materials are seeing increasing use in aerospace and some non-aerospace structures. An advantage of these materials is that their elastic properties can be tailored to give improved buckling strength, stiffness and aeroelastic properties as well as reduced weight when compared to structures made with conventional materials. In order to use this advantage effectively it is necessary to accurately determine the basic stiffness properties of the material.

This study considers the problem of testing the stiffness properties of graphite/epoxy. A series of tests were carried out to determine these properties. Some existing testing and analysis methods were employed and new ones developed. This test program allows the comparison of different test methods and may help determine if certain test methods are applicable to certain design problems.

In the process of making the test specimens, testing them, and analyzing the data there were several additional objectives. First, extra effort was put into automating the production process and producing test specimens that were precisely made and accurately measured. Second, a test method was developed that allowed speedy, accurate, and consistent collection of data. Third and last, computer programs were developed to speed up the analysis of data and present it in a useful form.

Consequently, the results of these tests should be accurate , easily reproducible, and provide a means of comparing stiffness properties from different types of tests.

SECTION 2

TEST SPECIMENS

2.1 Types of Specimens Tested

There were three general types of specimens tested. First, four point bending sandwich beam specimens for testing laminates in tension and compression. Second, tensile coupons that are relatively easy to build, test and provide additional data for comparison. Third, cantilever beams that were tested with static tip loads and also dynamically tested to determine natural frequencies and modulus.

2.2 Types of Laminates Tested

Three basic types of laminates were tested:

1. $(0°)_N$ where N = 2, 4, or 8
2. $(90°)_N$ where N = 4 or 8
3. $(+/- \ 45°)_{NS}$ where N = 1 or 2: $(+/- 45°, +/- 45)_S$

The $(0°)_N$ laminates were used to determine longitudinal modulus, E_L on all three types of specimens as well as major Poisson's Ratio, ν_{LT} from sandwich beam and coupon tests. Similarly, $(90°)_N$ laminates determined transverse modulus E_T and minor Poisson's Ratio, ν_{TL} for sandwich beam and coupon tests. Lastly, $(+/- \ 45°)_{NS}$ laminates were tested to determine shear stress-strain behavior and shear modulus, G.

A total of 70 laminates were tested. Twenty-six laminates were tested in 13 sandwich beams. Thirty-two laminates were tested as tensile coupons. Twelve laminates were tested as cantilever beams.

2.3 Sandwich Beams

At first, sandwich beam specimens were tested rather than tensile coupons for several reasons. The relatively thin laminates (2 to 4 plies) tested were easier to handle and less susceptible to damage when bonded onto a core material. Also, beam specimens could be tested easily at low stress levels. When testing was began this was not true for tensile coupons because hydraulic grips were not readily available for holding and testing tensile coupons. The grips that were then available tended to slip with only small loads at low stress levels. Most importantly thought, sandwich beams allowed the testing of each laminate in tension and compression without elaborate testing jigs.

2.4 Tensile Coupons

Sandwich beam tests with 2 and 4 ply laminates indicated very little difference between tensile and compressive stiffness properties. Also, a new testing machine with hydraulic grips suitable for testing tensile coupons was purchased and installed. Consequently, a series of tests were performed using tensile coupons made from 8 ply and some 4 ply laminates. The 8 ply laminates had a lower per ply thickness and thus they made it possible to test the stiffness properties of material with a lower fraction of epoxy matrix, and a higher fiber volume. The 4 ply laminates allowed the comparison of data with earlier beam tests.

Tensile coupon tests have some significant advantages. The test specimens are easy to construct accurately. Also, unlike sandwich beams

their is no core material which may affect laminate properties particularly Poisson's Ratio.

2.5 Cantilever Beam Specimens

Cantilever beam specimens are used to determine stiffness properties under static tip loads, and dynamically from the determination of natural frequencies.

In the cantilever beam test, the strain is linearly distributed through the thickness such that the strains on the top and bottom are approximately equal in magnitude and opposite in direction. This is considerably different from sandwich beam or coupon tests where there is little or no variation in strain through the laminate. The strain distribution found in cantilever beams may be similiar to that found in many aerospace structures including, vibration of fan blades or the buckling of shell structures. Therefore, it will be worthwhile to compare results from cantilever beam tests to other test methods.

SECTION 3

CONSTRUCTION AND MEASUREMENT OF TEST SPECIMENS

3.1 Construction of Laminates

All laminates were made from 12 inch wide 3501/AS1-6 pre-preg tape. Layups for each type of laminate were made by using sheet aluminum templates to cut out pieces to the correct size, shape, and fiber orientation. These pieces were stacked up to produce the desired sequence and orientation of plies. Each layup was then placed between aluminum plates with peel ply, porous teflon, correct number of fiberglass bleeders, and non-porous teflon on each side of the layup. The laminate was then cured in a hot press according to the cure cycle shown in Table 1.

After curing, laminates were cut from each layup using a table saw with a diamond coated, water cooled saw blade.

3.2 Sandwich Beam Construction

The beam cores are constructed of styrofoam and mahogany as shown in Figure 1. The mahogany was cut roughly to size (2 x 7.5 x 13 cm) in a table saw. The styrofoam was cut roughly to size (2.5 x 7.5 x 13.5 cm) with a hot wire. The mahogany and styrofoam were glued together with Titebond glue and allowed to set overnight. The beams were sanded down until they were flat in a milling machine with the milling head replaced by a sanding disk.

TABLE 1: Cure Cycle

TEMP (°F)	PRESSURE (PSI)	TIME (MINUTES)
275	15	18
RAISE TO 300	15	5
300	100	30
RAISE TO 350	100	7
350	100	35

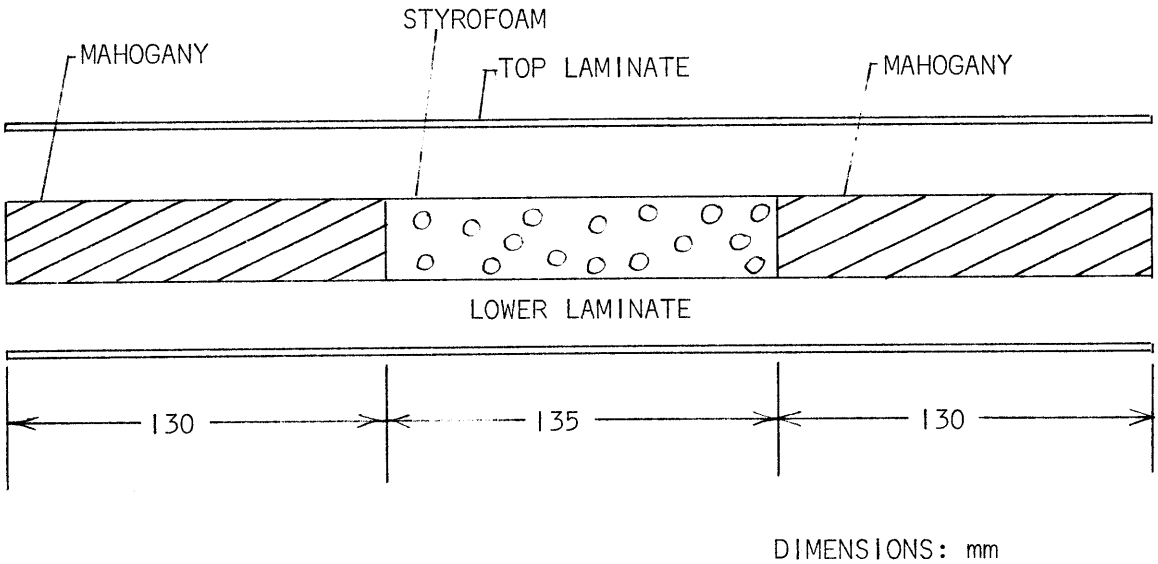

FIG. 1: SANDWICH BEAM CONSTRUCTION

Before the beams were bonded together thickness measurements were taken on the cores and the laminates at the 18 locations shown in Fig. 2.

The laminates were bonded to the cores using Smooth-on EA-40 Epoxy adhesive. This bonding process was carried out on a jig constructed from aluminum and placed inside a vacuum bag during the bonding process. The jig and vacuum bag assured that the laminates were kept flat and correctly aligned; also importantly, the adhesive was squeezed out so that only a thin layer remained.

After the beams were removed from the vacuum bag the edges were sanded down to remove excess dried epoxy. The beam thicknesses were then measured at the same 18 locations as before and widths were measured at the 6 locations shown in Fig. 2.

Four strain gages were glued onto each beam. The strain gages used were Micro-Measurements type EA-09-125AD-120 or type EA-06-125AD-120. Each laminate had two strain gages glued on to give longitudinal strain and transverse strain as shown in Fig. 3.

After the strain gages were glued on and wires soldered on, the beams were ready to be tested.

3.3 Construction of Tensile Coupons

Tensile coupons consisted of a test laminate and loading tabs as indicated in Fig. 4. The gage length was 275 mm for the $(+/- 45°)_{NS}$ laminates and 200 mm for other laminates.

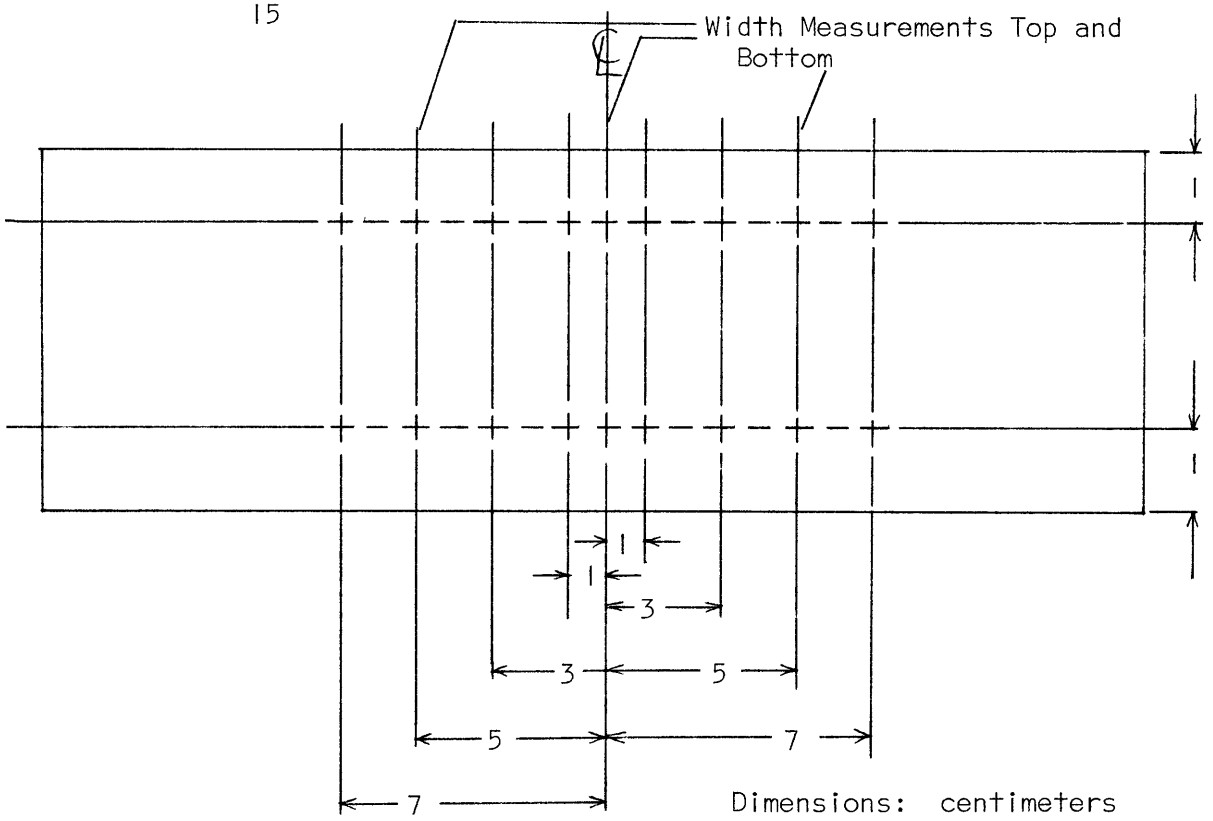

FIG. 2: SANDWICH BEAM AND LAMINATE MEASUREMENT LOCATIONS

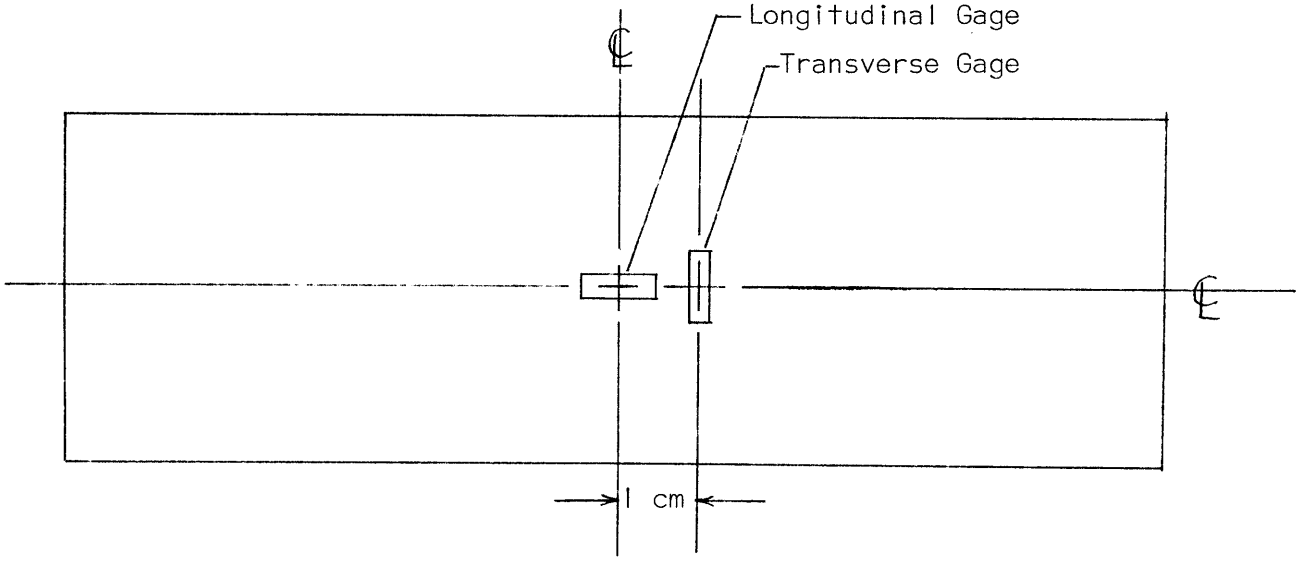

FIG. 3: STRAIN GAGE LOCATIONS

Test laminates were cut as described previously. Then sanded to a constant width. After which width measurements were taken at five locations and thickness measurements at ten as indicated in Fig. 5.

The loading tabs were cut from $(0°, 90°)_{2S}$ sheets of 3M Scotchply, fiberglass/epoxy. These were cured in the same way as graphite/epoxy except that the cure cycle consisted of 40 minutes at 50 psi and 330°F followed by a gradual cool down to room temperature.

The loading tabs were bonded onto the test laminate with Cyanamid FM123 film adhesive cured at 240°F, 40 psi for 90 minutes.

Longitudinal and transverse strain gages of the same types used on beam specimens were then attached to the test coupons. They were centered at the equivalent locations to those shown for beam specimens in Fig. 3.

3.4 Fabrication of Cantilever Beam Specimens

To make the cantilever beam specimens the cured graphite/epoxy was cut as before and sanded carefully to be straight and square. After which the mass of each laminate was measured. Measurements of thickness were taken at 12 locations and width was measured at 6 locations as indicated in Fig. 7. The next step was to bond onto the base a 25 mm x 25 mm loading tab machined from 1/8" aluminum as indicated in Fig. 6. Finally, a strain gage was bonded on each laminate 5 mm from the loading tab.

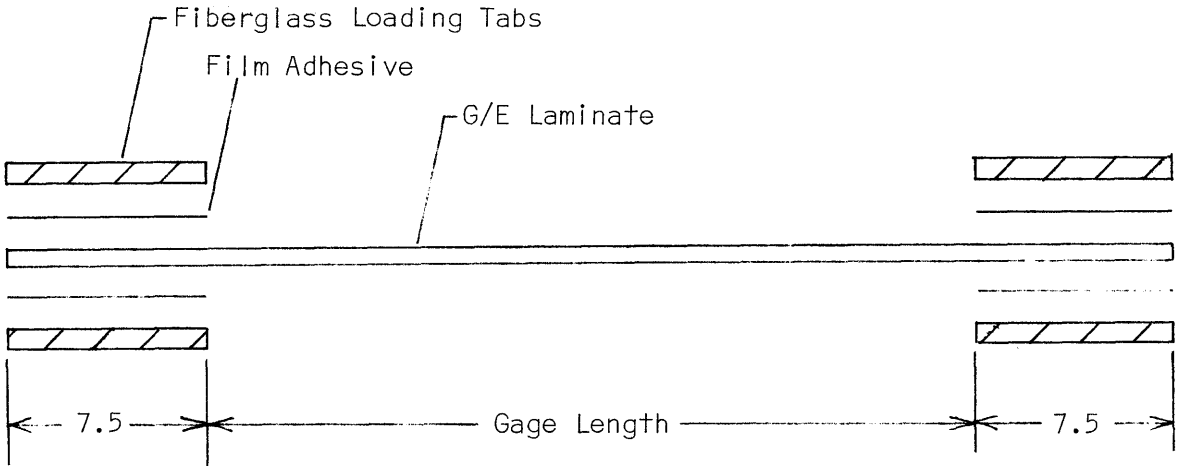

FIG. 4: TENSILE COUPON CONSTRUCTION

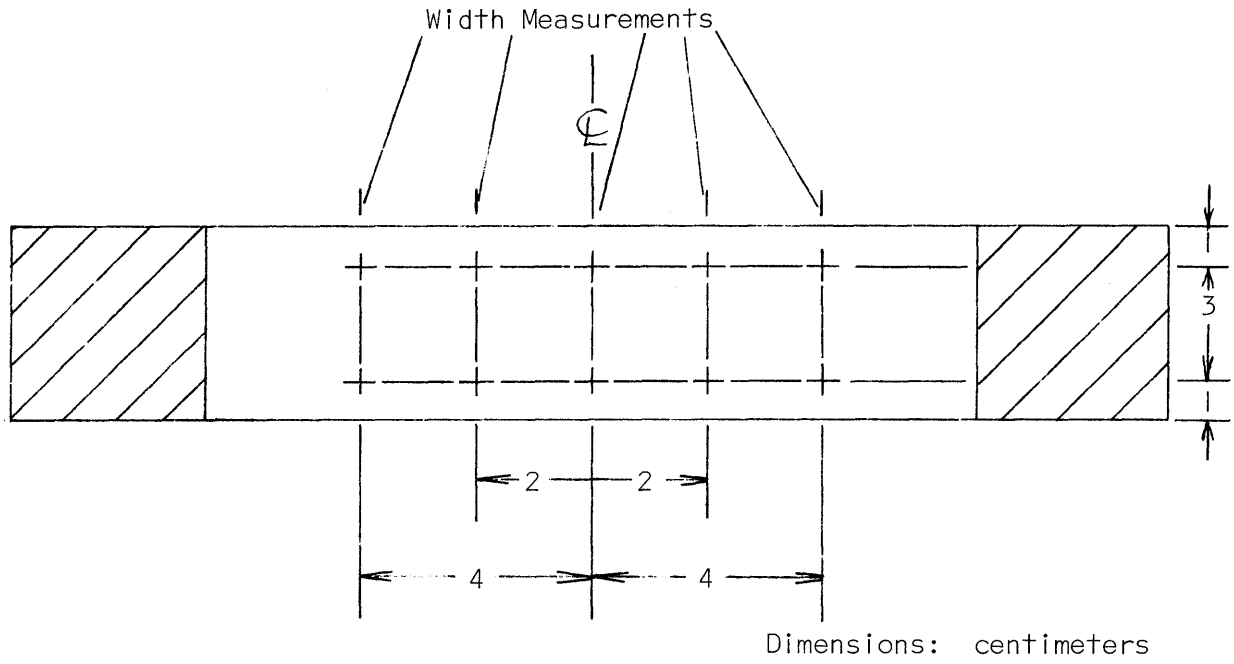

FIG. 5: COUPON MEASUREMENT LOCATIONS

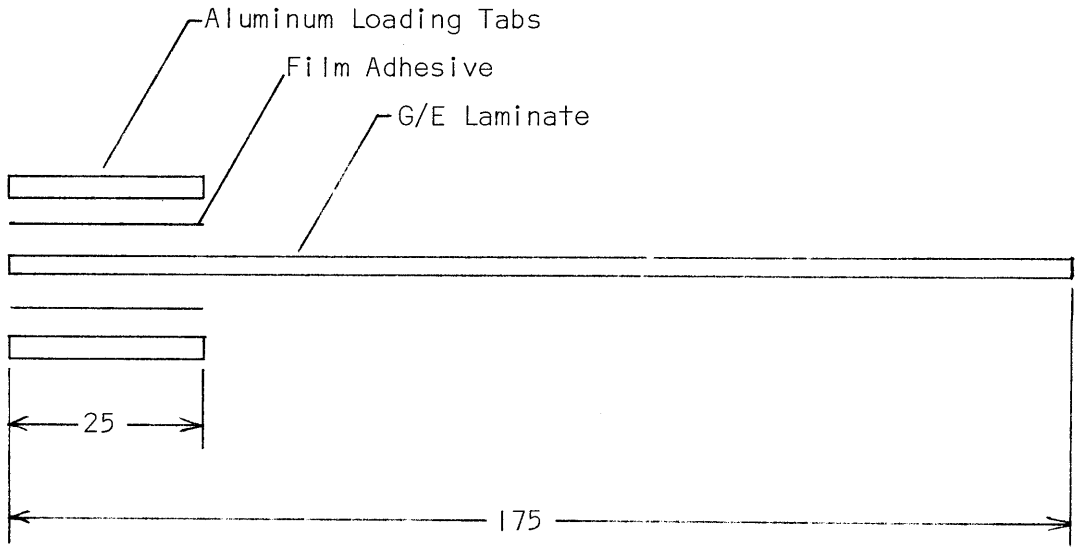

FIG. 6: CANTILEVER BEAM CONSTRUCTION

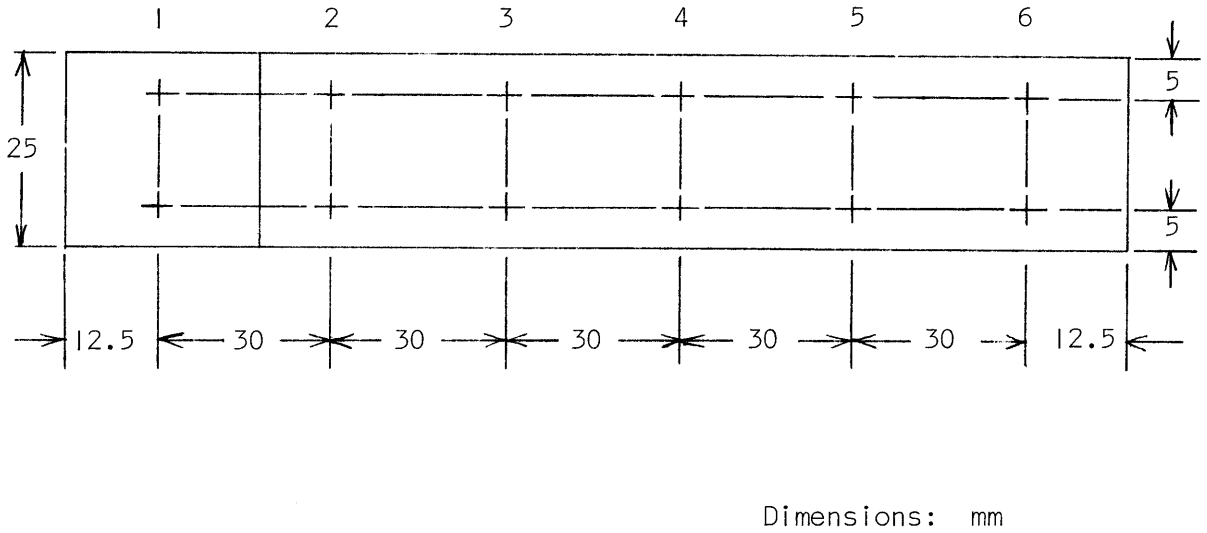

FIG. 7: CANTILEVER BEAM MEASUREMENT LOCATIONS

SECTION 4

TEST EQUIPMENT AND PROCEDURE

4.1 Sandwich Beam Tests

The sandwich beams were tested in a four point bending test jig made from aluminum I-beams. The test jig transfered the load from the Baldwin-Emery SR-4 test machine to the test specimen through four cylindrical rollers. The strain gages were attached to four BLH-1200 strain indicators. Figure 8 shows the aluminum test jig in the test machine with beam 3 after failure.

One person ran the test machine and called out the load every 10 or every 20 pounds and four volunteers wrote down the strain readings: Fig. 9.

Each beam was first tested upside down in the test jig up to a load between 100 and 200 pounds depending on the type of laminate. Then the beam was removed and tested right side up until it reached failure load. This prodedure was followed so that data could be collected for each laminate both in tension and compression.

4.2 Tensile Coupon Tests

The tensile coupons were tested in a 100,000 pound MTS testing machine using hydraulic grips: Fig. 10. Strain indicators were used as before.

The test procedure was similar to that used for sandwich beams: one person ran the test machine and called out the load every few

hundred pounds and two others wrote down the strain readings. However, the coupons were only tested in tension. As before, each specimen was tested to failure.

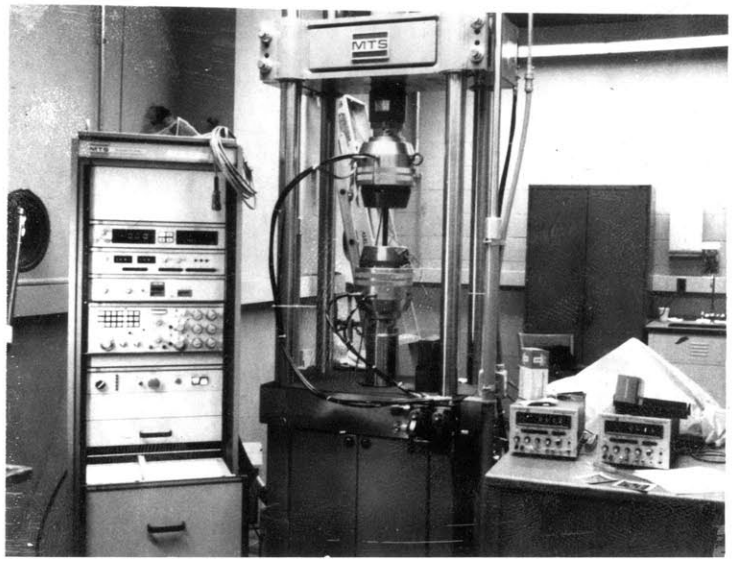

FIG. 10: TENSILE/COUPON TEST SETUP

4.3 Cantilever Beam Experiments

The cantilever beams were first tested with static tip loads and then tested dynamically with a shaker to find natural frequencies.

The static test was performed by first, clamping the test specimen onto a 12" x 12" x 3" base of aluminum. Then a Kevlar thread was taped on and draped over the center of the end of the specimen. Three different weights were hung from the thread and the tip displacment was measured for no load and then the three weights individually. An Edmund

direct measuring microscope, NO. 70,266, was used to measure these displacements accurately.

After each beam was tested statically it was tested to find the frequencies of the first 3 natural modes of vibration. This was done by clamping the specimen in an aluminum block attached to a Ling Model 420 shaker.[5] An Endevco 7701-50 "Isoshear" accelerometer was mounted to the aluminum block. This accelerometer and the specimen strain gage were used to produce a signal that was amplified and displayed on an oscilloscope.

By monitoring these signals resonances could be determined by maximum signal amplitude and most clearly from a 90° phase shift.

SECTION 5

THEORY AND DATA ANALYSIS

5.1 Sandwich Beams With $(0°)_2$, $(0°)_4$, and $(90°)_4$ Laminates

The sandwich beam data is analyzed by a computer program on an IBM 370. The beam, laminate dimensions, and load vs. strain data are input into the program. The program converts the load into metric units and then calculates moments. The program finds the two best straight lines through the moment vs. longitudinal strain data by linear regression.

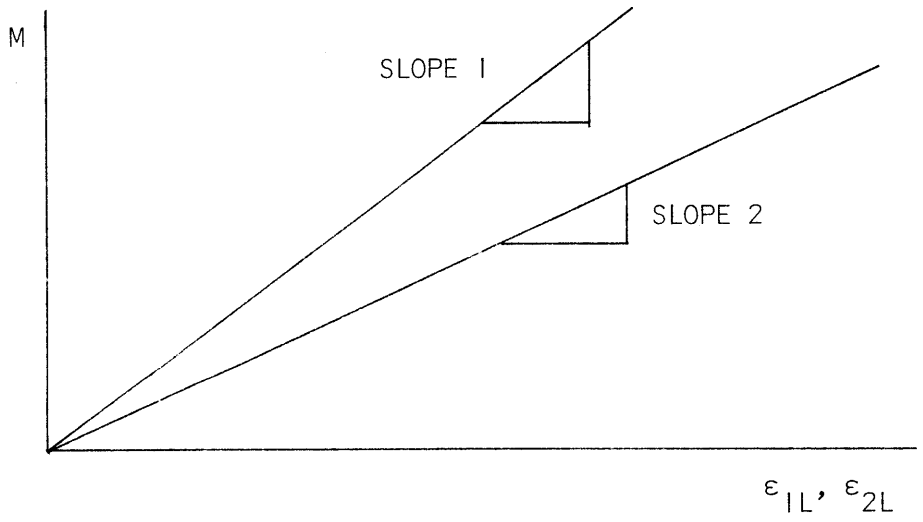

M = Moment

ε_{1L} = Upper Laminate Longitudinal Strain

ε_{2L} = Lower Laminate Longitudinal Strain

The location of the neutral axis is calculated:

$$Z_{NA} = t \left(\frac{1}{1 + \left| \frac{\text{SLOPE 1}}{\text{SLOPE 2}} \right|} \right)$$

The moment of inertia for each laminate about the neutral axis is calculated:

$$I_1 = A_1[t_1^2/12 + (Z_1 - Z_{NA})^2]$$

$$I_2 = A_1[t_2^2/12 + (Z_2 - Z_{NA})^2]$$

Where

I_1 = Moment of Inertia for the Upper Laminate

I_2 = Moment of Inertia for the Lower Laminate

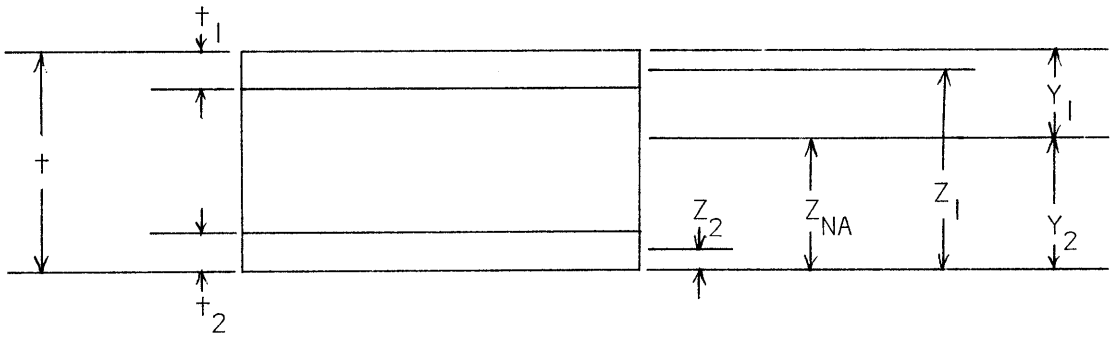

Beam Cross Section

$$A_1 = W_1 t_1$$

$$A_2 = W_2 t_2$$

W_1 = Width of Upper Laminate

W_2 = Width of Lower Laminate

Moment and force equilibrium yield the formulas used to determine Young's Moduli, E_1, E_2:

$$E_2 = \frac{A_1(\text{SLOPE } 1)Y_1}{A_2I_2\left(\frac{Z_{NA} - Z_2}{Z_1 - Z_{NA}}\right) + I_2A_1}$$

$$E_1 = [(\text{SLOPE } 1)Y_1 - E_2Y_2]/I_1$$

The stresses are

$$\sigma_1 = \frac{E_1Y_1M}{E_1I_1 + E_2I_2}$$

$$\sigma_2 = \frac{E_2Y_2M}{E_1I_1 + E_2I_2}$$

Poisson's Ratio's are

$$\nu_1 = -\frac{\varepsilon_{1T}}{\varepsilon_{1L}}$$

$$\nu_2 = -\frac{\varepsilon_{2T}}{\varepsilon_{2L}}$$

The program plots stress vs. strain, Poisson's Ratio vs. strain, and the best straight line through the stress-strain data for each laminate in tension and compression.

The graphical results are Figs. 14 to 23 and Figs. 40 to 47.

5.2 Sandwich Beams with $(+/- 45)_S$ Laminates

The sandwich beams with $(+/- 45)_S$ laminates are used to determine the shear stress-strain behavior and shear modulus, G. Using a $(+/- 45)_S$ laminate in a uniaxial stress state to determine shear properties was proposed by Petit[1] and others.[2,3,4] Testing the laminates on beams made it possible to further check the validity of the test by seeing if it worked equally well for a laminate in tension and compression.

The test data was again analyzed with a computer program on an IBM 370. This program calculates the longitudinal stresses σ_{1L}, σ_{2L} in the same way as the previous program. Rotating the axis 45° gives the shear stresses:

$$\tau_1 = \frac{1}{2}\sigma_{1L}$$

$$\tau_2 = \frac{1}{2}\sigma_{2L}$$

and the shear strains

$$\gamma_1 = \varepsilon_{1L} - \varepsilon_{1T}$$

$$\gamma_2 = \varepsilon_{2L} - \varepsilon_{2T}$$

The program performs a linear regression analysis on the shear stress-strain data to calculate the shear moduli:

$$G_1 = \frac{d\tau_1}{d\gamma_1}$$

$$G_2 = \frac{d\tau_2}{d\gamma_2}$$

The shear stress-strain behavior becomes nonlinear above a strain of 3000 microstrain. Therefore, only data points with a shear strain of less than 3000 microstrain are used in the linear regression analysis.

The program plots shear stress vs. strain and the best straight line through the data for each $(+/- 45)_S$ laminate in tension and compression.

The graphical results are Figs. 56 to 63.

5.3 Analysis of Tensile Coupons

Computer programs are also used to analyze data from tensile coupons. Longitudinal stresses are just calculated on the basis of load divided by cross sectional area. Longitudinal and transverse strain data having been read during the test.

The modulus of the $(0°)_N$ and $(90°)_N$ laminates is calculated directly by doing a linear regression analysis on the stress-strain data. The program plots stress vs. strain, Poisson's Ratio vs. strain, and the best straight line through the stress-strain data for each laminate. The graphical results are Figs. 23 to 36 and Figs. 45 to 52.

For the $(+/- 45)_{NS}$ laminates the shear stress is half the longitudinal stress and the shear strain is the difference between the longitudinal and transverse strain, The shear modulus, G is determined by performing a linear regression on the shear stress-strain data for shear

strain of less than 3000 microstrain. Shear stress vs. strain is plotted along with the best straight line through the data for each of the $(+/- 45)_{NS}$ laminate. The graphical output is given in Figs. 64 to 74.

5.4 Analysis of Cantilever Beam Experiments

In the static tip load test the modulus can be determined from simple beam theory:

$$q = \frac{L^3}{3EI} Q$$

differentiating

$$\frac{dq}{dQ} = \frac{L^3}{3EI}$$

Then

$$E = \left(\frac{dQ}{dq}\right) \frac{L^3}{3I}$$

where

L = length of beam: from tab to tip

I = moment of inertia: assumed constant along the beam

$\frac{dQ}{dq}$ = the slope of tip load vs. displacement

$\frac{dQ}{dq}$ being determined from a linear regression analysis done on tip load vs. displacment data.

For the $(0°)_8$ laminates E is the longitudinal modulus, E_L and for the $(90°)_8$ laminates E is the transverse modulus, E_T. For the $(+/- 45°)_{2S}$ laminates E is some effective longitudinal modulus, the significance of which will be discussed later.

The cantilever beams are also tested dynamically to determine the lowest 3 resonances. From beam theory the first 3 natural frequencies of a clamped-free beam are

$$\omega_1 = (1.8751041)^2 \sqrt{\frac{EI}{mL^4}}$$

$$\omega_2 = (4.6940911)^2 \sqrt{\frac{EI}{mL^4}}$$

$$\omega_3 = (7.8547574)^2 \sqrt{\frac{EI}{mL^4}}$$

Employing these formulas the modulus can be determined from the frequencies. As with the static tests E_L and E_T are found from the $(0°)_8$ and $(90°)_8$ laminates.

Now to consider how to effectively analyze cantilever beams made with $(+/- 45°)_{2S}$ laminates. One difficulty with analyzing these laminates is that they exhibit bending-twisting coupling. That is to say, if one considers one of these laminates as plate, the bending stiffness terms D_{1112}, $D_{2212} \neq 0$. If simple beam theory is to be applied it is necessary to neglect these terms.

Therefore, with this approximation a straightforward analysis can be performed assuming the only stress acting is a stress along the axis of the beam:

$$\sigma_{11} = - \frac{Mz}{I}$$

$$\sigma_{22} = 0$$

For each +45° ply

$$\begin{bmatrix} \sigma_{11} \\ \sigma_{22} \\ \sigma_{12} \end{bmatrix} = \begin{bmatrix} E_{1111}^{[45]} & E_{1122}^{[45]} & 2E_{1112}^{[45]} \\ E_{2211}^{[45]} & E_{2222}^{[45]} & 2E_{2212}^{[45]} \\ E_{1211}^{[45]} & E_{1222}^{[45]} & 2E_{1212}^{[45]} \end{bmatrix} \begin{bmatrix} \varepsilon_{11} \\ \varepsilon_{22} \\ \varepsilon_{12} \end{bmatrix}$$

With the approximation of no twist, $\varepsilon_{12} = 0$, this becomes

$$\begin{bmatrix} \sigma_{11} \\ \sigma_{22} \end{bmatrix} = \begin{bmatrix} E_{1111}^{[45]} & E_{1122}^{[45]} \\ E_{2211}^{[45]} & E_{2222}^{[45]} \end{bmatrix} \begin{bmatrix} \varepsilon_{11} \\ \varepsilon_{22} \end{bmatrix}$$

This last relationship also holds for the -45° plies. Inverting the above relationship and using $\sigma_{22} = 0$:

$$\varepsilon_{11} = E_{1111}^{[45]^{-1}} \sigma_{11}$$

Therefore, the effective modulus determined from tip loads and beam natural frequencies is

$$E = \frac{1}{E_{1111}^{[45]^{-1}}}$$

or

$$E = \frac{E_{1111}^{[45]} E_{2222}^{[45]} - E_{1122}^{[45]} E_{2211}^{[45]}}{E_{2222}^{[45]}}$$

In terms of the orthotropic properties for a 0° ply

$$E_{1111}^{[45]} = \frac{1}{4} E_{1111}^{*} + \frac{1}{4} E_{2222}^{*} + \frac{1}{2} E_{1122}^{*} + E_{1212}^{*}$$

$$E_{1122}^{[45]} = \frac{1}{4} E_{1111}^{*} + \frac{1}{4} E_{2222}^{*} + \frac{1}{2} E_{1122}^{*} - E_{1212}^{*}$$

Also,

$$E_{1111}^{[45]} = E_{2222}^{[45]}$$

$$E_{1122}^{[45]} = E_{2211}^{[45]}$$

For convenience define

$$A = \frac{1}{4} E_{1111}^{*} + \frac{1}{4} E_{2222}^{*} + \frac{1}{2} E_{1122}^{*}$$

and note that

$$E_{1212}^{*} = G$$

Then

$$E = \frac{4\ G}{1 + \frac{G}{A}}$$

or

$$G = \frac{1}{\left(\frac{4}{E} - \frac{1}{A}\right)}$$

Putting in previously determined properties to calculate A and G shows that changing the value of A by 20% only changes G by 2.5%: showing the results for G determined by this method are not overly sensitive to values assumed for other stiffness properties. Therefore, the values of G are calculated from cantilever beam tests with $(+/- 45°)_{2S}$ laminates.

SECTION 6

COMPARISON OF TEST RESULTS

6.1 Difference in Test Methods

Of the three different test methods employed: sandwich beams, tensile coupons, and cantilever beams, the first two methods are basically similar and give comparable results. Therefore, results from these two methods will be considered together. Then the results from the cantilever beam tests will be analyzed and compared to the other test methods.

All test results are summarized and tabulated in Appendix B for easy comparison.

6.2 Stiffness Properties Determined from Sandwich Beams & Tensile Coupons

When looking at the test results it is worthwhile to try and determine what parameters seem to affect the stiffness properties. One would expect the fraction of material that is graphite fibers, the fiber volume, V_F should be one of the parameters.

Test results clearly show the effect of fiber volume, V_F on material properties. Laminates of only a few plies have a greater per ply thickness and consequently a lower fiber volume. The effect of this on material properties is apparent in Table 4 where the average stiffness properties are summarized for 2, 4, and 8 ply laminates.

The dependence of E_L on fiber volume is shown by Fig. 13. This includes data from $(0)_N$, 1, 2 and 4 ply, laminates tested on sandwich

beams. This graph shows similar results for E_L in tension and compression. Also, a linear regression through this data has a near zero intercept indicating that it is possible to approximate the affect of V_F on E_L by neglecting the stiffness of the epoxy matrix.

Table 4 indicates that the transverse modulus, E_T goes down very slightly with fiber volume. This is certainly not expected and could just be an anomaly from a small amount of test data. Looking at the results for the $(90°)_8$ laminates on Table II it appears that laminates cut from one sheet have a 15% lower E_T than those cut from another sheet. However, the slope of the load vs. stroke graphs made during each test indicate there is less than 3% variation in the overall stiffness of all $(90°)_8$ coupons. Therefore, it is felt that the variation in E_T must indicate some local soft or hard spots in the material. This may be a significant problem in testing $(90°)_N$ laminates. Consequently, it is likely that E_T is not reduced for high fiber volume G/E.

On the other hand the properties ν_{LT} and G vary with V_F in the direction expected. The major Poisson's Ratio goes down with increasing fiber volume because the graphite fibers have a lower Poisson's Ratio than the epoxy matrix. Similarly, G increases slightly with increasing fiber volume as expected. The nonlinear nature of the shear stress-strain behavior is shown in Figs. 56 to 74. Figure 11 is a photograph of beam 5 being tested. It shows the large deflection and distinct anticlastic bending caused by the large longitudinal and transverse strains of $(+/- 45°)_s$ specimens. For the laminates tested on sandwich beams, the measured value of ν_{TL} is about half that needed to satisfy the relation $E_L\nu_{TL} = E_T\nu_{LT}$

which should hold for ideally orthotropic laminates. However, for the 8 ply laminates tested on coupons the average properties agree with this relationship within 10%. Perhaps testing the laminates on sandwich beams restricts the transverse strains and affects the measured Poisson's Ratios. Also, there is a certain amount of inaccuracy in the measurement of ν_{TL} for small stresses. This is the result of a small amount of drift in the strain readings due to temperature variation. This has its greatest effect on the small strain readings of the transversely mounted gage (parallel to the fibers). Looking at the plots of ν_{TL}, Figs. 37 to 52 and comparing the results from sandwich beams to those from tensile coupons, it is noticeable that, temperature drift was not a problem for the tensile coupons. Consequently, the coupon data for ν_{TL} is probably more reliable than that from sandwich beams and the coupon data agrees closely with the previous relatinship indicating that ν_{TL} can be determined from the other stiffness properties.

Taking into account the variation of stiffness properties with fiber volume, values for these properties are calculated for the manufacture's specified per ply thickness. These values are included in Table 3.

6.3 Stiffness Properties from Cantilever Beam Tests

In looking at the stiffness properties determined from cantilever beam tests there are several important considerations. First, are the test results consistent and are there explanations for any variation. Second, how do stiffness properties determined statically and from the first three bending frequencies compare. Third, how do the cantilever

beam results compare with results from the other test methods and particularly with tensile coupons cut from the same sheets of cured G/E.

To address the first consideration, look at Tables 9, 12, and 16. It is clear that, there is little variation in the E_T determined for the 4 $(90°)_8$ laminates. However, for the $(0°)_8$ and $(+/- 45°)_{2S}$ laminates both have a test specimen that appears to have significantly lower stiffness properties than the other laminates. In the first bending frequency where this difference is most pronounced the $(0°)_8$ - 2 - B specimen has a modulus 12% lower than the other 3 $(0°)_8$ cantilever beams and the $(+/- 45°)_{2S}$ - 2 - D specimen has a modulus 16% lower than the other $(+/- 45°)_{2S}$ laminates. The measurements of these 2 specimens indicate they are thicker at the tip than the root and the 6 remaining $(0°)_8$ and $(+/- 45°)_{2S}$ specimens are thicker at the root than the tip. It is possible to approximate this thickness variation as straight taper from root to tip. A taper involving a difference between root and tip thickness of about 4% for the $(0°)_8$ specimens and as much as 8% for the $(+/- 45°)_{2S}$ specimens. A Ritz analysis is performed in Appendix A on the effect of beam taper on first bending frequency. This analysis indicates that to get the 12% and 16% difference in moduli found in the $(0°)_8$ and $(+/- 45°)_{2S}$ laminates would require a thickness taper of 5% and 6% respectively. This compares fairly well with the 4% and 8% measured thickness variation. Consequently, the variation in measured stiffness is easily explained.

The second consideration is how the properties determined from the first 3 bending frequencies and from static tests compare for the cantilever beam specimens. The difference between static and dynamic modulus is only 2 to 3% for the $(0°)_8$, $(90°)_8$ specimens, and as much as 6% for the $(+/- 45°)_{2S}$ specimens. A 2 to 3% difference is insignificant and the small 6% difference for the $(+/- 45°)_{2S}$ could easily be caused by the bending-twisting-coupling they exhibit, or the variation in thickness. The difference in modulus determined from each of the 3 bending modes is insignificant when the moduli are averaged for the 4 specimens of each type. Something that is noticeable is that the moduli data is less scattered for the higher natural frequencies of the $(0°)_8$ and $(+/- 45°)_{2S}$ which could be because the thickness variation of these laminates has less effect on the frequencies of the higher modes. Consequently, there are no significant differences between the moduli determined from the 3 lowest natural frequencies and the static tests of the cantilever beam specimens.

The third and most interesting consideration is how the cantilever beam test results compare to moduli from the other test methods. Table 3 provides a summary of moduli from the cantilever beam tests compared to the results from the other test methods and design stiffness properties used by Grumman. The shear modulus, G is not significantly different from that determined from the other tests. The transverse modulus, E_T is somewhat lower. However, the longitudinal modulus, E_L is some 30% lower than that found in other test methods.

The difference in measured E_L is a direct result of the test method rather than a difference in material properties between the cantilever beam specimens and other test specimens. Consult Table 8, the $(0°)_8$ - 2 laminates cut from the same sheet of cured G/E as the $(0°)_8$ cantilever beams and tested as tensile coupons have a much higher E_L than found in the cantilever beam tests. As a final confirmation the $(0°)_8$ cantilever beam specimens were made into tensile coupons by cutting off the aluminum tabs and bonding on 25 cm x 25 cm fiberglass loading tabs. The specimens were strain gaged and tested like other tensile coupons. The results are included in Table 9 and the test data is Figs. 37 to 39. These results agree with the other tensile coupon data. This indicates that the same material tested with different methods exhibits a different modulus E_L.

In summary, it appears that cantilever beam specimens give consistent results from the beam natural frequencies and static tip loads but E_L is significantly lower than that found by other test methods. The cantilever beams are sufficiently long and thin that transverse shear will have little effect on test results. Therefore, it would appear that the stiffness may vary through the thickness perhaps due to the distribution of fibers.

SECTION 7

CONCLUSIONS AND RECOMMENDATIONS

The test results and analysis in this report make it possible to draw some significant conclusions about the stiffness properties of Graphite/Epoxy and the test and analysis methods used to determine those properties for composite materials. First, useable stiffness properties and some variables that may affect those properties have been determined. Second, the effectiveness of the test and analysis methods has been confirmed but some important differences have been found in stiffness properties from tests that involve laminate bending or flexure.

Considering the stiffness properties first, Tables 3 and 4 give a good summary of stiffness properties that can be expected from ASI/3501-6 G/E used at M.I.T. One important conclusion is that these properties are the same in tension and compression. Also, the per ply thickness or fiber volume has some effect on all the stiffness properties. The longitudinal modulus is most sensitive: the quantity of fiber being the most important item in determining this property.

From comparison of the test and analysis methods several conclusions can be drawn. First, tests using coupon specimens are easier to perform than those using sandwich beams but they both give similar results. Also, cantilever beam tests indicate that laminates exhibit different material properties in bending.

The results in this report indicate some techniques that may be useful in the future and some areas that warrant further investigation.

The use of several types of laminates such as $(0°)_N$, $(90°)_N$, and $(+/- 45°)_{NS}$ laminates to determine basic material properties can be useful in finding other characteristics of composite materials. This approach could be applicable to finding strength characteristics, damping properties, and fatigue damage. One area that warrants further investigation is the determination of stiffness properties in flexure: particularly, E_L. Making $(0°)_N$ laminates with different numbers of plies and then testing them as 4 point bending flexure specimens could provide insight into why E_L is apparently lower in bending.

In conclusion, this work has determined stiffness properties, compared test methods, and also in indicated where more research could be worthwhile.

REFERENCES

1. Petit, P. H., "A Simplified Method of Determining the In Plane Shear Stress-Strain Response of Unidirectional Composites," Composite Materials: Testing and Design, ASTM STP460, American Society for Testing and Materials, 1969.

2. Rosen, B. W., "A Simple Procedure for Experimental Determination of the Longitudinal Shear Modulus of Unidirectional Composites," J. Composite Materials, Vol. 6 (1972), pp. 552-554.

3. Sims, D. F., "In-Plane Shear-Strain Response of Unidirectional Composite Materials," J. Composite Materials, Vol. 7 (1972), pp. 124-126.

4. Hahn, H. T., "A Note on Determination of the Shear Stress-Strain Response of Unidirectional Composites," J. Composite Materials, Vol. 7 (1973), pp. 383-386.

5. Crawley, E. F., "The Natural Mode Shapes and Frequencies of Graphite/Epoxy Cantilevered Plates and Shells," S.M. Thesis, June 1978, M.I.T.

6. Young, D., and Felgar, R. P., "Table of Characteristic Functions Representing the Normal Modes of Vibration of a Beam," Engineering Research Series, No. 44, July 1, 1949, University of Texas, Austin, Texas.

APPENDIX A

RITZ ANALYSIS OF EFFECT OF BEAM THICKNESS TAPER ON FIRST BENDING FREQUENCY

A Ritz analysis is performed using the first mode shape for a uniform cantilever beam. This analysis will yield a good approximation of the frequency of the first mode for a slightly tapered beam.

For the harmonic transverse vibration of a beam the displacement is of the form

$$w(x,t) = \phi(x)e^{i\omega t}$$

The maximum potential and kinetic energy are

$$V = \frac{1}{2}\int_0^L EI(x)(\phi'')^2 dx$$

$$T = \frac{1}{2}\omega^2 \int_0^L m(x)\phi^2 dx$$

For convenience a new variable is introduced:

$$\xi = 2\frac{x}{L} - 1$$

The beam thickness of a uniformly tapered beam is

$$h(\xi) = \bar{h} + \frac{\xi}{2}(h_{TIP} - h_{ROOT})$$

Where $\bar{h}$ is the average thickness. If $\bar{m}$ and $\overline{EI}$ are the mass distribution and stiffness for a uniform beam of thickness $\bar{h}$, then for the tapered beam

$$\frac{m}{\bar{m}} = \frac{h}{\bar{h}}$$

$$\frac{EI}{\overline{EI}} = \left(\frac{h}{\bar{h}}\right)^3$$

$$\omega^2 = \frac{\overline{EI}}{\bar{m}L^4} \frac{\int_{-1}^{+1} \left(\frac{h}{\bar{h}}\right)^3 (L^2\phi'')^2 d\xi}{\int_{-1}^{+1} \left(\frac{h}{\bar{h}}\right) \phi^2 d\xi}$$

The function used for ϕ is the first bending mode for a uniform beam:

$$\phi = \cos\frac{\beta x}{L} - \cos\frac{\beta x}{L} - \alpha\left(\sin\frac{\beta x}{L} - \sin\frac{\beta x}{L}\right)$$

Values of α and β are in Ref. 6 along with tables of $\phi(x)$ and $\phi''(x)$. However, ϕ and ϕ'' can easily be calculated on a programmable calculator.

The expression for ω^2 is evaluated for 5 cases: a uniform beam and tapered beams with the tip thickness 4% less, 8% less, 4% greater, and 8% greater than the root thickness. The necessary integrals were evaluated numerically using Gauss quadrature on 6 points. In the case of the uniform beam the integrals are equal to the exact result up to the sixth decimal place.

The results of this analysis are presented in Table 2 and plotted in Fig. 12.

TABLE 2: EFFECT OF BEAM TAPER ON FIRST BENDING FREQUENCY

$\frac{h_{ROOT} - h_{TIP}}{\bar{h}}$	$\frac{\omega^2}{\left(\frac{\overline{EI}}{\bar{m}L^4}\right)}$	$\frac{\omega^2 - \bar{\omega}^2}{\bar{\omega}^2}$
.08	13.63453	.10291
.04	12.9833	.05023
0	12.362364	0
-.04	11.7703	-.04790
-.08	11.2058	-.09356

$\bar{h}$ = Average beam thickness

$\bar{m}$ = Mass distribution for uniform beam of thickness $\bar{h}$

$\overline{EI}$ = Bending stiffness for uniform beam of thickness $\bar{h}$

$\bar{\omega}$ = First bending frequency for uniform beam of thickness $\bar{h}$

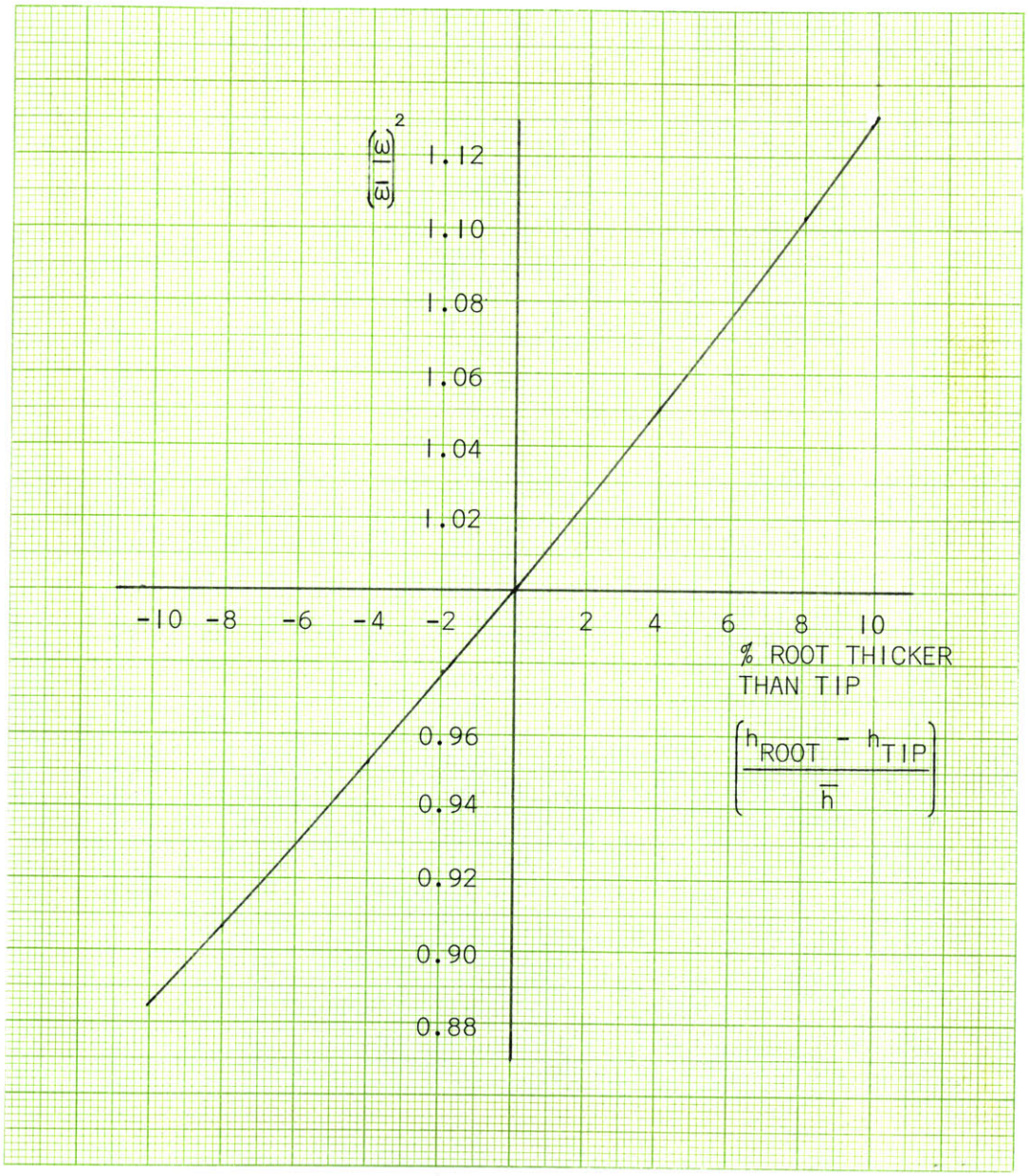

FIG. 12: EFFECT OF BEAM TAPER ON FIRST BENDING FREQUENCY

APPENDIX B

TABLE 3: SUMMARY OF IN-PLANE STIFFNESS PROPERTIES OF AS1/3501-6 GRAPHITE/EPOXY

PROPERTY	VALUE USED BY GRUMMAN	FROM SANDWICH BEAM AND COUPON DATA*	8 PLY LAMINATES IN FLEXURE†
E_L	128 GPa (18.5 msi)	134 GPa (19.4 msi)	98 GPa (14.2 msi)
E_T	11.0 GPa (1.60 msi)	10.0 GPa (1.45 msi)	7.9 GPa (1.15 msi)
ν_{LT}	.25	.28	---
G	4.5 GPa (.65 msi)	5.7 GPa (.83 msi)	5.6 GPa (.81 msi)

$msi = 10^6$ psi

*Values estimated for manufacture's per ply thickness = .13335 mm.

†Based on cantilever beam tests with per ply thickness = .130 mm.

TABLE 4: EFFECT OF PER PLY THICKNESS ON THE STIFFNESS PROPERTIES OF 2, 4, AND 8 PLY LAMINATES BASED ON SANDWICH BEAM AND TENSILE COUPON TESTS

PROPERTY	2 PLY LAMINATE MEASURED PER PLY THICKNESS = .169 mm	4 PLY LAMINATE MEASURED PER PLY THICKNESS = .146 mm	8 PLY LAMINATE MEASURED PER PLY THICKNESS = .130 mm
E_L (GPa)	104	125	142
E_T (GPa)	---	10.6	9.4
ν_{LT}	.33	.29	.27
G(GPa)	---	5.5	6.0

TABLE 5: SUMMARY OF $(0°)_2$ SANDWICH BEAM DATA

RUN	BEAM	LAMINATE	AVERAGE LAMINATE THICKNESS (mm)	E_L (GPa)		ν_{LT}
				TENSION	COMPRESSION	
1	3	$(0)_2$-2-3	.341	103.255	100.477	.325
1	3	$(0)_2$-2-2	.338	102.105	104.564	.338
8	7	$(0)_2$-2-4	.332	103.469	104.835	.325
8	7	$(0)_2$-2-1	.341	100.702	101.340	.325
7	10	$(0)_2$-1-2	.348	106.754	111.468	.350
7	10	$(0)_2$-1-3	.341	104.476	106.999	.338
5	11	$(0)_2$-1-4	.327	99.876	102.853	.338
5	11	$(0)_2$-1-1	.332	99.411	104.329	.325

Average E_L Tension = 102.505 GPa (14.876 msi)
Standard Deviation = 2.489 GPa (2.4%)

Average E_L Compression = 104.608 GPa (15.172 msi)
Standard Deviation = 3.459 GPa (3.3%)

Average of E_L Tension & E_L Compression = 103.557 GPa (15.020 msi)
Standard Deviation = 3.107 GPa (3.0%)

Average ν_{LT} = .333
Standard Deviation = .009 (2.7%)

Average Thickness = .338 mm
Standard Deviation = .007 mm (2.1%)

TABLE 6: SUMMARY OF $(0°)_4$ SANDWICH BEAM DATA

RUN	BEAM	LAMINATE	AVERAGE LAMINATE THICKNESS (mm)	E_L (GPa)		ν_{LT}
				TENSION	COMPRESSION	
12	16	$(0)_4$-1-4	.575	127.213	120.205	.313
12	16	$(0)_4$-1-1	.571	118.174	114.231	.318

Average E_L Tension = 122.694 GPa (17.795 msi)
Standard Deviation = 6.392 GPa (5.2%)

Average E_L Compression = 117.218 GPa (17.001 msi)
Standard Deviation = 4.224 GPa (3.6%)

Average of E_L Tension & E_L Compression = 119.956 GPa (17.398 msi)
Standard Deviation = 5.437 GPa (4.5%)

Average ν_{LT} = .315

Average Thickness = .573 mm

TABLE 7: SUMMARY OF $(0°)_4$ TENSILE COUPON DATA

RUN	LAMINATE	AVERAGE LAMINATE THICKNESS (mm)	E_L (GPa)	ν_{LT}
11	$(0)_4$-2-1	.572	129.224	.287
12	$(0)_4$-2-2	.584	130.768	.264
13	$(0)_4$-2-3	.549	121.093	.317
14	$(0)_4$-2-4	.564	126.234	.268

Average E_L = 126.830 GPa (18.395 msi)
Standard Deviation = 4.263 GPa (3.4%)

Average ν_{LT} = 0.284
Standard Deviation = .024 (8.5%)

Average Thickness = 0.567 mm
Standard Deviation = .015 mm (2.6%)

TABLE 8: SUMMARY OF $(0°)_8$ TENSILE COUPON DATA

RUN	LAMINATE	AVG. THICKNESS (mm)	E_L (GPa)	ν_{LT}
1	$(0)_8$-1-1	1.053	134.183	.272
4	$(0)_8$-1-2	1.080	141.784	.281
5	$(0)_8$-1-3	1.055	142.091	.259
3	$(0)_8$-1-4	1.034	140.708	.280
6	$(0)_8$-1-5	1.000	142.165	.257
7	$(0)_8$-2-1	1.020	144.325	.292
8	$(0)_8$-2-2	1.069	142.679	.297
9	$(0)_8$-2-3	1.070	144.430	.270
10	$(0)_8$-2-4	1.038	145.265	.254

Average E_L = 141.959 GPa (20.589 GPa)
Standard Deviation = 3.265 GPa (2.3%)

Average ν_{LT} = 0.274
Standard Deviation = .015 (5.6%)

Average Thickness = 1.047 mm
Standard Deviation = .026 mm (2.5%)

TABLE 9: SUMMARY OF $(0°)_8$ CANTILEVER BEAM DATA

EAM	THICKNESS (mm)	E(GPa) STATIC (TIP LOAD)	E(GPa) 1st MODE	E(GPa) 2nd MODE	E(GPa) 3rd MODE	E(GPa) STATIC (COUPON)	ν_{LT} STATIC (COUPON)
$)_8$-2-A	1.029	100.599	101.433	98.636	98.129	142.236	.304
$)_8$-2-B	1.055	91.696	89.252	92.283	93.176	138.330	.310
$)_8$-2-C	1.044	99.716	101.060	97.669	96.627	142.253	.296
$)_8$-2-D	1.031	101.996	102.447	99.900	98.941	-------	----
ERAGE	1.040	98.502	98.548	97.122	96.718	140.940	.303
).DEV.	.012 (1.2%)	4.633 (4.7%)	6.225 (6.3%)	3.353 (3.5%)	2.549 (2.6%)	2.260 (1.6%)	.007 (2.3%)

TABLE 10: SUMMARY OF $(90°)_4$ SANDWICH BEAM DATA

RUN	BEAM	LAMINATE	AVERAGE LAMINATE THICKNESS (mm)	E_T (GPa)	
				TENSION	COMPRESSION
3	13	$(90)_4$-3-2	.591	10.470	10.154
3	13	$(90)_4$-3-3	.595	9.807	11.275
9	1	$(90)_4$-4-3	.583	10.263	10.472
9	1	$(90)_4$-4-2	.581	10.477	10.532
11	4	$(90)_4$-3-4	.581	11.342	11.231
11	4	$(90)_4$-3-1	.587	10.380	11.380
10	15	$(90)_4$-4-4	.577	10.740	10.702
10	15	$(90)_4$-4-1	.578	10.190	10.702

Average E_T Tension = 10.459 GPa (1.517 msi)

Standard Deviation = .477 GPa (4.3%)

Average E_T Compression = 10.807 GPa (1.567 msi)

Standard Deviation = .441 GPa (4.1%)

Average of E_T Tension and Compression = 10.633 GPa (1.542 msi)

Standard Deviation = .465 GPa (4.4%)

Poissons Ratio $\doteq$ .016 for all Laminates Tension and Compression

Average Thickness = .584 mm

Standard Deviation = .006 mm (1.0%)

TABLE II: SUMMARY OF $(90°)_8$ TENSILE COUPON DATA

RUN	LAMINATE	AVG. THICKNESS (mm)	E_T(GPa)	ν_{TL}
14	$(90)_8$-1-1	1.037	10.187	.020
15	$(90)_8$-1-2	1.029	10.083	.020
16	$(90)_8$-1-3	1.041	9.877	.023
17	$(90)_8$-1-4	1.056	10.223	.020
21	$(90)_8$-2-1	1.054	8.423	.016
20	$(90)_8$-2-2	1.045	8.701	.017
18	$(90)_8$-2-3	1.029	8.485	.016
19	$(90)_8$-2-4	1.040	8.825	.018

Average E_T = 9.351 GPa (1.356 msi)
Standard Deviation = .809 GPa (8.7%)

Average ν_{TL} = .019
Standard Deviation = .002 (13%)

Average Thickness = 1.041 mm
Standard Deviation = .010 mm (1.0%)

TABLE 12: SUMMARY OF $(90°)_8$ CANTILEVER BEAM DATA

BEAM	THICKNESS (mm)	E_T (GPa)			
		STATIC (TIP LOAD)	1st MODE	2nd MODE	3rd MODE
$(90)_8$-2-A	1.071	7.724	7.961	7.998	7.878
$(90)_8$-2-B	1.083	7.777	7.960	7.809	8.001
$(90)_8$-2-C	1.073	7.822	7.971	8.362	8.168
$(90)_8$-2-D	1.064	7.841	7.854	7.921	8.025
AVERAGE	1.073	7.791	7.937	8.023	8.018
STD.DEV.	.008 (.7%)	.052 (0.7%)	.055 (0.7%)	.239 (3.0%)	.119 (1.5%)

TABLE 13: SUMMARY OF $(+/- 45°)_S$ SANDWICH BEAM DATA

RUN	BEAM	LAMINATE	AVERAGE LAMINATE THICKNESS (mm)	G(GPa)	
				TENSION	COMPRESSION
6	5	$(+/- 45°)_S$-3-4	.596	5.184	5.238
6	5	$(+/- 45°)_S$-3-1	.611	5.974	5.964
13	8	$(+/- 45°)_S$-4-3	.589	5.623	5.673
13	8	$(+/- 45°)_S$-4-2	.590	5.710	5.740
14	9	$(+/- 45°)_S$-4-4	.595	5.619	5.542
14	9	$(+/- 45°)_S$-4-1	.601	6.057	5.936
4	12	$(+/- 45°)_S$-4-3	.594	5.008	4.789
4	12	$(+/- 45°)_S$-4-2	.594	5.048	5.109

Average G Tension = 5.528 GPa (.802 msi)
Standard Deviation = .405 GPA (7.3%)

Average G Compression = 5.499 GPa (.798 msi)
Standard Deviation = .418 GPa (7.6%)

Average of G Tension and G Compression = 5.513 GPa (.800 msi)
Standard Deviation = .398 GPa (7.2%)

Average Thickness = .596 mm
Standard Deviation = .007 mm (1.2%)

TABLE 14: SUMMARY OF $(+/- 45°)_S$ TENSILE COUPON DATA

RUN	LAMINATE	AVG. THICKNESS (mm)	G(GPa)
31	$(+/- 45°)_S$-1-3	.586	5.474
32	$(+/- 45°)_S$-1-4	.586	5.042

Average G = 5.258 GPa

Standard Deviation = .305 GPa (5.8%)

Average Thickness = .586 mm

Standard Deviation = 0

TABLE 15: SUMMARY OF $(+/- 45°)_{2S}$ TENSILE COUPON DATA

RUN	LAMINATE	AVG. THICKNESS (mm)	G(GPa)
22	$(+/- 45°)_{2S}$-1-1	1.042	6.509
23	$(+/- 45°)_{2S}$-1-2	1.005	6.142
24	$(+/- 45°)_{2S}$-1-3	1.021	5.583
25	$(+/- 45°)_{2S}$-1-4	1.032	6.145
26	$(+/- 45°)_{2S}$-1-5	1.063	5.765
27	$(+/- 45°)_{2S}$-2-1	1.089	5.867
28	$(+/- 45°)_{2S}$-2-2	1.059	6.117
29	$(+/- 45°)_{2S}$-2-3	1.032	6.162
30	$(+/- 45°)_{2S}$-2-4	1.040	5.423

Average G = 5.971 GPa (.866 msi)

Standard Deviation = .335 GPa (5.6%)

Average Thickness = 1.043 mm

Standard Deviation = .025 mm (2.4%)

TABLE 16: SUMMARY OF $(+/- 45°)_{2S}$ CANTILEVER BEAM DATA

BEAM	THICKNESS (mm)	G(GPa)			
		STATIC (TIP LOAD)	1st MODE	2nd MODE	3rd MODE
$(+/- 45°)_{2S}$-2-A	1.095	5.172	5.685	5.466	5.641
$(+/- 45°)_{2S}$-2-B	1.074	5.453	6.170	5.692	5.856
$(+/- 45°)_{2S}$-2-C	1.076	5.483	6.193	5.843	5.984
$(+/- 45°)_{2S}$-2-D	1.100	5.082	4.952	5.320	5.692
AVERAGE	1.086	5.298	5.750	5.580	5.793
STD. DEV.	.013(1.2%)	.201(3.8%)	.581(10.1%)	.233(4.2%)	.157(2.7%)

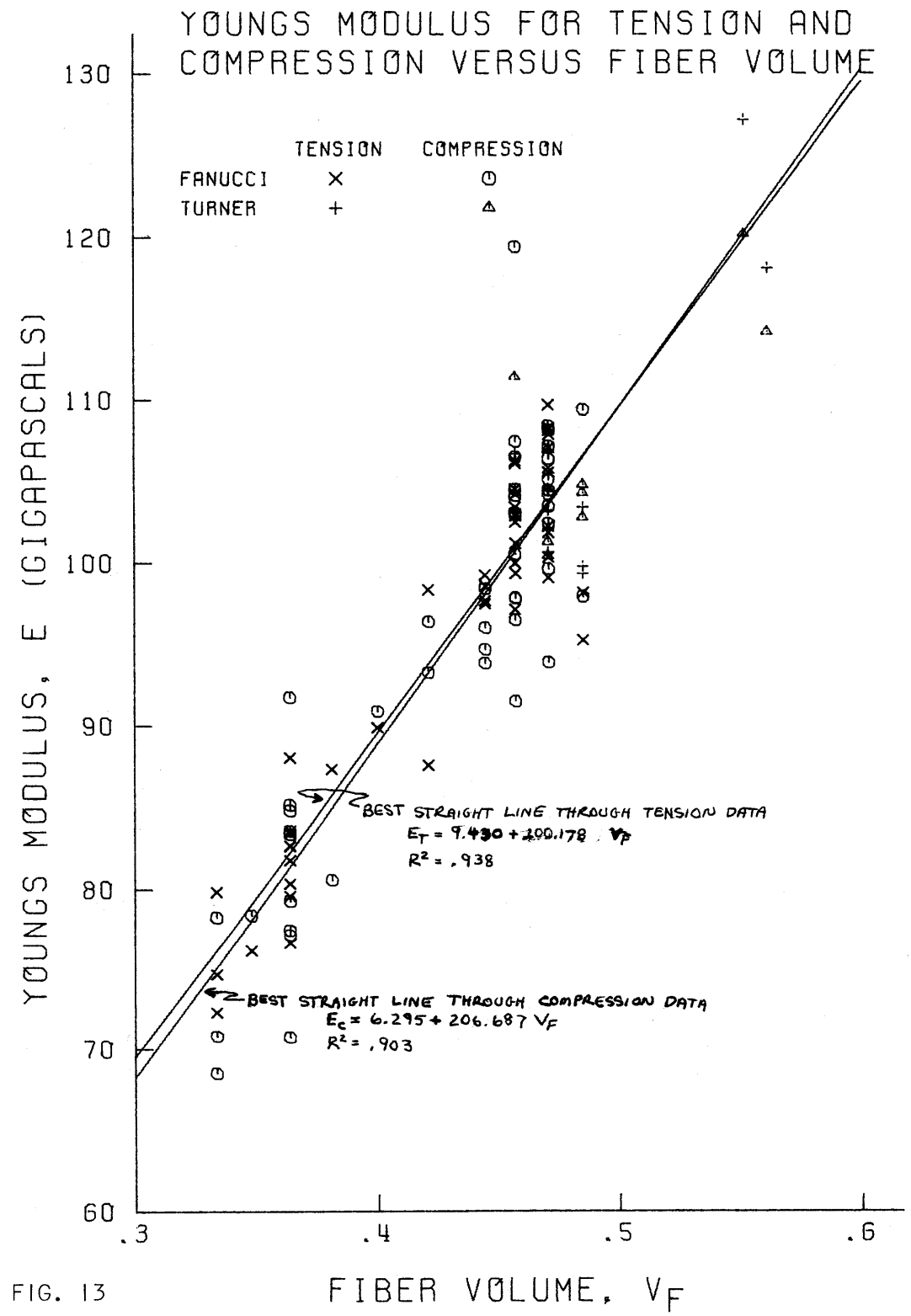
YOUNGS MODULUS FOR TENSION AND COMPRESSION VERSUS FIBER VOLUME
TENSION
COMPRESSION
FANUCCI
TURNER
BEST STRAIGHT LINE THROUGH TENSION DATA
$E_T = 9.430 + 200.178\ V_F$
$R^2 = .938$
BEST STRAIGHT LINE THROUGH COMPRESSION DATA
$E_C = 6.295 + 206.687\ V_F$
$R^2 = .903$
YOUNGS MODULUS, E (GIGAPASCALS)
130
120
110
100
90
80
70
60
.3
.4
.5
.6
FIBER VOLUME, V_F

FIG. 13

FIG. 14

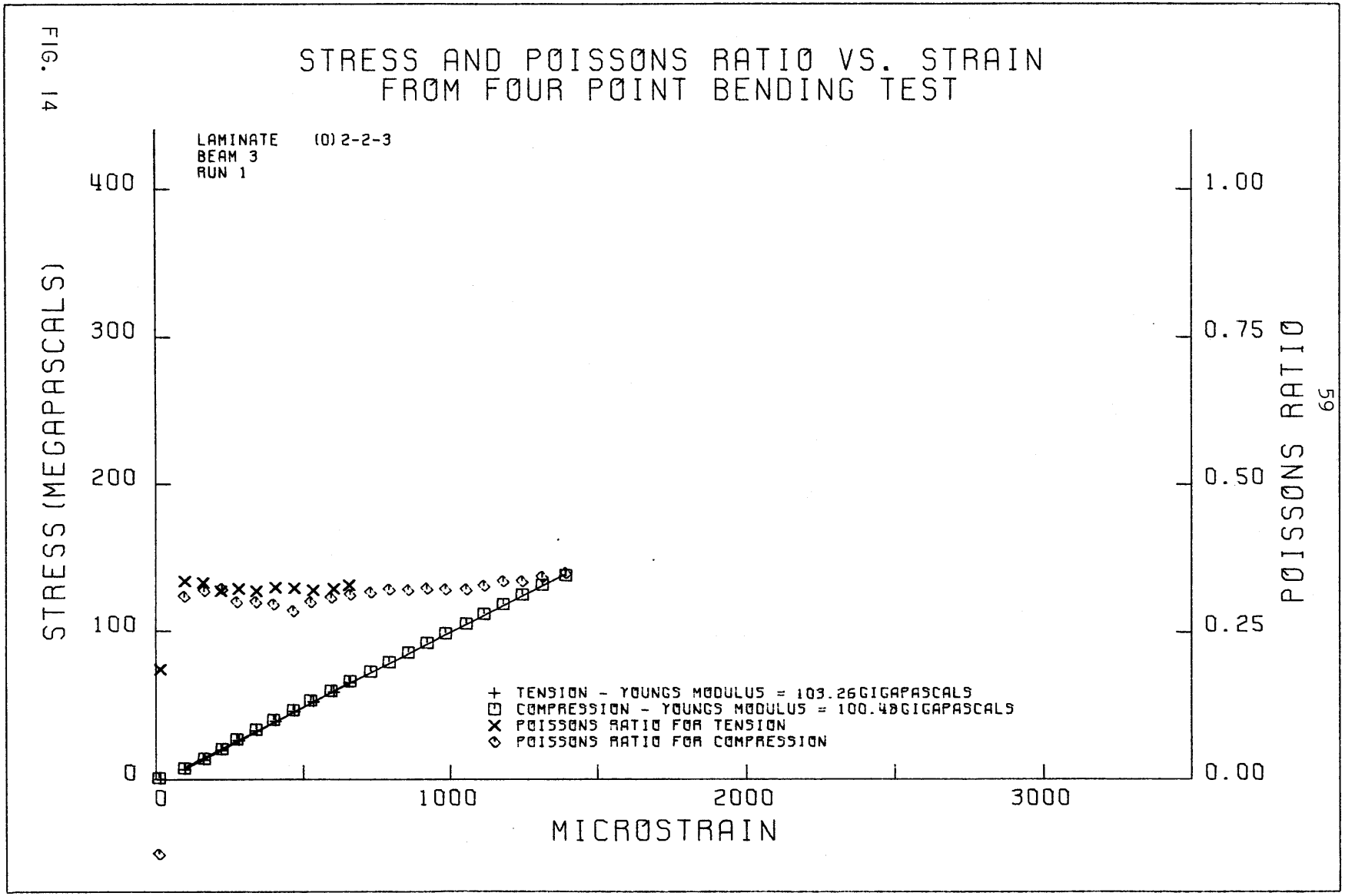
STRESS AND POISSONS RATIO VS. STRAIN
FROM FOUR POINT BENDING TEST
LAMINATE (0)2-2-3
BEAM 3
RUN 1
STRESS (MEGAPASCALS)
400
300
200
100
0
1.00
0.75
0.50
0.25
0.00
POISSONS RATIO
0
1000
2000
3000
MICROSTRAIN
+ TENSION - YOUNGS MODULUS = 103.26GIGAPASCALS
□ COMPRESSION - YOUNGS MODULUS = 100.48GIGAPASCALS
× POISSONS RATIO FOR TENSION
◇ POISSONS RATIO FOR COMPRESSION

FIG. 15

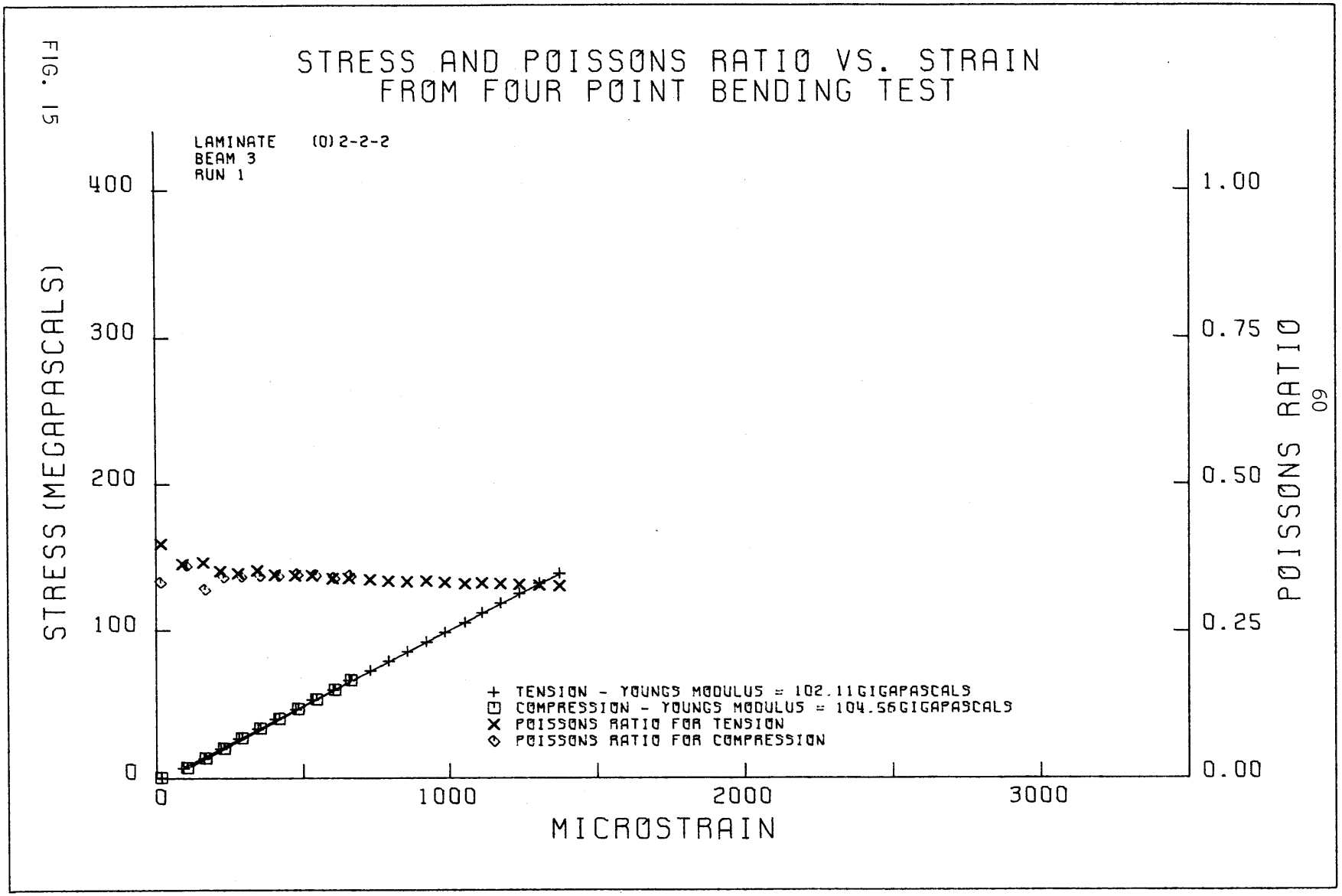
STRESS AND POISSONS RATIO VS. STRAIN
FROM FOUR POINT BENDING TEST
LAMINATE (0)2-2-2
BEAM 3
RUN 1
STRESS (MEGAPASCALS)
400
300
200
100
0
0
1000
2000
3000
MICROSTRAIN
1.00
0.75
0.50
0.25
0.00
POISSONS RATIO
+ TENSION - YOUNGS MODULUS = 102.11GIGAPASCALS
⊡ COMPRESSION - YOUNGS MODULUS = 104.56GIGAPASCALS
× POISSONS RATIO FOR TENSION
◇ POISSONS RATIO FOR COMPRESSION

09

FIG. 16

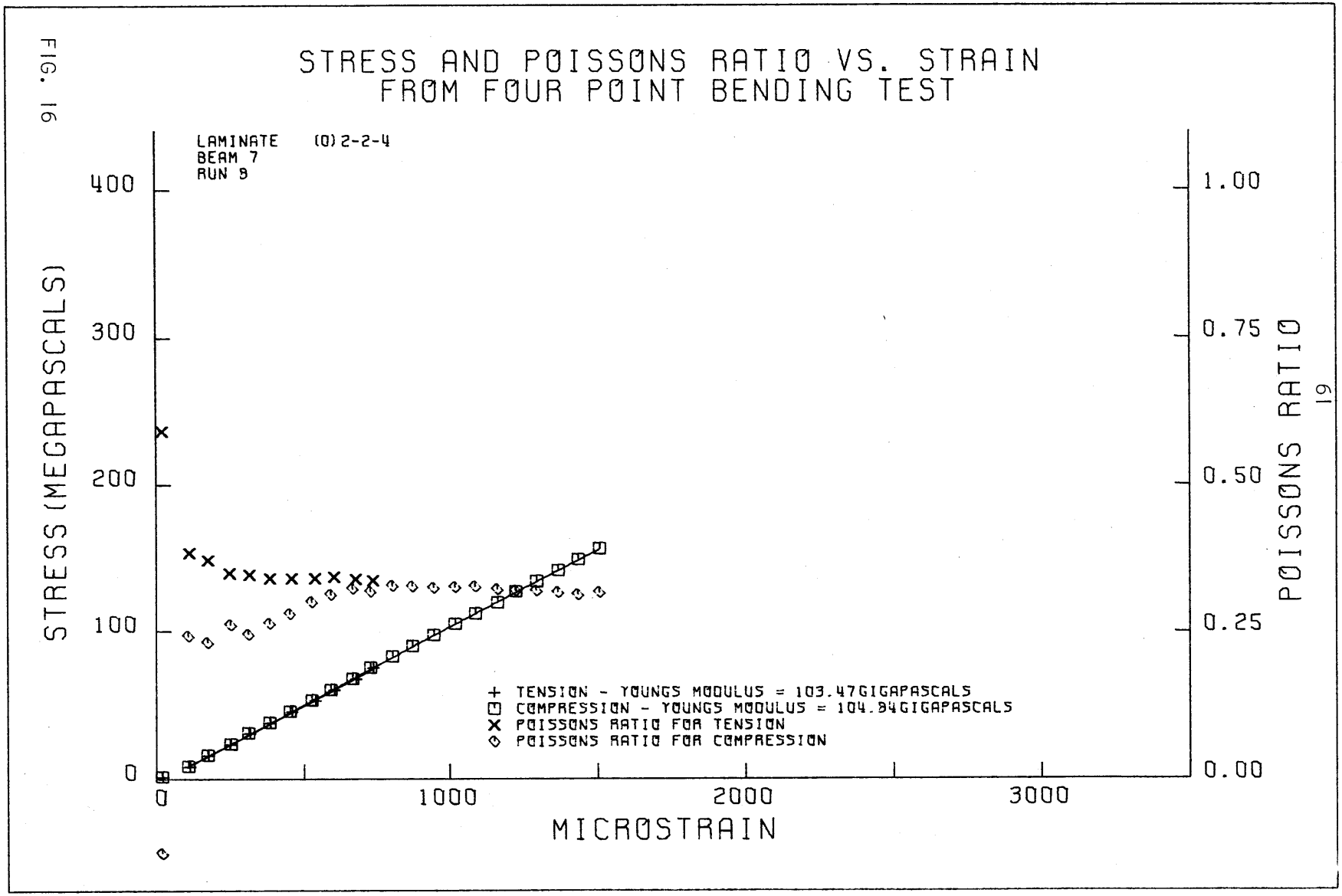
STRESS AND POISSONS RATIO VS. STRAIN
FROM FOUR POINT BENDING TEST
LAMINATE (0)2-2-4
BEAM 7
RUN 8
STRESS (MEGAPASCALS)
400
300
200
100
0
1.00
0.75
0.50
0.25
0.00
POISSONS RATIO
0
1000
2000
3000
MICROSTRAIN
+ TENSION - YOUNGS MODULUS = 103.47GIGAPASCALS
□ COMPRESSION - YOUNGS MODULUS = 104.84GIGAPASCALS
× POISSONS RATIO FOR TENSION
◇ POISSONS RATIO FOR COMPRESSION

FIG. 17

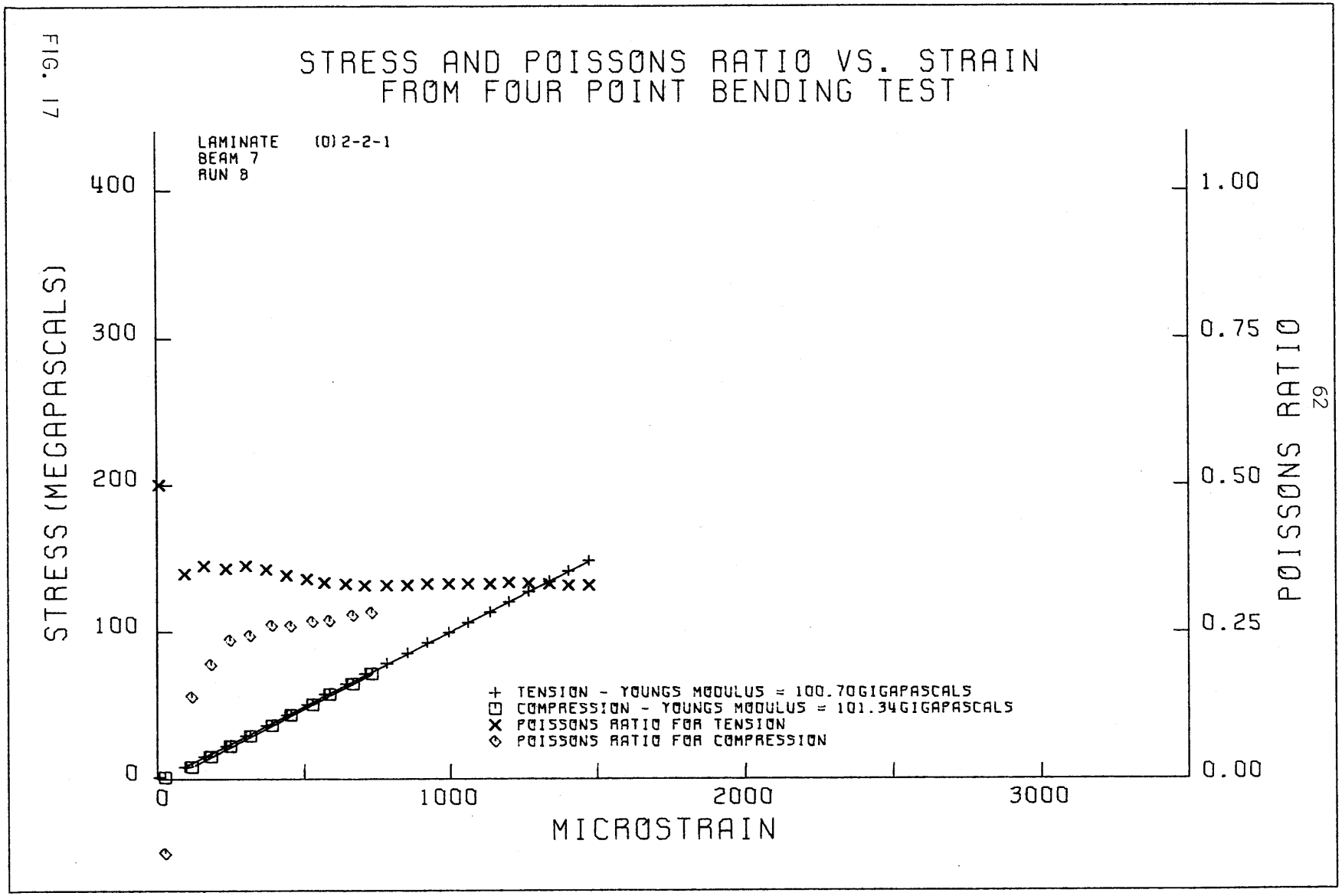
STRESS AND POISSONS RATIO VS. STRAIN
FROM FOUR POINT BENDING TEST
LAMINATE (0)2-2-1
BEAM 7
RUN 8
STRESS (MEGAPASCALS)
400
300
200
100
0
0
1000
2000
3000
MICROSTRAIN
1.00
0.75
0.50
0.25
0.00
POISSONS RATIO
+ TENSION - YOUNGS MODULUS = 100.70GIGAPASCALS
□ COMPRESSION - YOUNGS MODULUS = 101.34GIGAPASCALS
× POISSONS RATIO FOR TENSION
◇ POISSONS RATIO FOR COMPRESSION

FIG. 18

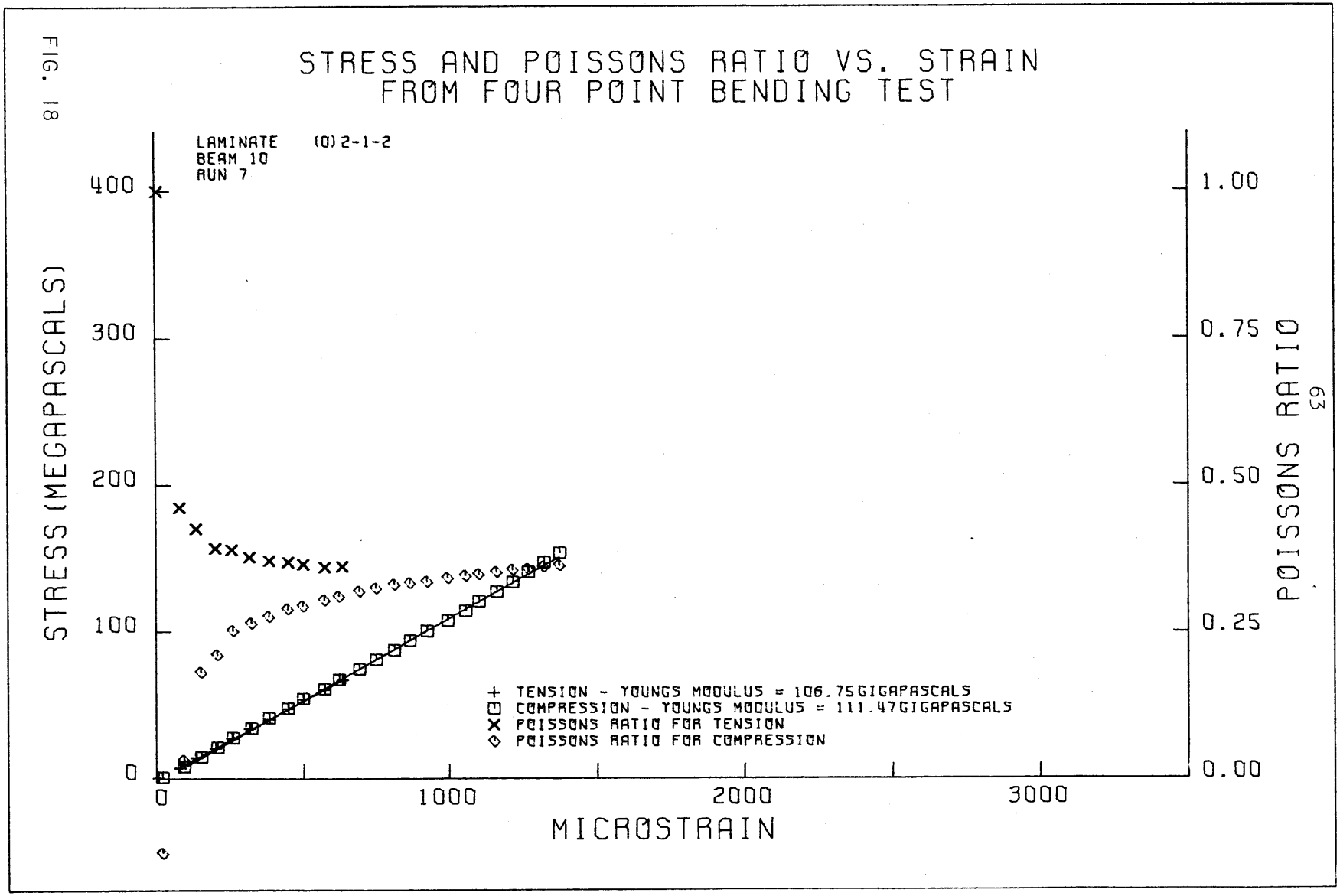
STRESS AND POISSONS RATIO VS. STRAIN
FROM FOUR POINT BENDING TEST
LAMINATE (0)2-1-2
BEAM 10
RUN 7
STRESS (MEGAPASCALS)
400
300
200
100
0
0
1000
2000
3000
MICROSTRAIN
1.00
0.75
0.50
0.25
0.00
POISSONS RATIO
+ TENSION - YOUNGS MODULUS = 106.75GIGAPASCALS
□ COMPRESSION - YOUNGS MODULUS = 111.47GIGAPASCALS
× POISSONS RATIO FOR TENSION
◇ POISSONS RATIO FOR COMPRESSION

FIG. 19

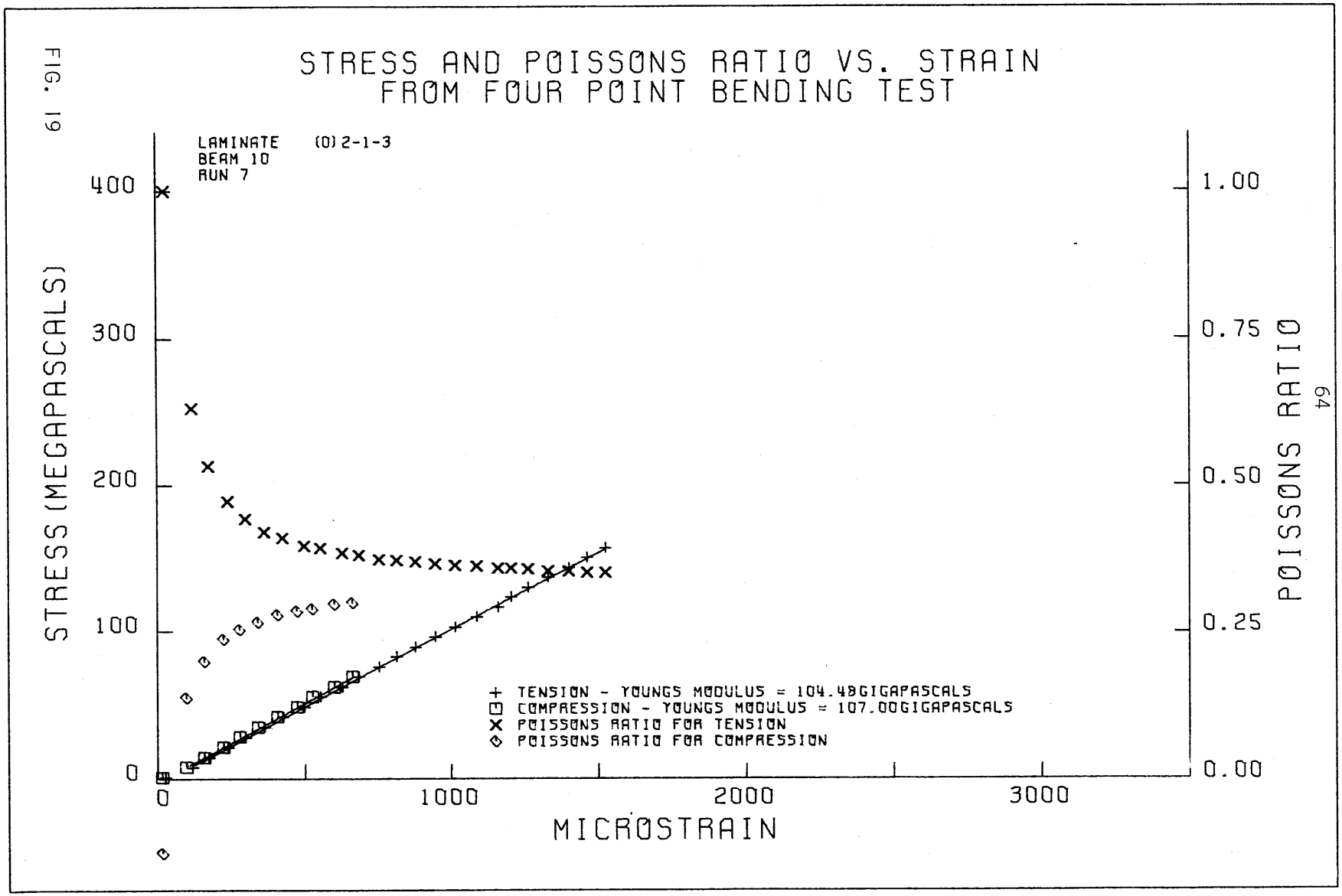
STRESS AND POISSONS RATIO VS. STRAIN
FROM FOUR POINT BENDING TEST
LAMINATE (0)2-1-3
BEAM 10
RUN 7
STRESS (MEGAPASCALS)
400
300
200
100
0
0
1000
2000
3000
MICROSTRAIN
1.00
0.75
0.50
0.25
0.00
POISSONS RATIO
+ TENSION - YOUNGS MODULUS = 104.48GIGAPASCALS
□ COMPRESSION - YOUNGS MODULUS = 107.00GIGAPASCALS
× POISSONS RATIO FOR TENSION
◇ POISSONS RATIO FOR COMPRESSION

FIG. 20

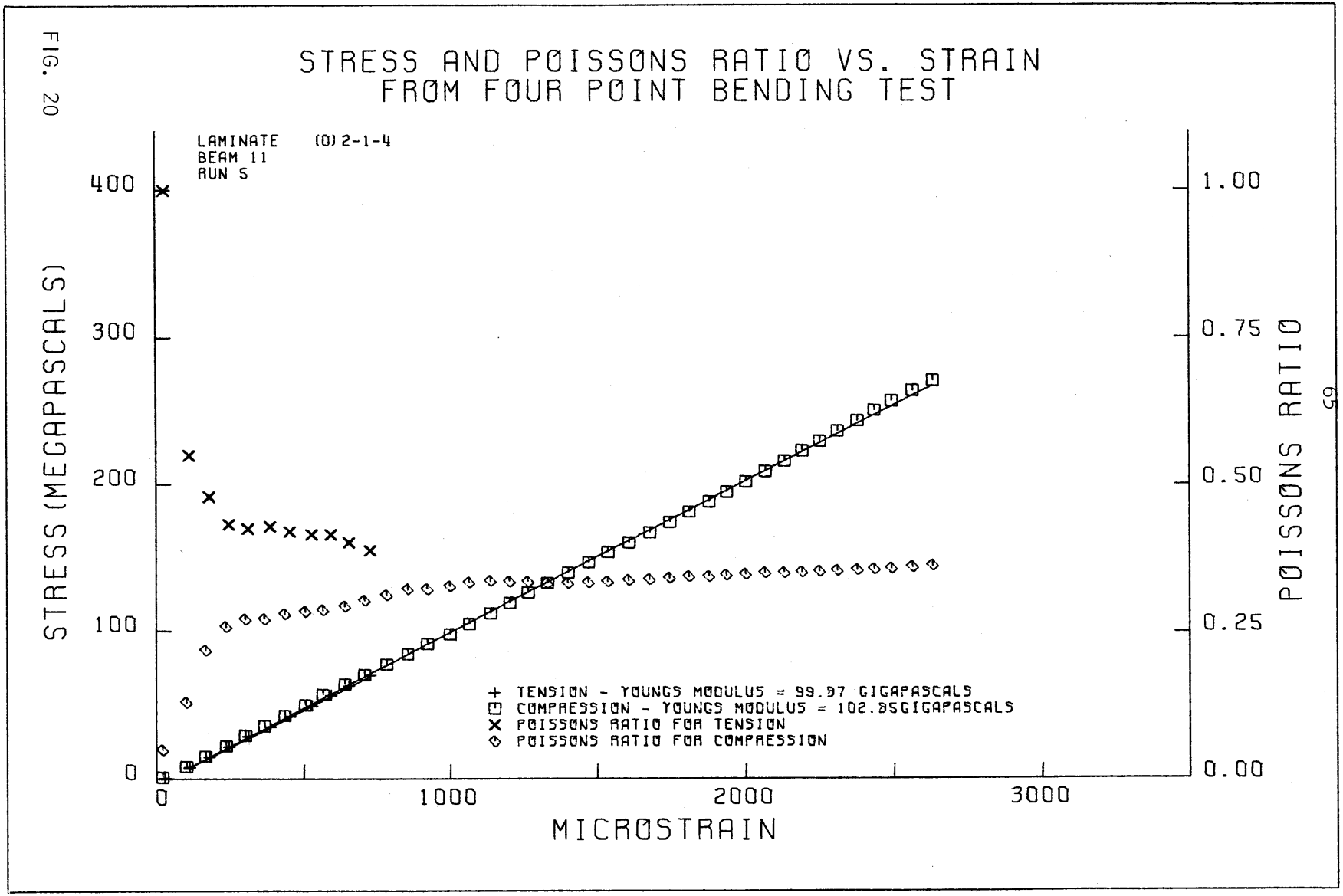
STRESS AND POISSONS RATIO VS. STRAIN
FROM FOUR POINT BENDING TEST
LAMINATE (0)2-1-4
BEAM 11
RUN 5
STRESS (MEGAPASCALS)
400
300
200
100
0
0
1000
2000
3000
MICROSTRAIN
1.00
0.75
0.50
0.25
0.00
POISSONS RATIO
+ TENSION - YOUNGS MODULUS = 99.97 GIGAPASCALS
COMPRESSION - YOUNGS MODULUS = 102.85GIGAPASCALS
POISSONS RATIO FOR TENSION
POISSONS RATIO FOR COMPRESSION

FIG. 21

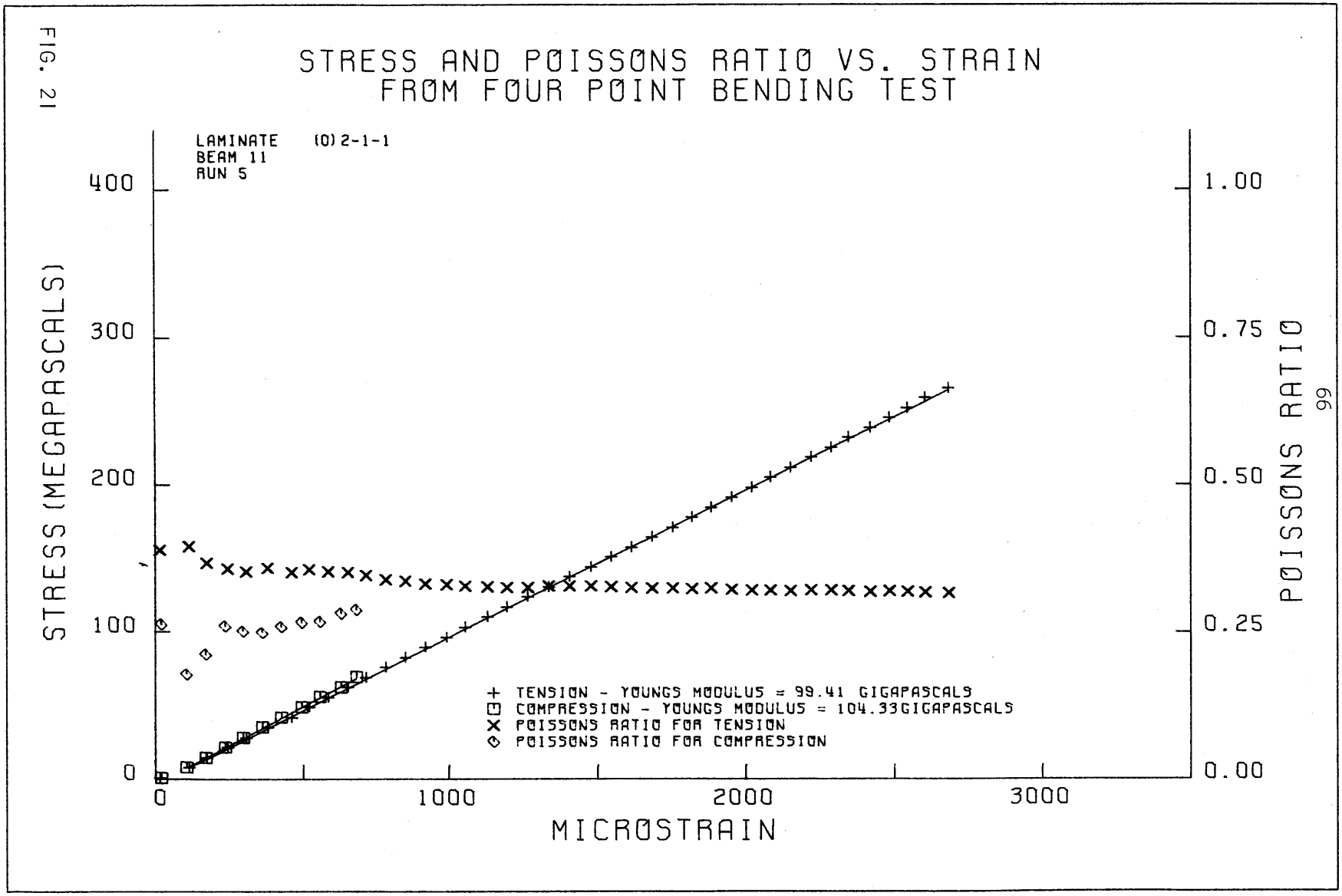
STRESS AND POISSONS RATIO VS. STRAIN
FROM FOUR POINT BENDING TEST
LAMINATE (0)2-1-1
BEAM 11
RUN 5
STRESS (MEGAPASCALS)
400
300
200
100
0
0
1000
2000
3000
MICROSTRAIN
1.00
0.75
0.50
0.25
0.00
POISSONS RATIO
+ TENSION - YOUNGS MODULUS = 99.41 GIGAPASCALS
COMPRESSION - YOUNGS MODULUS = 104.33GIGAPASCALS
POISSONS RATIO FOR TENSION
POISSONS RATIO FOR COMPRESSION

FIG. 22

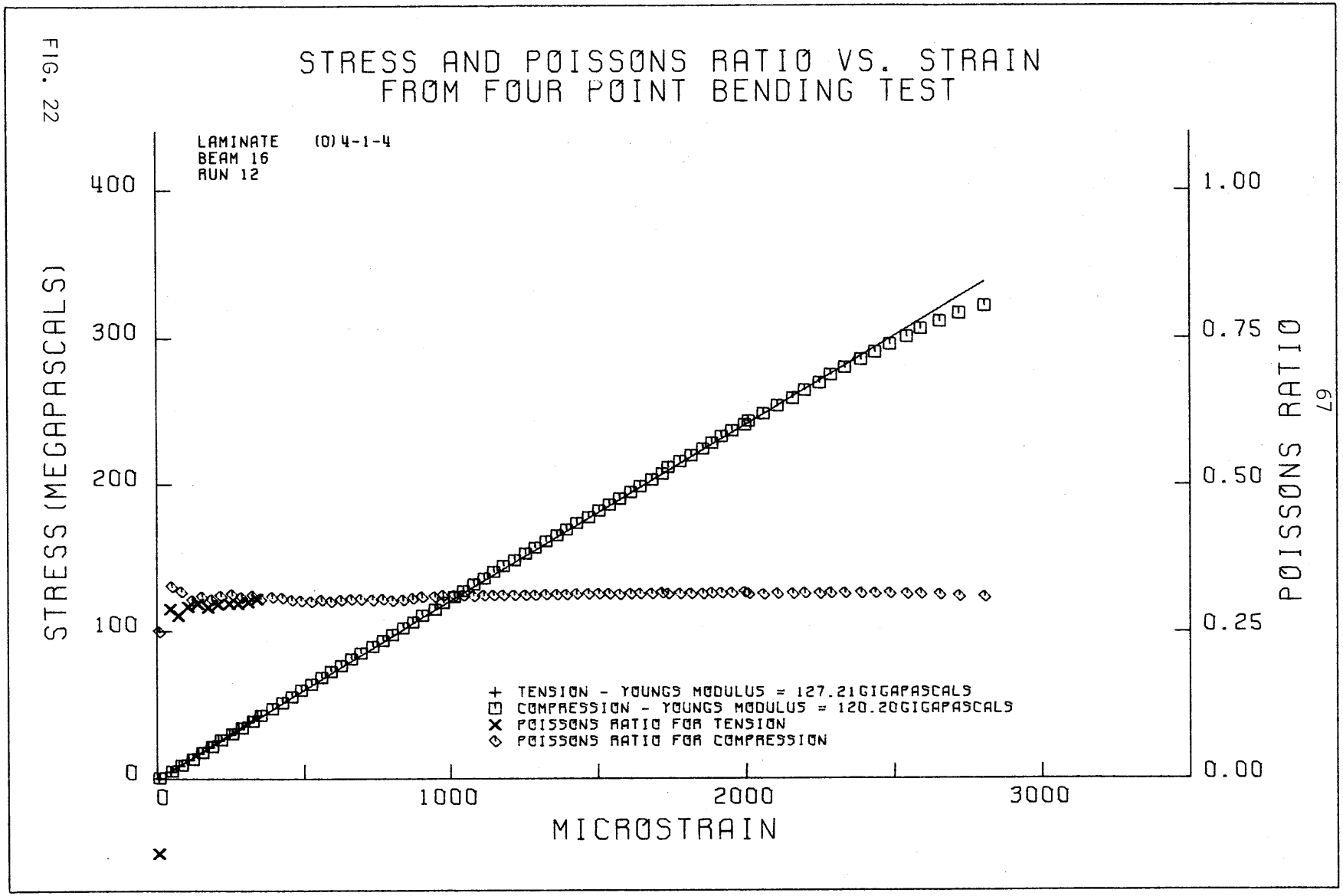
STRESS AND POISSONS RATIO VS. STRAIN
FROM FOUR POINT BENDING TEST
LAMINATE (0)4-1-4
BEAM 16
RUN 12
STRESS (MEGAPASCALS)
400
300
200
100
0
1.00
0.75
0.50
0.25
0.00
POISSONS RATIO
0
1000
2000
3000
MICROSTRAIN
+ TENSION - YOUNGS MODULUS = 127.21GIGAPASCALS
□ COMPRESSION - YOUNGS MODULUS = 120.20GIGAPASCALS
× POISSONS RATIO FOR TENSION
◇ POISSONS RATIO FOR COMPRESSION

FIG. 23

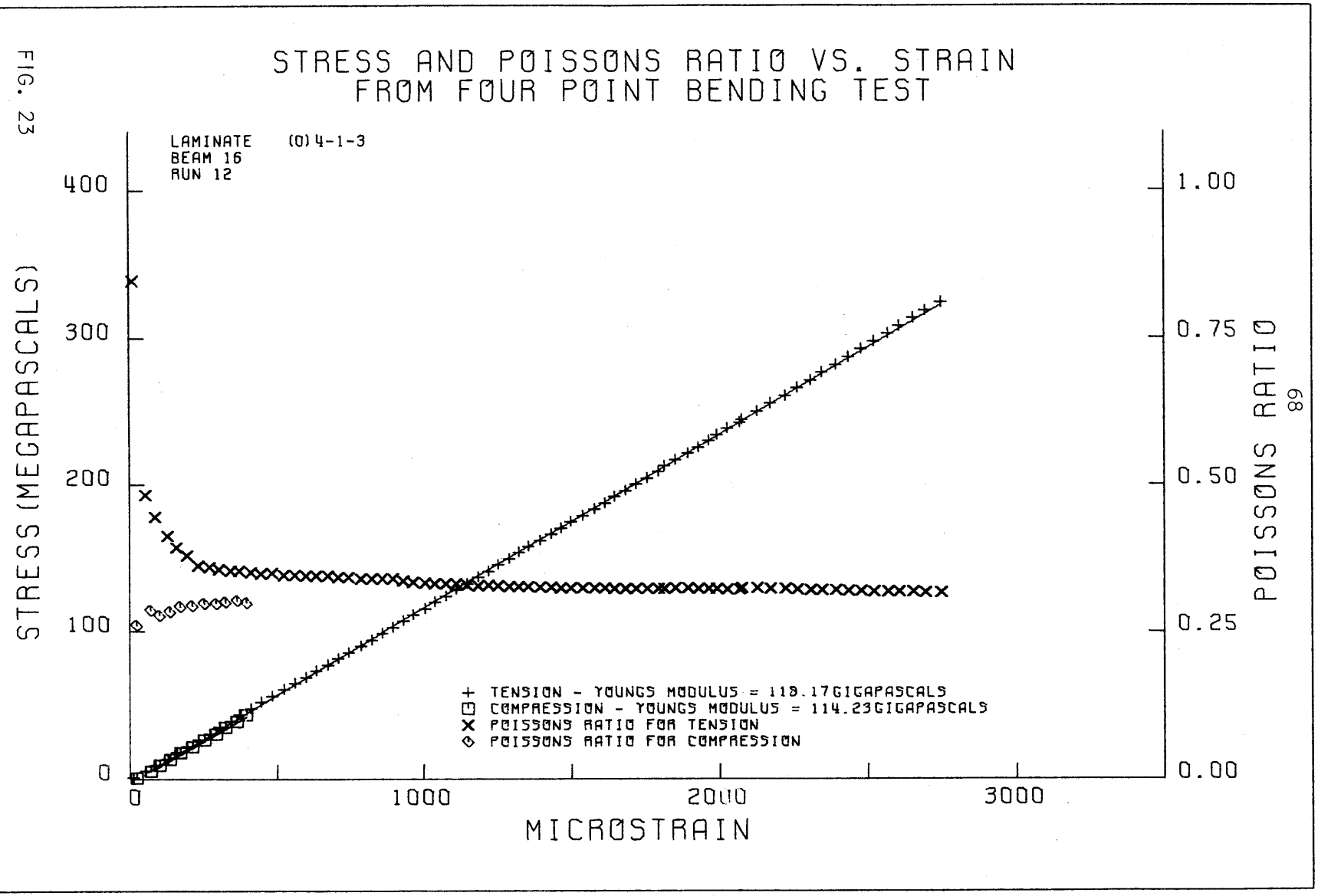
STRESS AND POISSONS RATIO VS. STRAIN
FROM FOUR POINT BENDING TEST
LAMINATE (0)4-1-3
BEAM 16
RUN 12
STRESS (MEGAPASCALS)
400
300
200
100
0
1.00
0.75
0.50
0.25
0.00
POISSONS RATIO
0
1000
2000
3000
MICROSTRAIN
+ TENSION - YOUNGS MODULUS = 118.17GIGAPASCALS
□ COMPRESSION - YOUNGS MODULUS = 114.23GIGAPASCALS
× POISSONS RATIO FOR TENSION
◇ POISSONS RATIO FOR COMPRESSION

FIG. 24

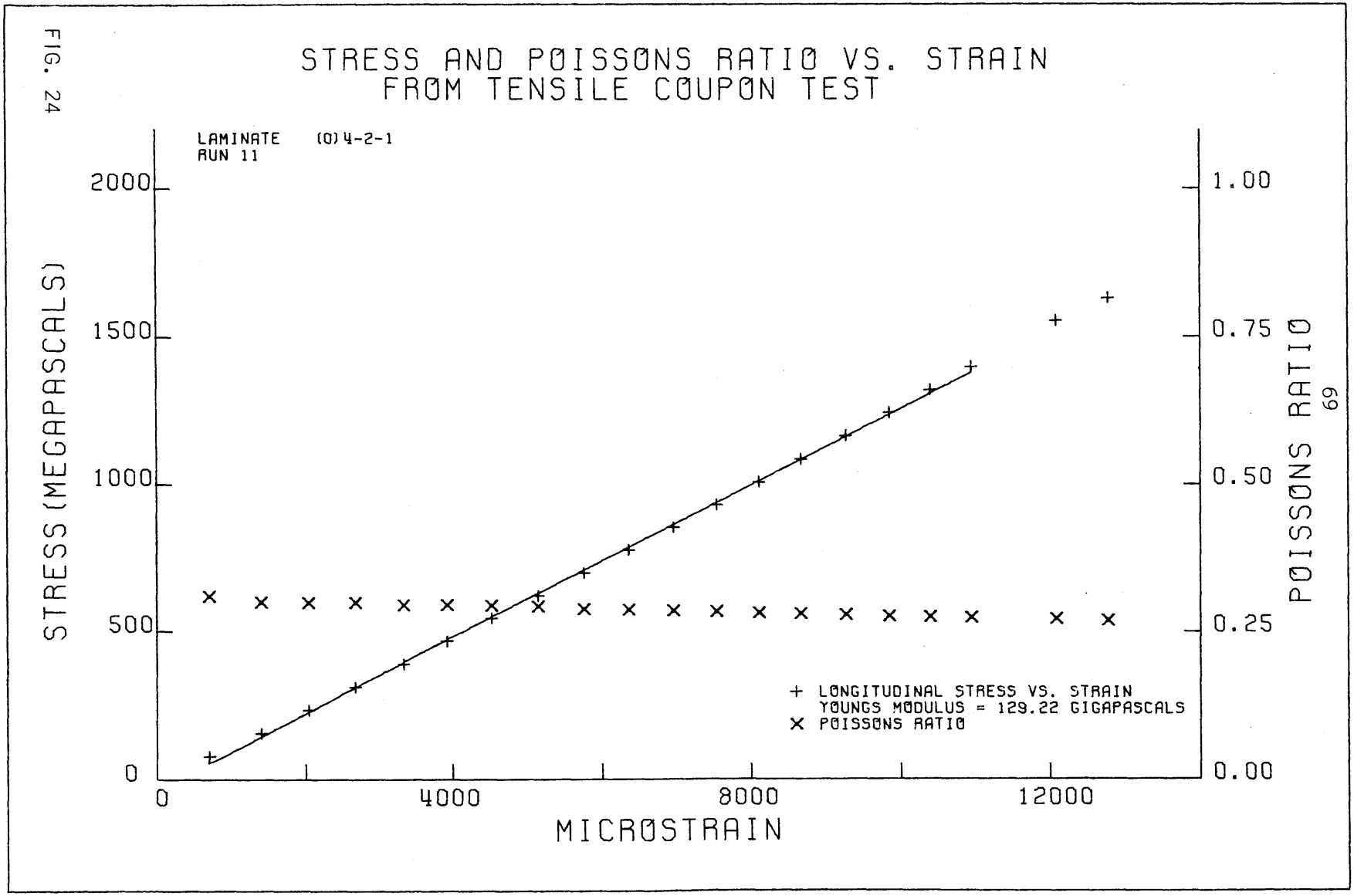
STRESS AND POISSONS RATIO VS. STRAIN
FROM TENSILE COUPON TEST
LAMINATE (0)4-2-1
RUN 11
STRESS (MEGAPASCALS)
2000
1500
1000
500
0
0
4000
8000
12000
MICROSTRAIN
1.00
0.75
0.50
0.25
0.00
POISSONS RATIO
+ LONGITUDINAL STRESS VS. STRAIN
YOUNGS MODULUS = 129.22 GIGAPASCALS
× POISSONS RATIO

FIG. 25

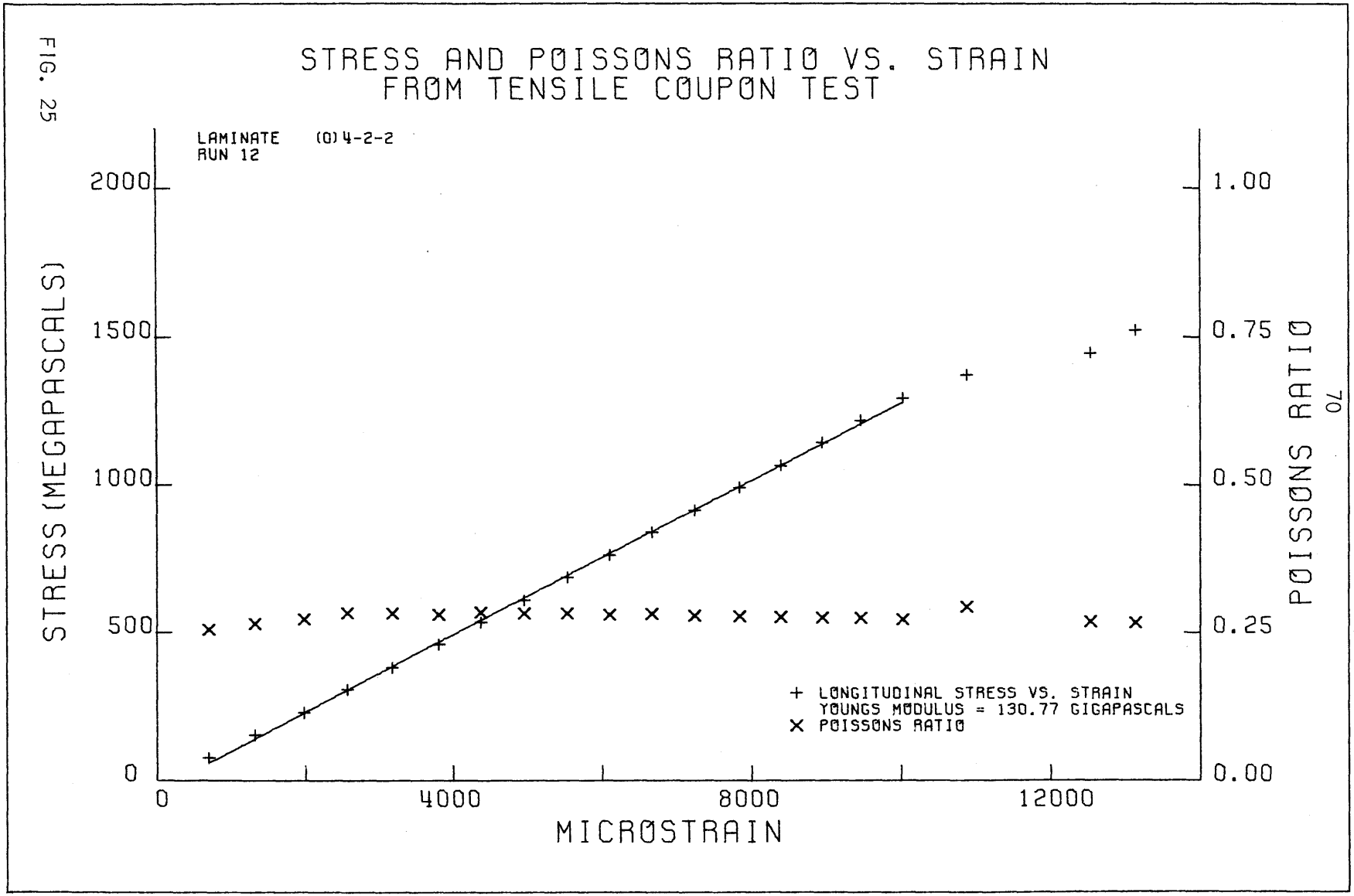
STRESS AND POISSONS RATIO VS. STRAIN
FROM TENSILE COUPON TEST
LAMINATE (0)4-2-2
RUN 12
2000
1500
1000
500
0
STRESS (MEGAPASCALS)
1.00
0.75
0.50
0.25
0.00
POISSONS RATIO
0
4000
8000
12000
MICROSTRAIN
+ LONGITUDINAL STRESS VS. STRAIN
YOUNGS MODULUS = 130.77 GIGAPASCALS
× POISSONS RATIO

FIG. 26

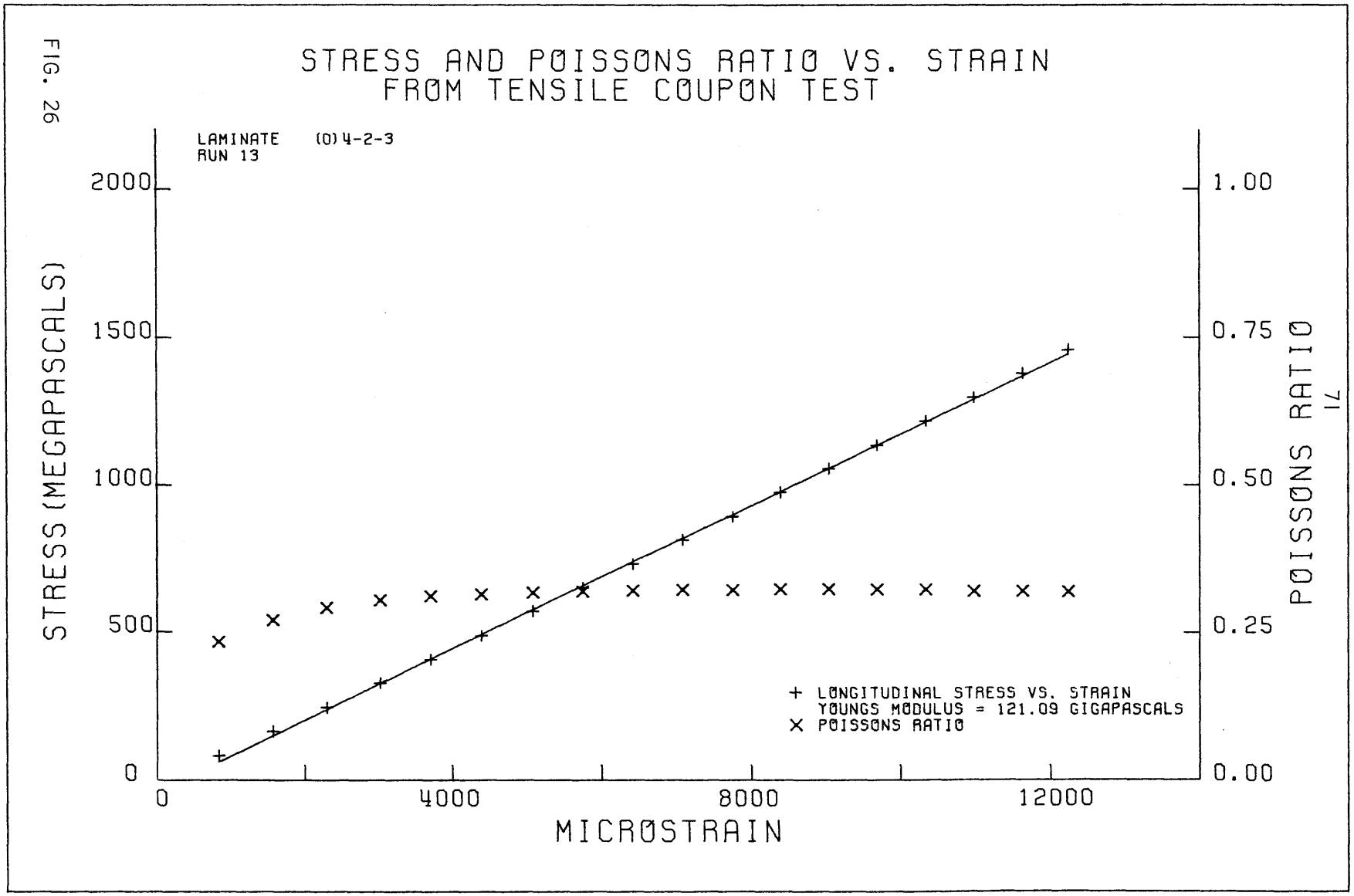
STRESS AND POISSONS RATIO VS. STRAIN
FROM TENSILE COUPON TEST
LAMINATE (0)4-2-3
RUN 13
STRESS (MEGAPASCALS)
2000
1500
1000
500
0
0
4000
8000
12000
MICROSTRAIN
1.00
0.75
0.50
0.25
0.00
POISSONS RATIO
+ LONGITUDINAL STRESS VS. STRAIN
YOUNGS MODULUS = 121.09 GIGAPASCALS
× POISSONS RATIO

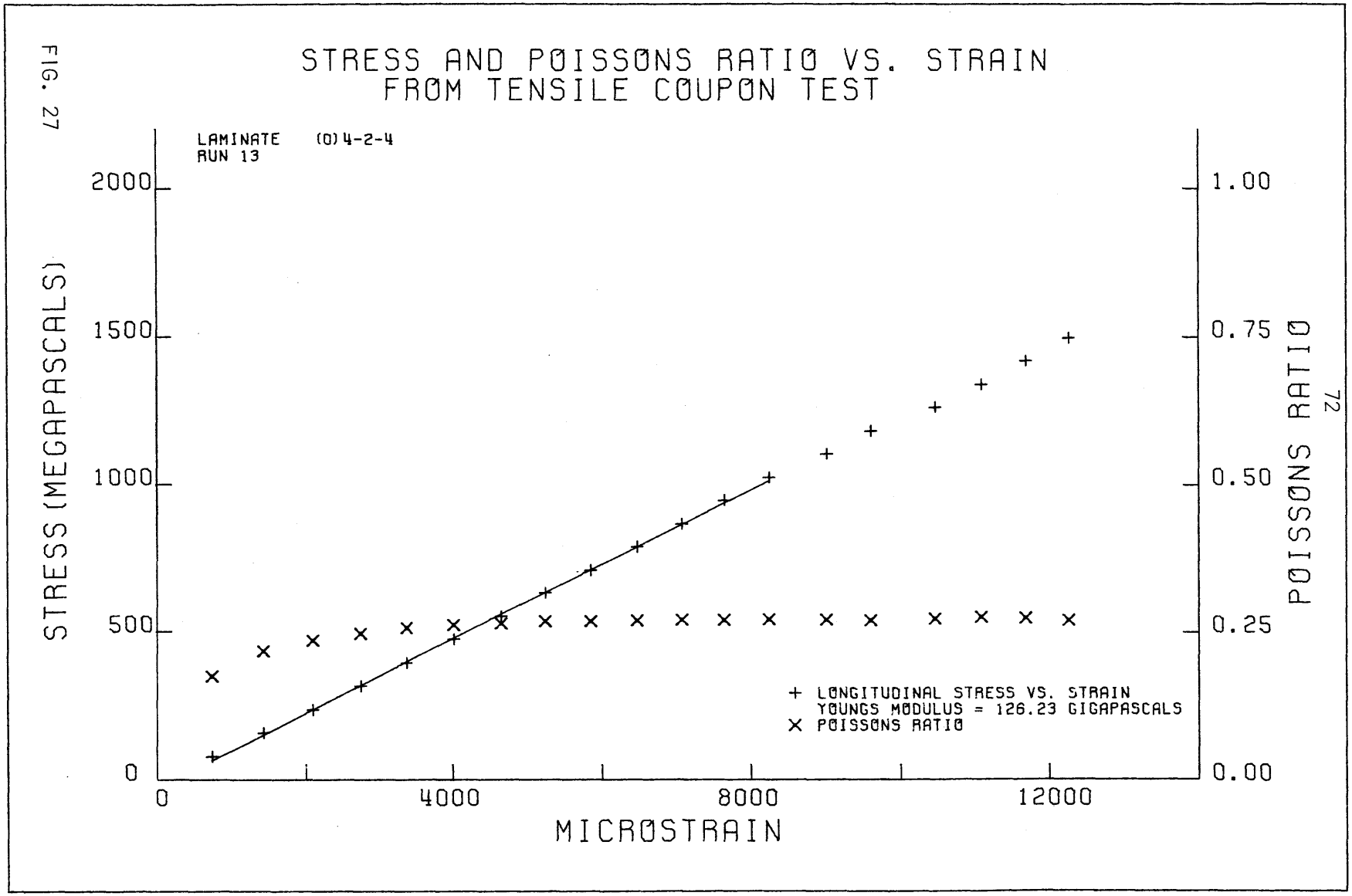
STRESS AND POISSONS RATIO VS. STRAIN
FROM TENSILE COUPON TEST
LAMINATE (0)4-2-4
RUN 13
STRESS (MEGAPASCALS)
2000
1500
1000
500
0
1.00
0.75
0.50
0.25
0.00
POISSONS RATIO
0
4000
8000
12000
MICROSTRAIN
+ LONGITUDINAL STRESS VS. STRAIN
YOUNGS MODULUS = 126.23 GIGAPASCALS
× POISSONS RATIO

FIG. 27

FIG. 28

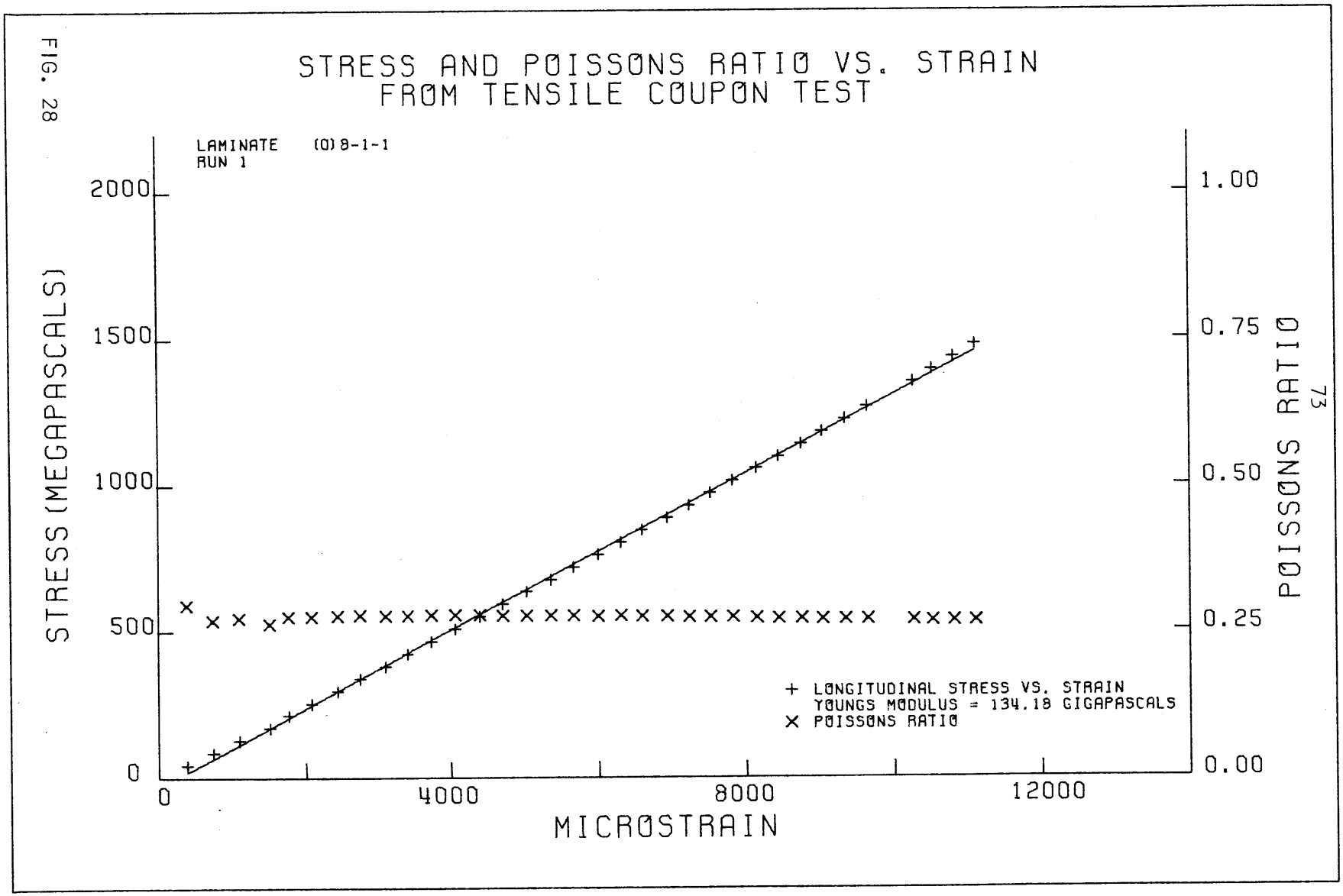
STRESS AND POISSONS RATIO VS. STRAIN
FROM TENSILE COUPON TEST
LAMINATE (0)8-1-1
RUN 1
STRESS (MEGAPASCALS)
2000
1500
1000
500
0
0
4000
8000
12000
MICROSTRAIN
1.00
0.75
0.50
0.25
0.00
POISSONS RATIO
+ LONGITUDINAL STRESS VS. STRAIN
YOUNGS MODULUS = 134.18 GIGAPASCALS
× POISSONS RATIO

FIG. 29

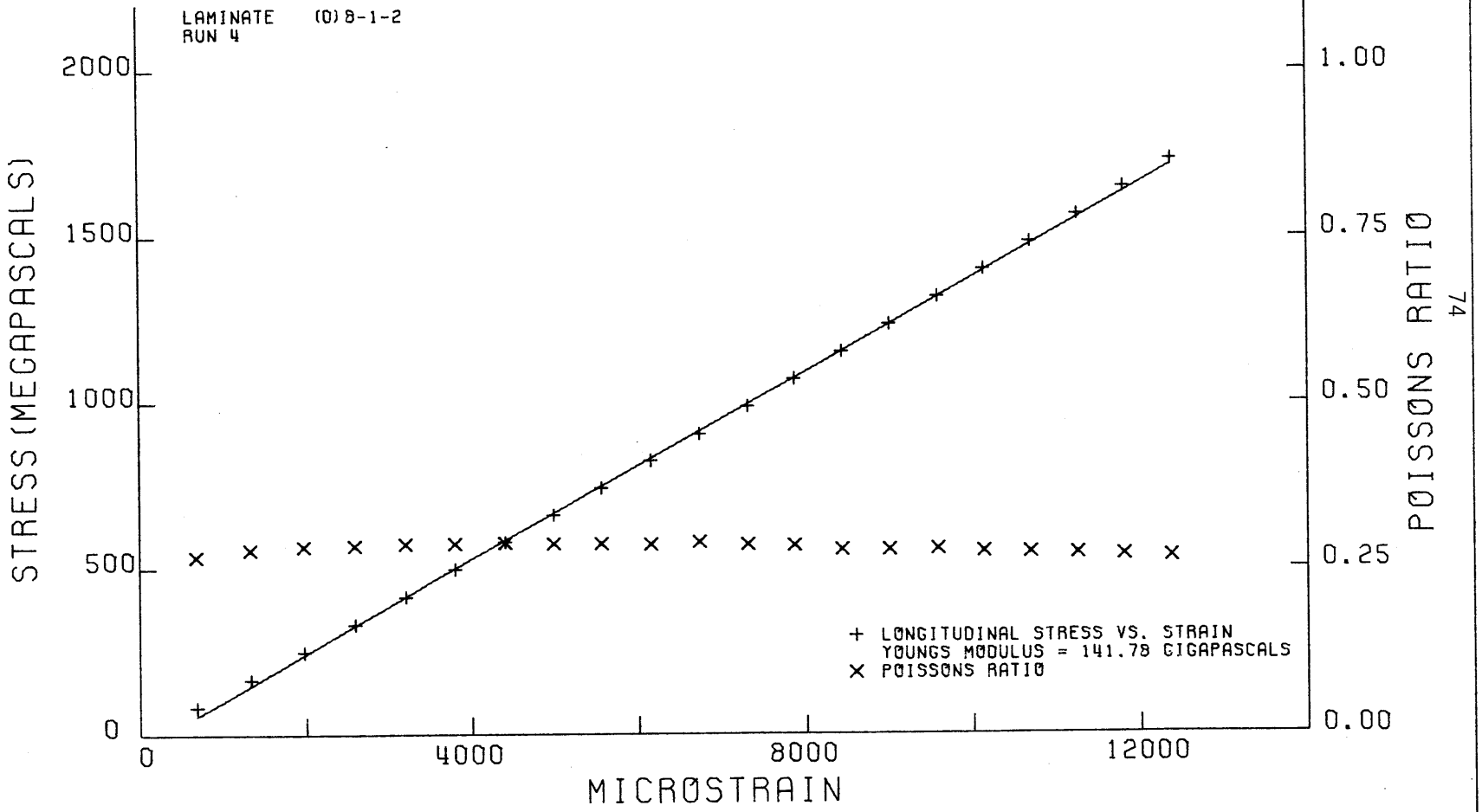
STRESS AND POISSONS RATIO VS. STRAIN
FROM TENSILE COUPON TEST
LAMINATE (0)8-1-2
RUN 4
STRESS (MEGAPASCALS)
2000
1500
1000
500
0
0
4000
8000
12000
MICROSTRAIN
1.00
0.75
0.50
0.25
0.00
POISSONS RATIO
+ LONGITUDINAL STRESS VS. STRAIN
YOUNGS MODULUS = 141.78 GIGAPASCALS
× POISSONS RATIO

FIG. 30

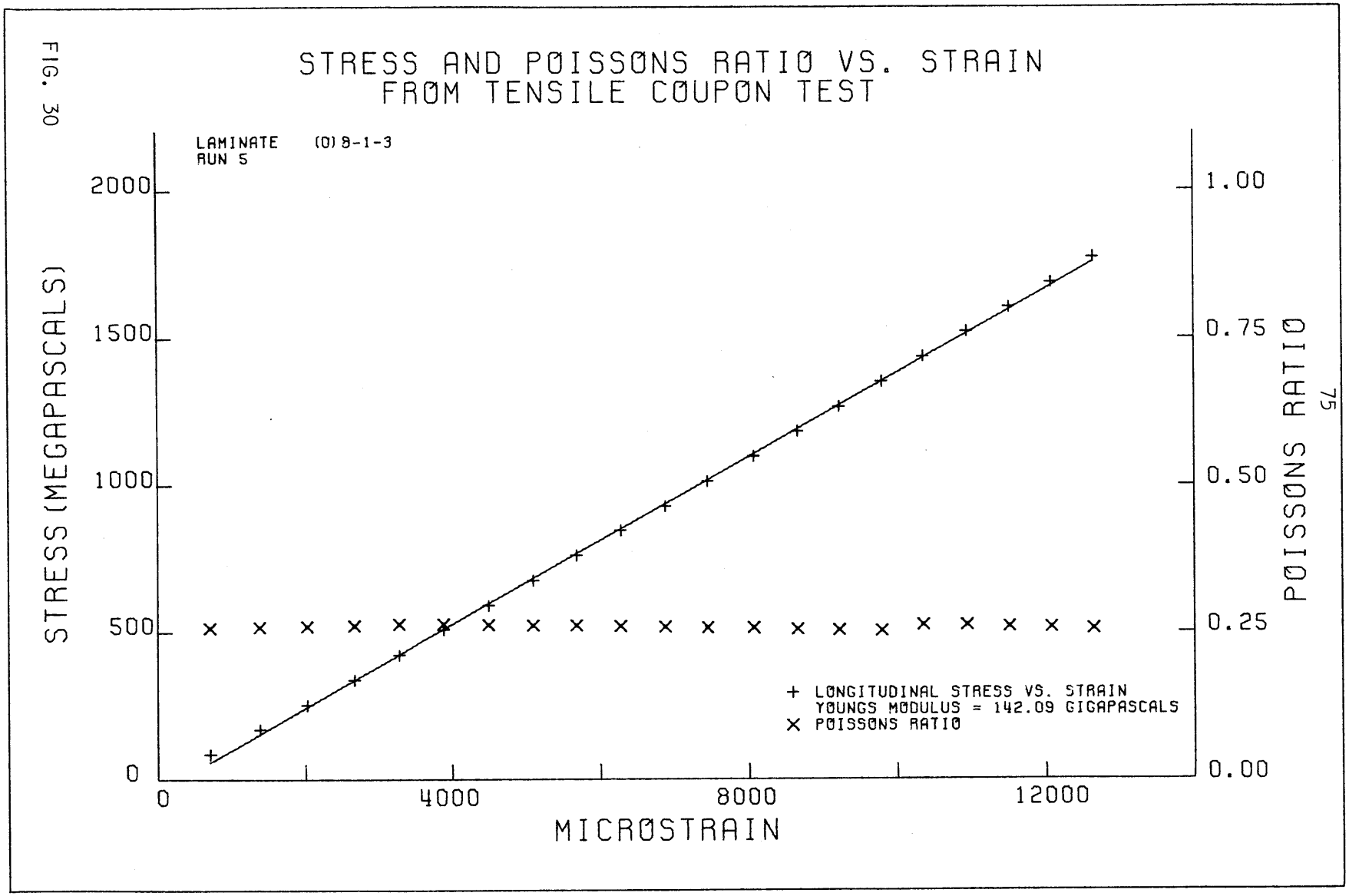
STRESS AND POISSONS RATIO VS. STRAIN
FROM TENSILE COUPON TEST
LAMINATE (0)8-1-3
RUN 5
STRESS (MEGAPASCALS)
2000
1500
1000
500
0
0
4000
8000
12000
MICROSTRAIN
1.00
0.75
0.50
0.25
0.00
POISSONS RATIO
+ LONGITUDINAL STRESS VS. STRAIN
YOUNGS MODULUS = 142.09 GIGAPASCALS
× POISSONS RATIO

FIG. 31

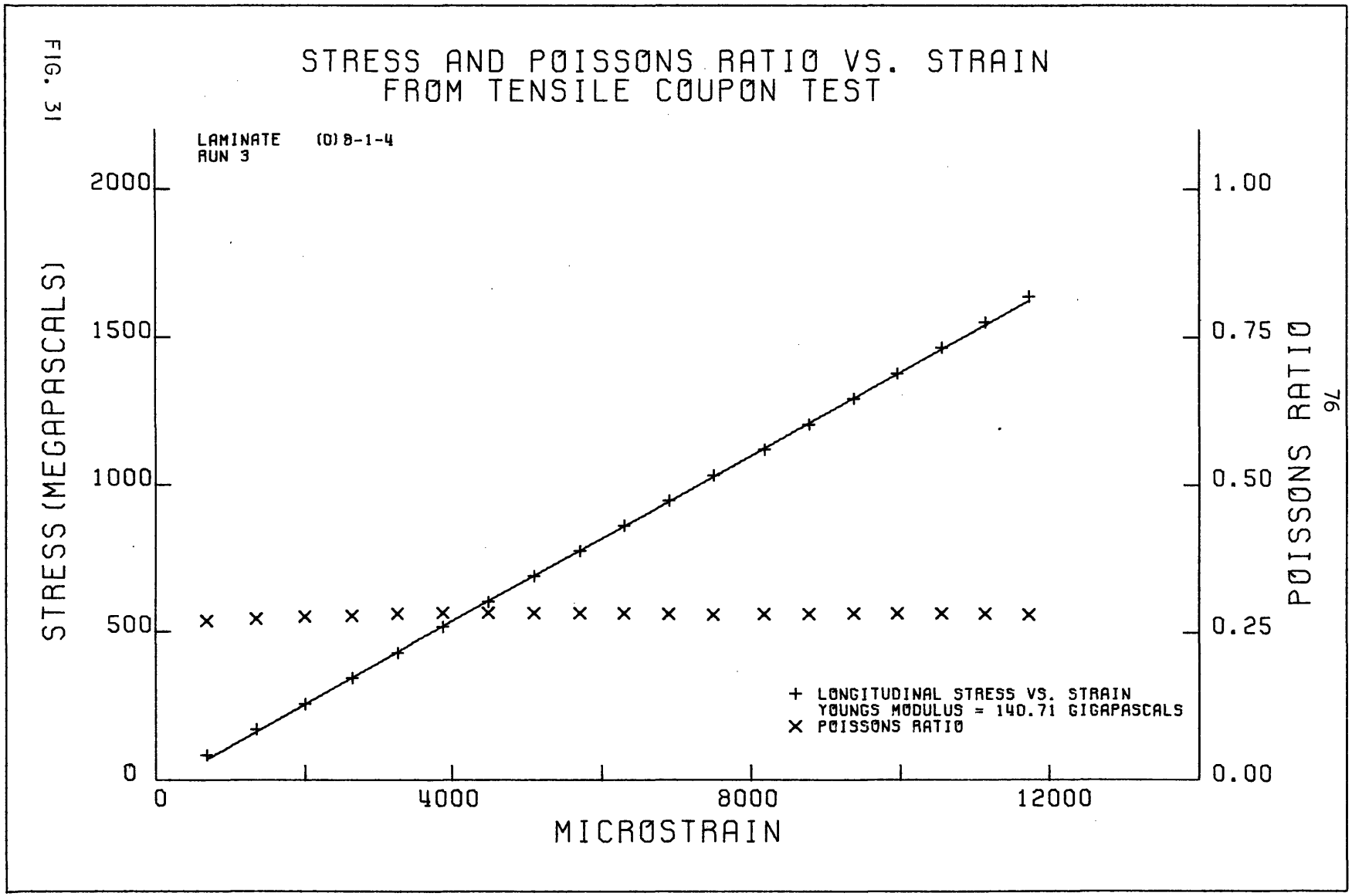
STRESS AND POISSONS RATIO VS. STRAIN
FROM TENSILE COUPON TEST
LAMINATE (0)8-1-4
RUN 3
STRESS (MEGAPASCALS)
2000
1500
1000
500
0
0
4000
8000
12000
MICROSTRAIN
1.00
0.75
0.50
0.25
0.00
POISSONS RATIO
+ LONGITUDINAL STRESS VS. STRAIN
YOUNGS MODULUS = 140.71 GIGAPASCALS
× POISSONS RATIO

FIG. 22

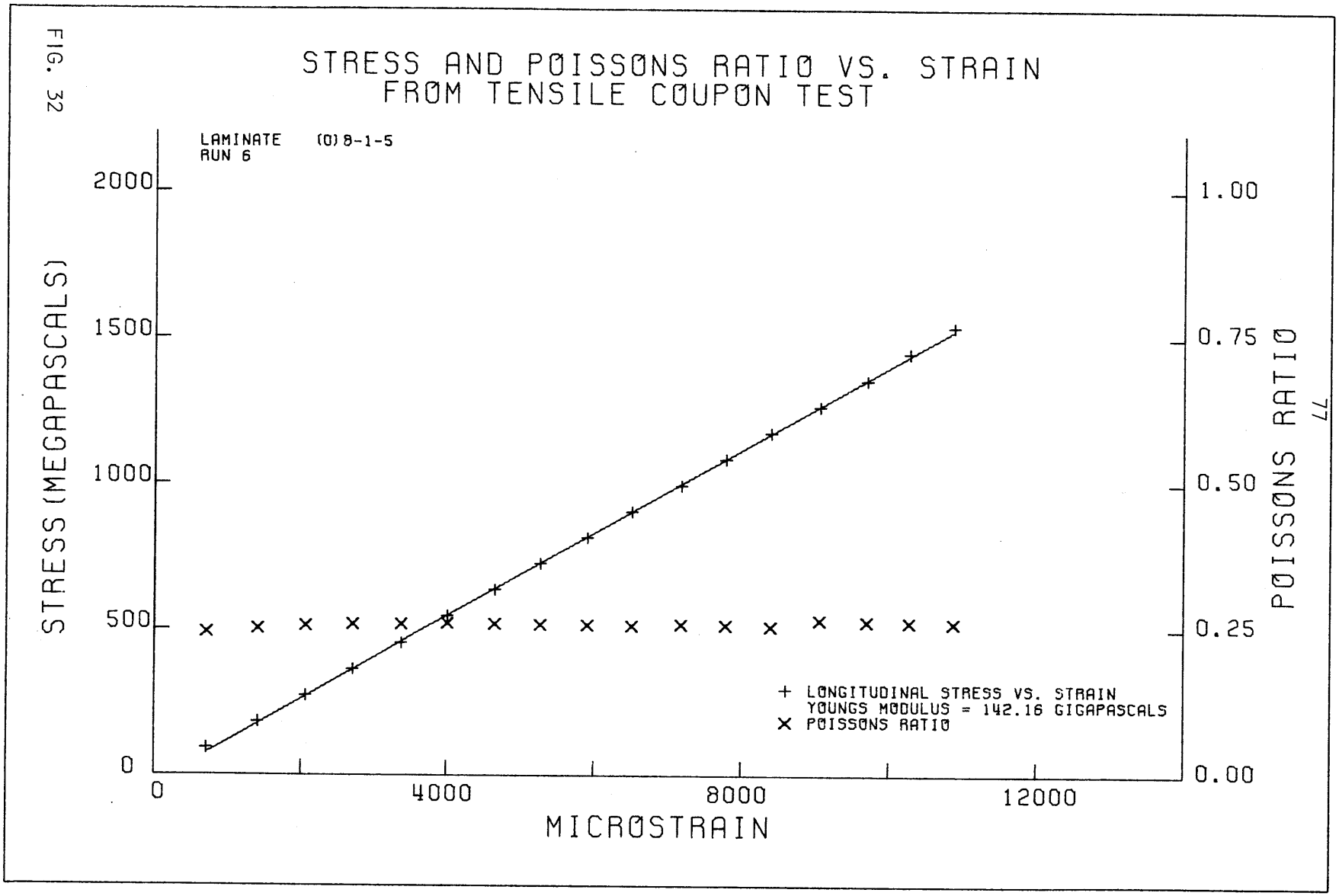
STRESS AND POISSONS RATIO VS. STRAIN
FROM TENSILE COUPON TEST
LAMINATE (0)8-1-5
RUN 6
STRESS (MEGAPASCALS)
2000
1500
1000
500
0
0
4000
8000
12000
MICROSTRAIN
1.00
0.75
0.50
0.25
0.00
POISSONS RATIO
+ LONGITUDINAL STRESS VS. STRAIN
YOUNGS MODULUS = 142.16 GIGAPASCALS
× POISSONS RATIO

FIG. 33

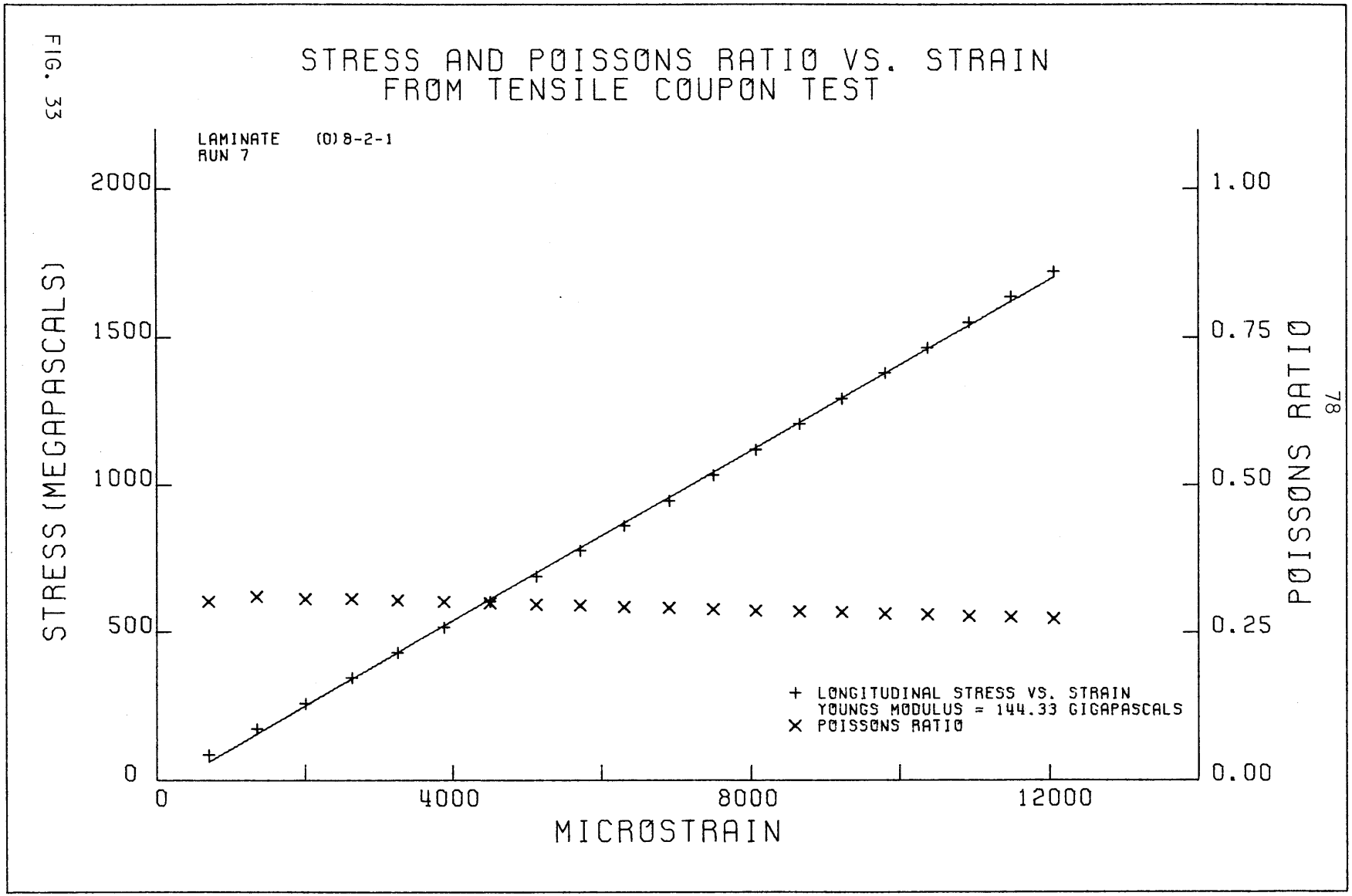
STRESS AND POISSONS RATIO VS. STRAIN
FROM TENSILE COUPON TEST
LAMINATE (0)8-2-1
RUN 7
STRESS (MEGAPASCALS)
2000
1500
1000
500
0
0
4000
8000
12000
MICROSTRAIN
1.00
0.75
0.50
0.25
0.00
POISSONS RATIO
+ LONGITUDINAL STRESS VS. STRAIN
YOUNGS MODULUS = 144.33 GIGAPASCALS
× POISSONS RATIO

FIG. 34

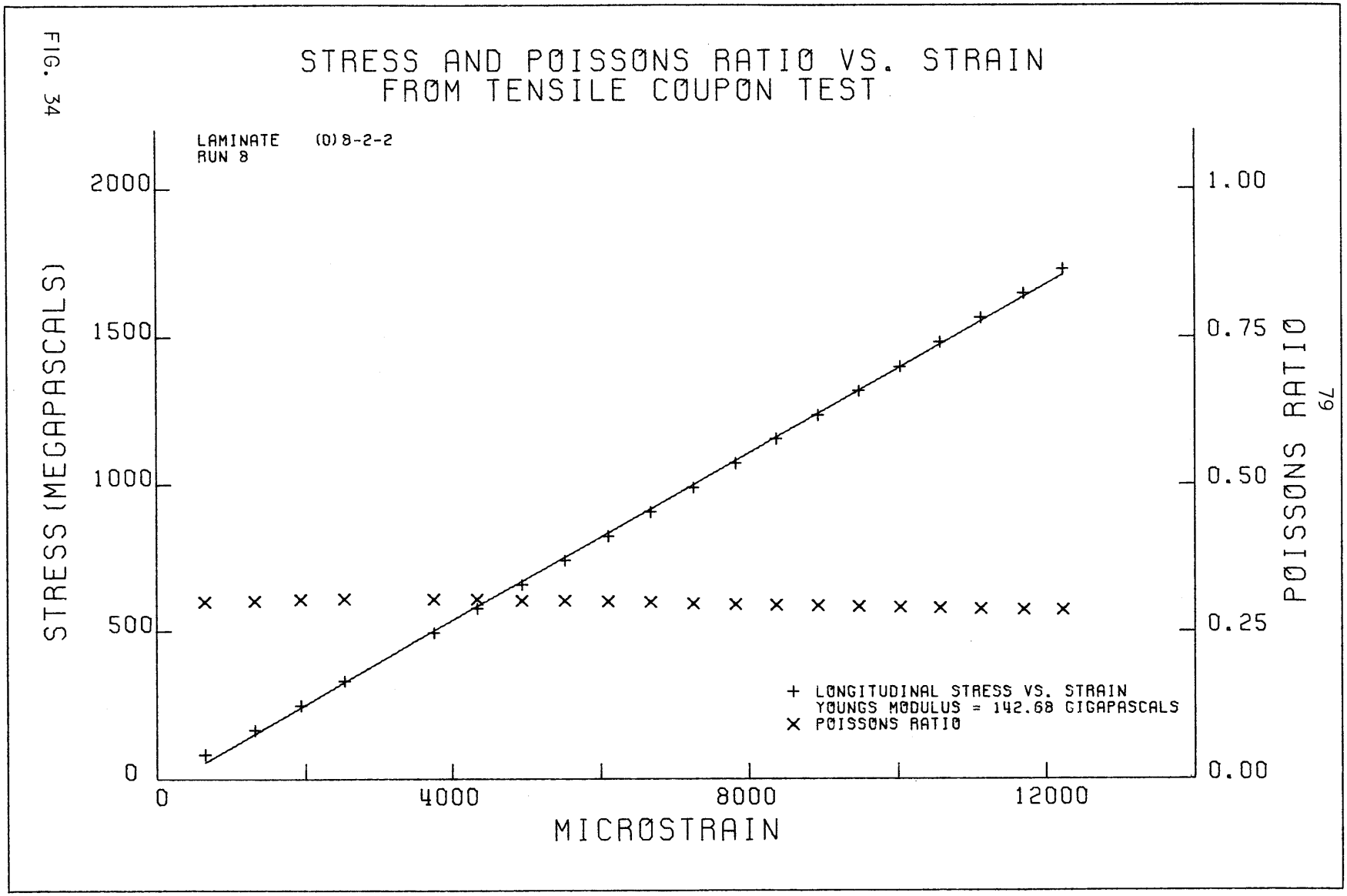
STRESS AND POISSONS RATIO VS. STRAIN
FROM TENSILE COUPON TEST
LAMINATE (0)8-2-2
RUN 8
STRESS (MEGAPASCALS)
2000
1500
1000
500
0
0
4000
8000
12000
MICROSTRAIN
1.00
0.75
0.50
0.25
0.00
POISSONS RATIO
+ LONGITUDINAL STRESS VS. STRAIN
YOUNGS MODULUS = 142.68 GIGAPASCALS
× POISSONS RATIO

FIG. 35

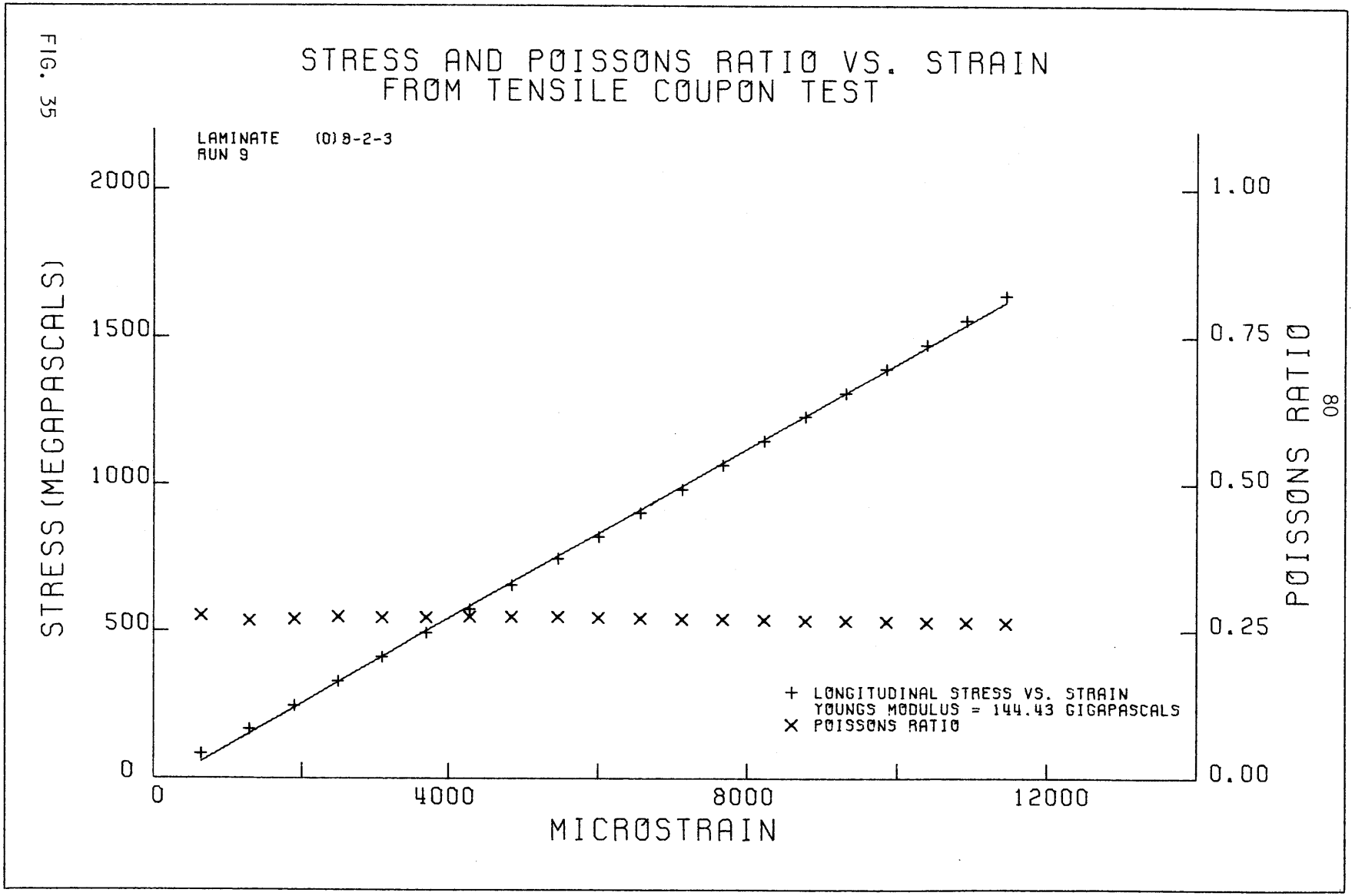
STRESS AND POISSONS RATIO VS. STRAIN
FROM TENSILE COUPON TEST
LAMINATE (0)8-2-3
RUN 9
STRESS (MEGAPASCALS)
2000
1500
1000
500
0
0
4000
8000
12000
MICROSTRAIN
1.00
0.75
0.50
0.25
0.00
POISSONS RATIO
+ LONGITUDINAL STRESS VS. STRAIN
YOUNGS MODULUS = 144.43 GIGAPASCALS
× POISSONS RATIO

FIG. 36

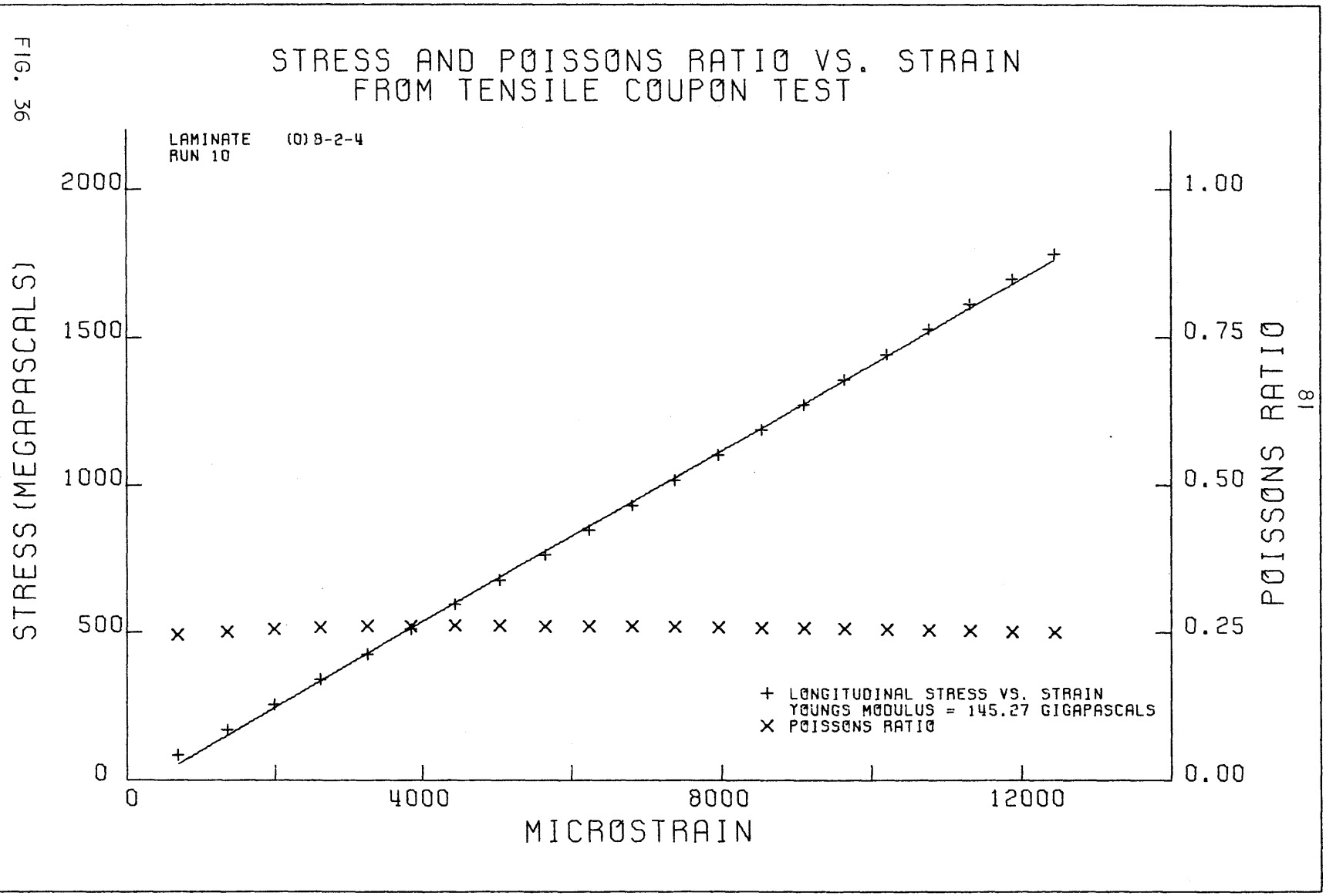
STRESS AND POISSONS RATIO VS. STRAIN
FROM TENSILE COUPON TEST
LAMINATE (0)8-2-4
RUN 10
STRESS (MEGAPASCALS)
2000
1500
1000
500
0
0
4000
8000
12000
MICROSTRAIN
1.00
0.75
0.50
0.25
0.00
POISSONS RATIO
+ LONGITUDINAL STRESS VS. STRAIN
YOUNGS MODULUS = 145.27 GIGAPASCALS
× POISSONS RATIO

FIG. 37

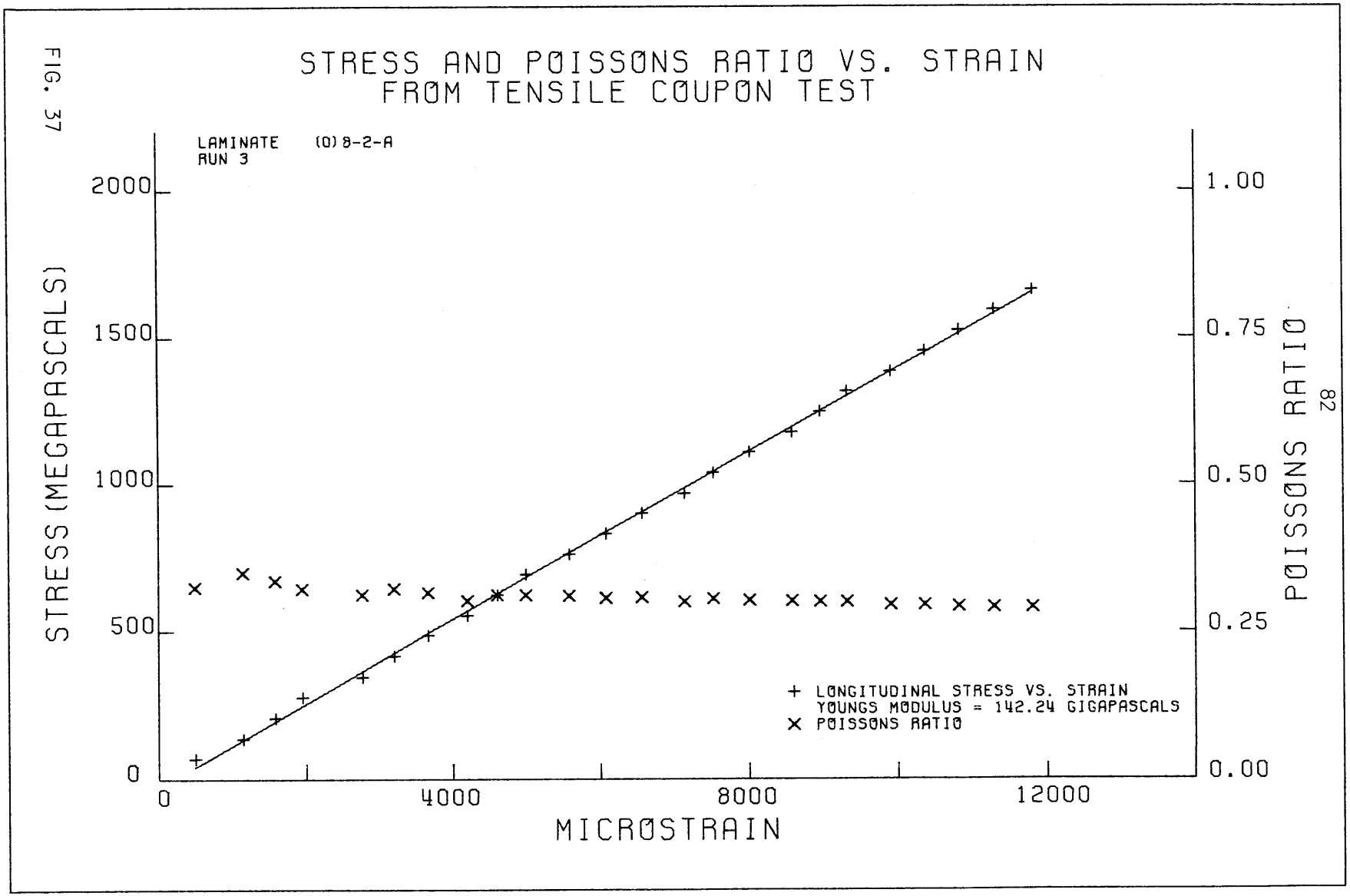
STRESS AND POISSONS RATIO VS. STRAIN
FROM TENSILE COUPON TEST
LAMINATE (0)8-2-A
RUN 3
STRESS (MEGAPASCALS)
2000
1500
1000
500
0
0
4000
8000
12000
MICROSTRAIN
1.00
0.75
0.50
0.25
0.00
POISSONS RATIO
+ LONGITUDINAL STRESS VS. STRAIN
YOUNGS MODULUS = 142.24 GIGAPASCALS
× POISSONS RATIO

FIG. 38

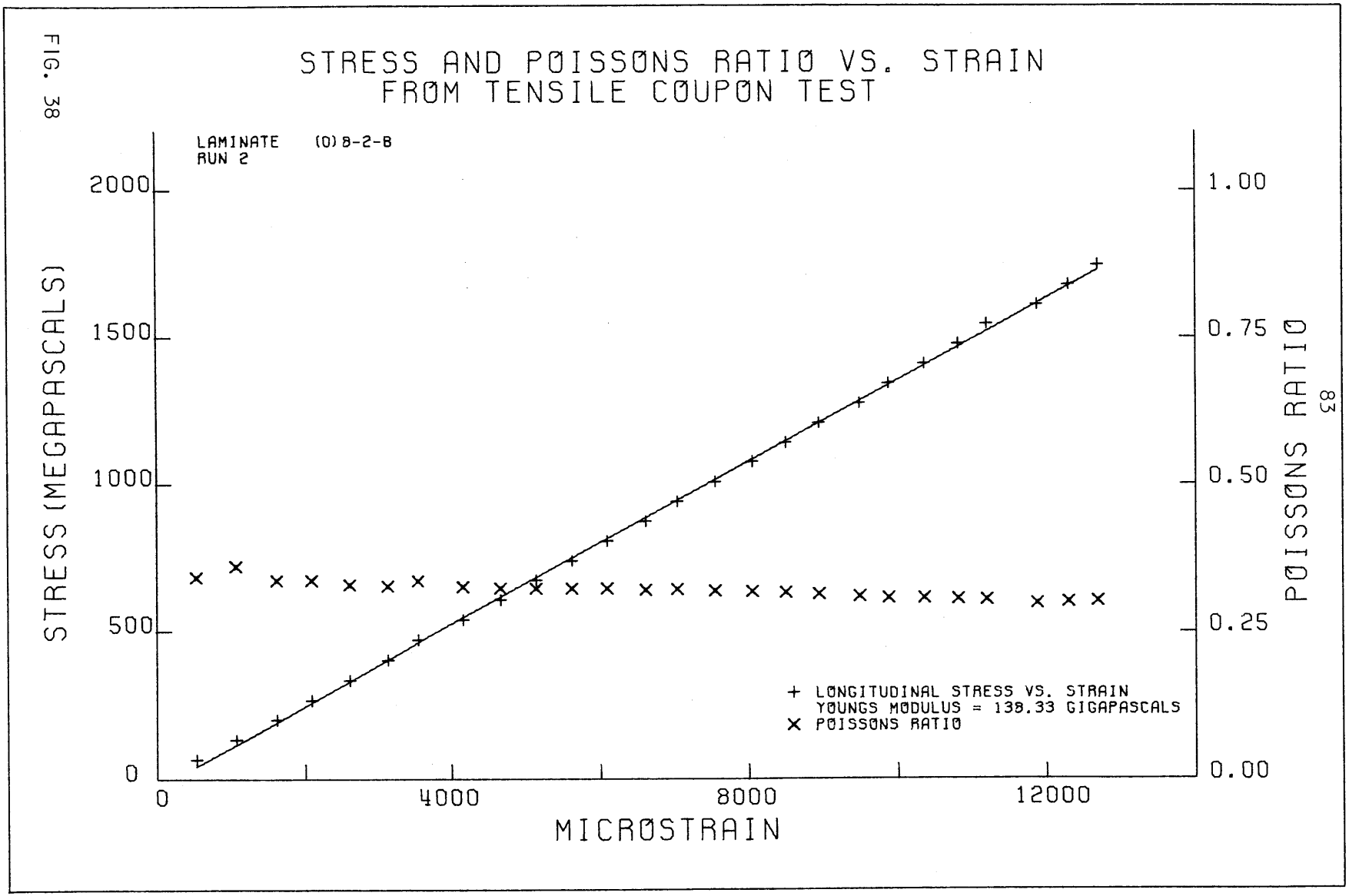
STRESS AND POISSONS RATIO VS. STRAIN
FROM TENSILE COUPON TEST
LAMINATE (0)8-2-B
RUN 2
STRESS (MEGAPASCALS)
2000
1500
1000
500
0
0
4000
8000
12000
MICROSTRAIN
1.00
0.75
0.50
0.25
0.00
POISSONS RATIO
+ LONGITUDINAL STRESS VS. STRAIN
YOUNGS MODULUS = 138.33 GIGAPASCALS
× POISSONS RATIO

FIG. 39

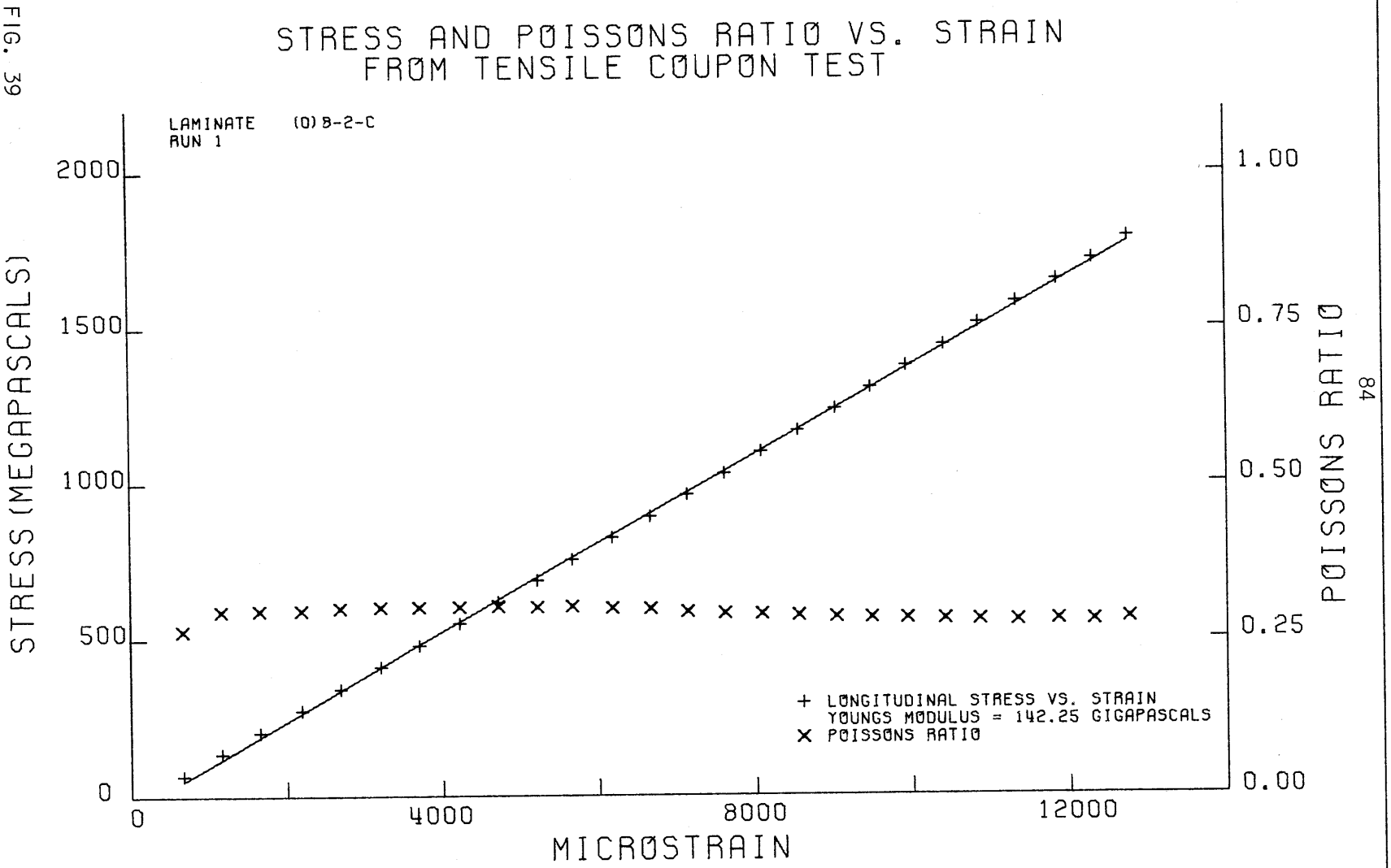
STRESS AND POISSONS RATIO VS. STRAIN
FROM TENSILE COUPON TEST
LAMINATE (0)8-2-C
RUN 1
STRESS (MEGAPASCALS)
2000
1500
1000
500
0
0
4000
8000
12000
MICROSTRAIN
1.00
0.75
0.50
0.25
0.00
POISSONS RATIO
+ LONGITUDINAL STRESS VS. STRAIN
YOUNGS MODULUS = 142.25 GIGAPASCALS
× POISSONS RATIO

FIG. 40

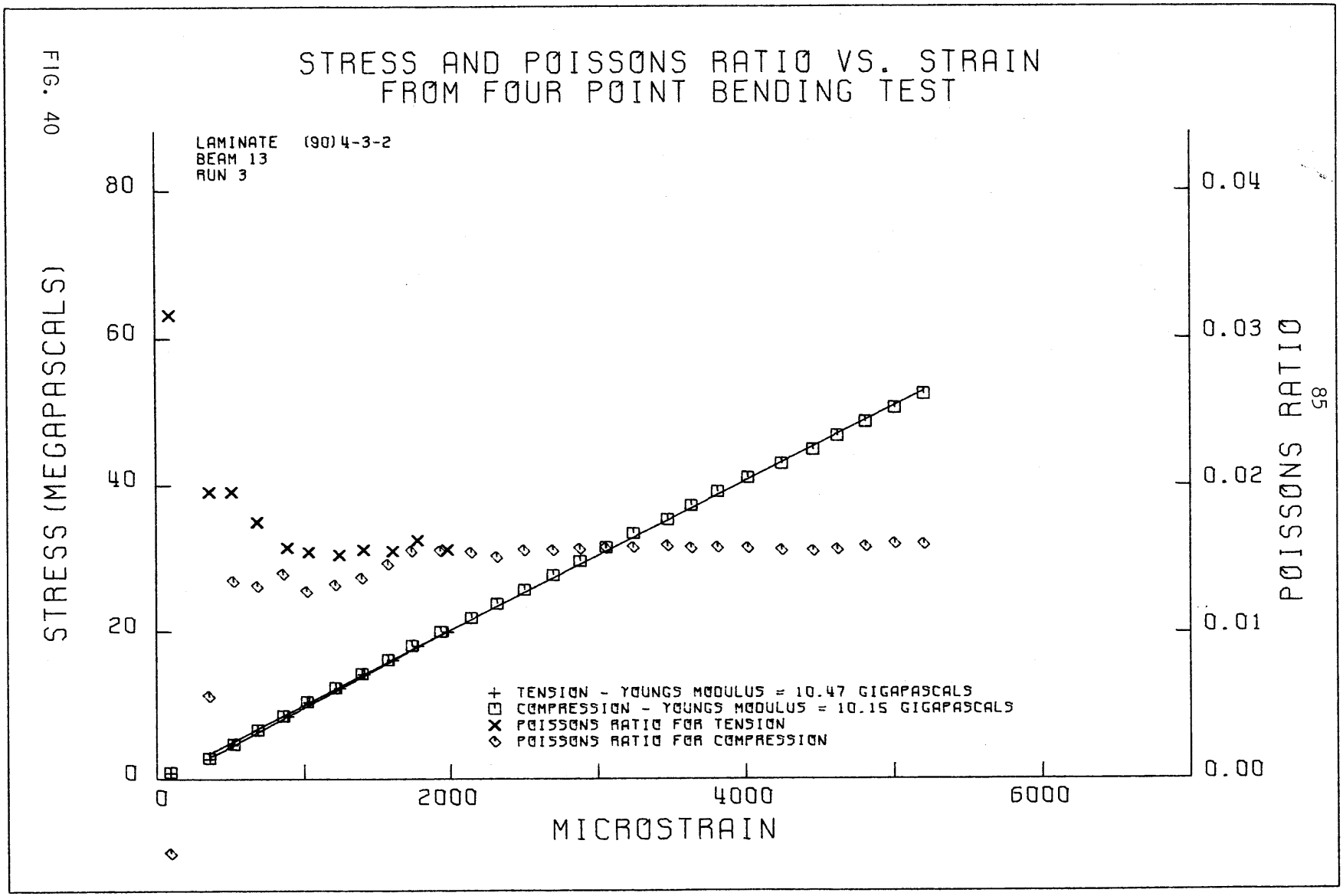
STRESS AND POISSONS RATIO VS. STRAIN
FROM FOUR POINT BENDING TEST
LAMINATE (90)4-3-2
BEAM 13
RUN 3
STRESS (MEGAPASCALS)
80
60
40
20
0
0
2000
4000
6000
MICROSTRAIN
0.04
0.03
0.02
0.01
0.00
POISSONS RATIO
+ TENSION - YOUNGS MODULUS = 10.47 GIGAPASCALS
□ COMPRESSION - YOUNGS MODULUS = 10.15 GIGAPASCALS
× POISSONS RATIO FOR TENSION
◇ POISSONS RATIO FOR COMPRESSION

FIG. 41

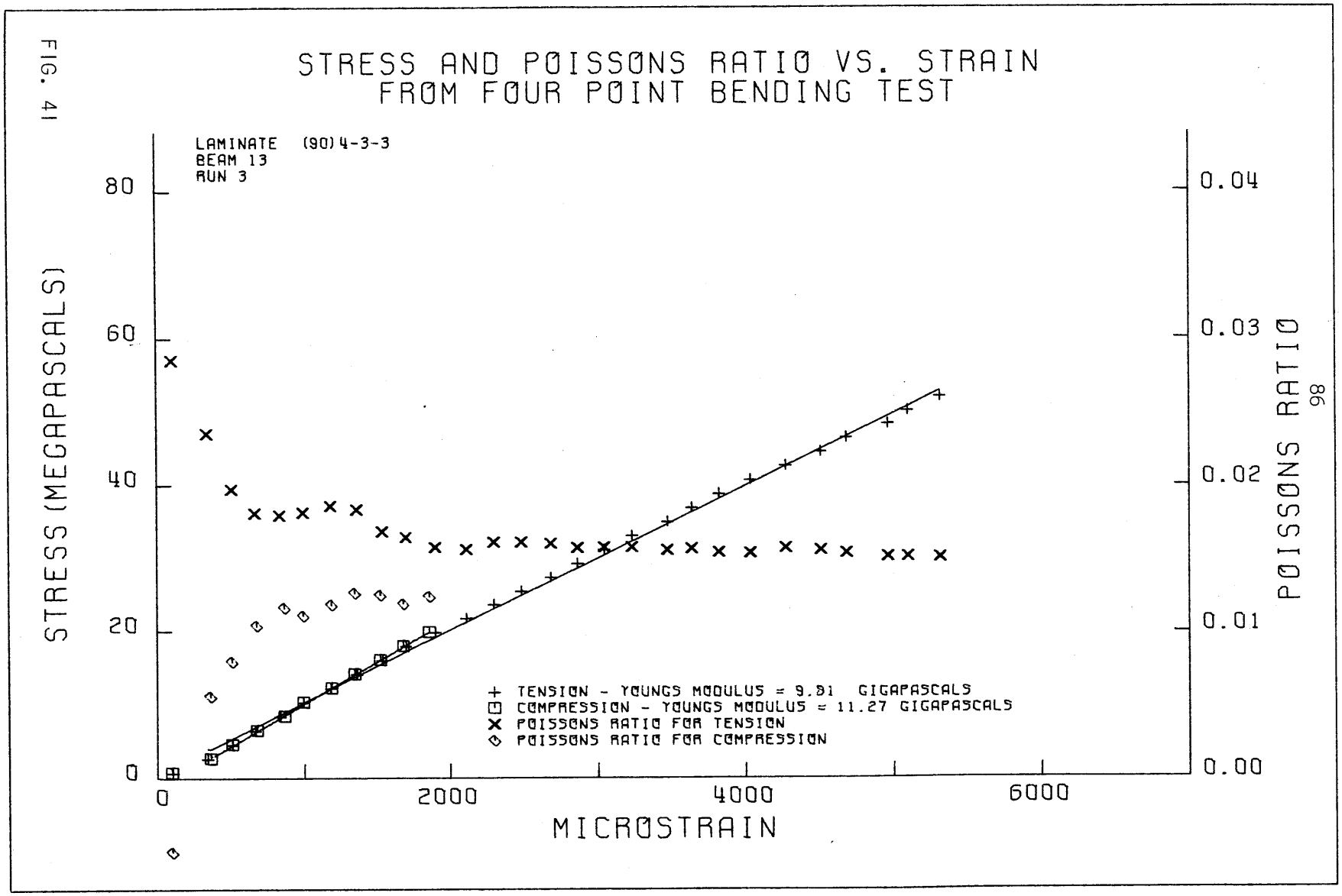
STRESS AND POISSONS RATIO VS. STRAIN
FROM FOUR POINT BENDING TEST
LAMINATE (90)4-3-3
BEAM 13
RUN 3
STRESS (MEGAPASCALS)
80
60
40
20
0
0
2000
4000
6000
MICROSTRAIN
0.04
0.03
0.02
0.01
0.00
POISSONS RATIO
+ TENSION - YOUNGS MODULUS = 9.81 GIGAPASCALS
□ COMPRESSION - YOUNGS MODULUS = 11.27 GIGAPASCALS
× POISSONS RATIO FOR TENSION
◇ POISSONS RATIO FOR COMPRESSION

FIG. 42

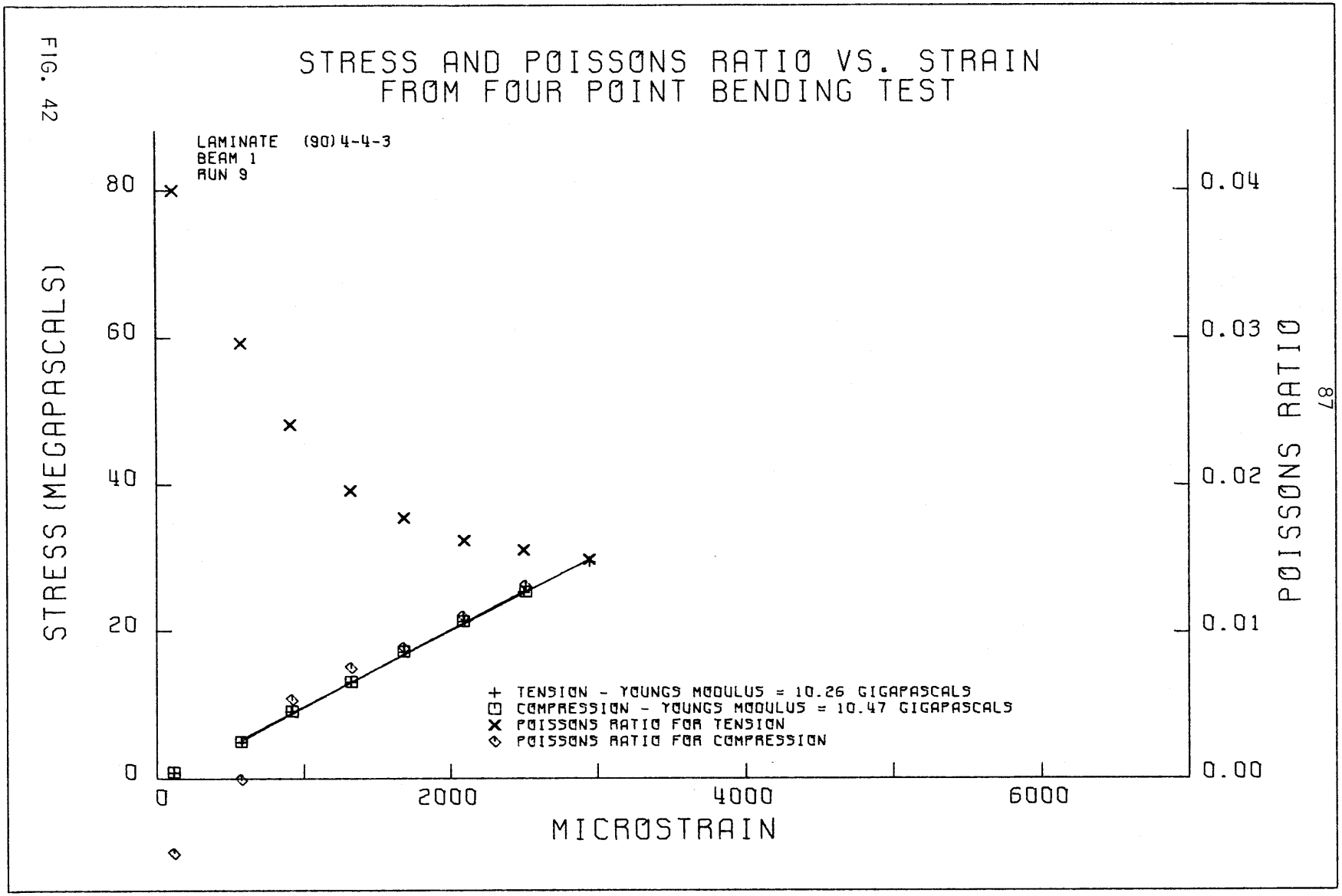
STRESS AND POISSONS RATIO VS. STRAIN
FROM FOUR POINT BENDING TEST
LAMINATE (90)4-4-3
BEAM 1
RUN 9
STRESS (MEGAPASCALS)
80
60
40
20
0
0
2000
4000
6000
MICROSTRAIN
0.04
0.03
0.02
0.01
0.00
POISSONS RATIO
+ TENSION - YOUNGS MODULUS = 10.26 GIGAPASCALS
□ COMPRESSION - YOUNGS MODULUS = 10.47 GIGAPASCALS
× POISSONS RATIO FOR TENSION
◇ POISSONS RATIO FOR COMPRESSION

FIG. 43

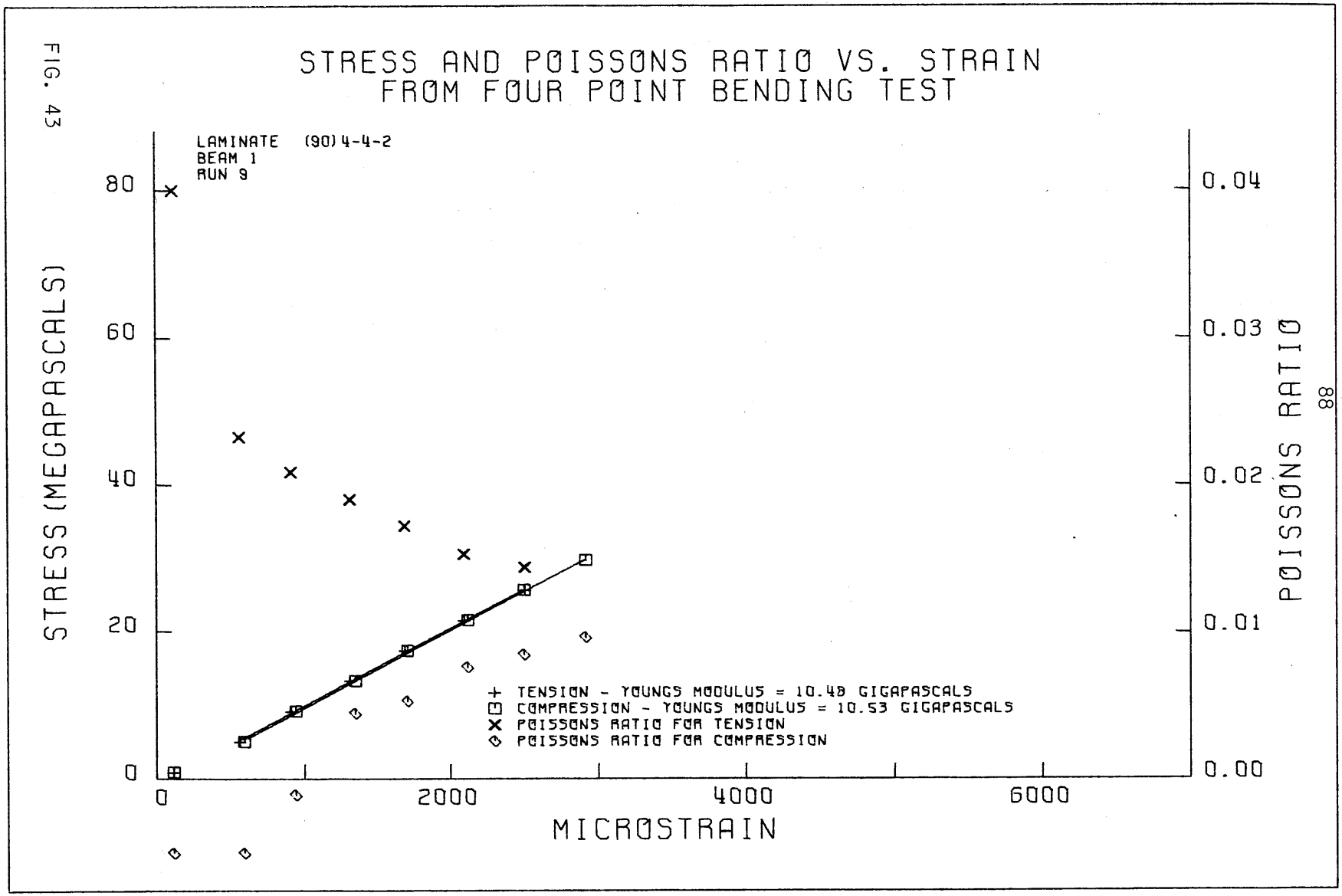
STRESS AND POISSONS RATIO VS. STRAIN
FROM FOUR POINT BENDING TEST
LAMINATE (90)4-4-2
BEAM 1
RUN 9
STRESS (MEGAPASCALS)
80
60
40
20
0
0
2000
4000
6000
MICROSTRAIN
0.04
0.03
0.02
0.01
0.00
POISSONS RATIO
+ TENSION - YOUNGS MODULUS = 10.48 GIGAPASCALS
□ COMPRESSION - YOUNGS MODULUS = 10.53 GIGAPASCALS
× POISSONS RATIO FOR TENSION
◇ POISSONS RATIO FOR COMPRESSION

FIG. 44

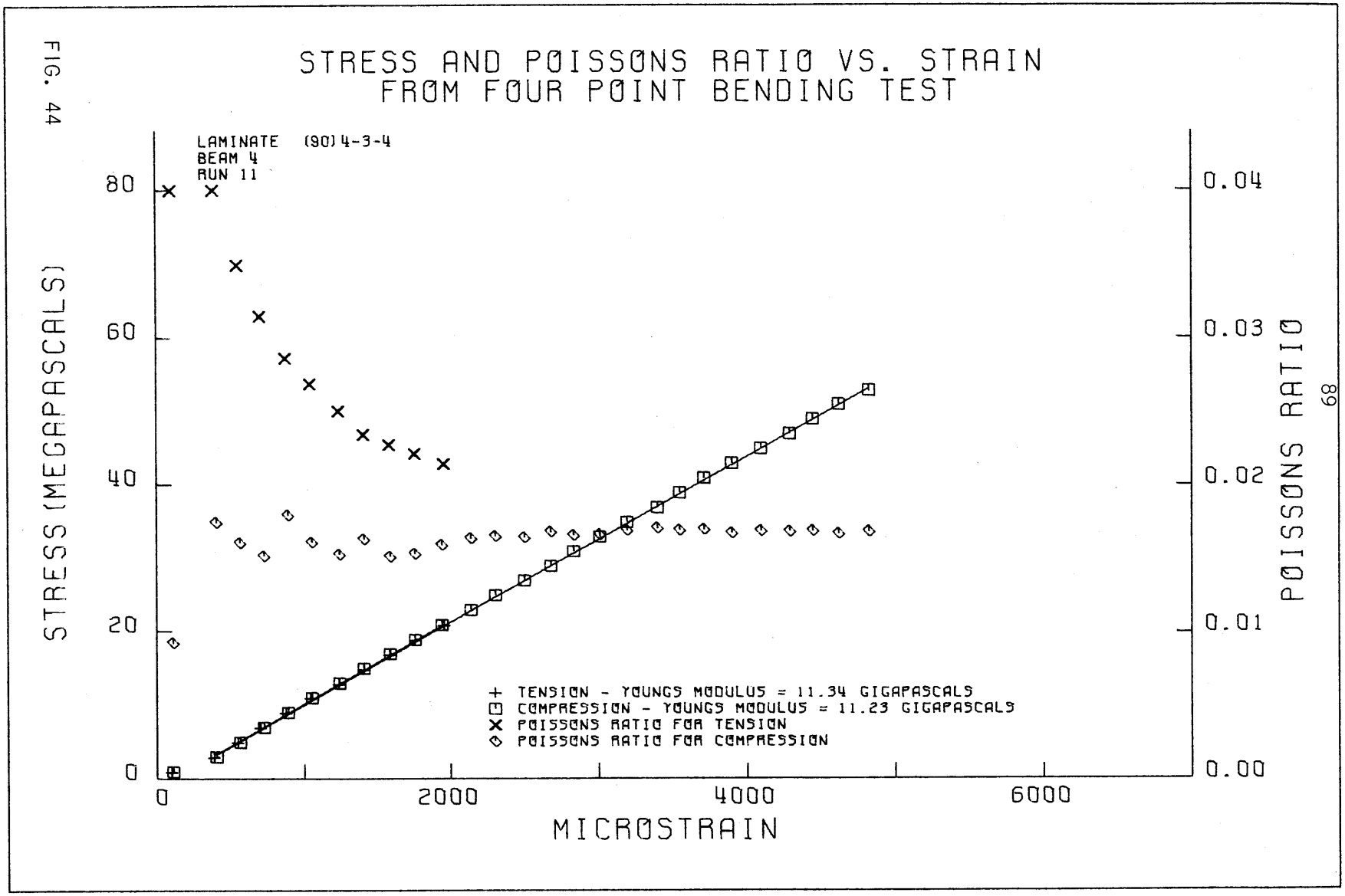
STRESS AND POISSONS RATIO VS. STRAIN
FROM FOUR POINT BENDING TEST
LAMINATE (90)4-3-4
BEAM 4
RUN 11
STRESS (MEGAPASCALS)
80
60
40
20
0
0
2000
4000
6000
MICROSTRAIN
0.04
0.03
0.02
0.01
0.00
POISSONS RATIO
+ TENSION - YOUNGS MODULUS = 11.34 GIGAPASCALS
□ COMPRESSION - YOUNGS MODULUS = 11.23 GIGAPASCALS
× POISSONS RATIO FOR TENSION
◇ POISSONS RATIO FOR COMPRESSION

FIG. 45

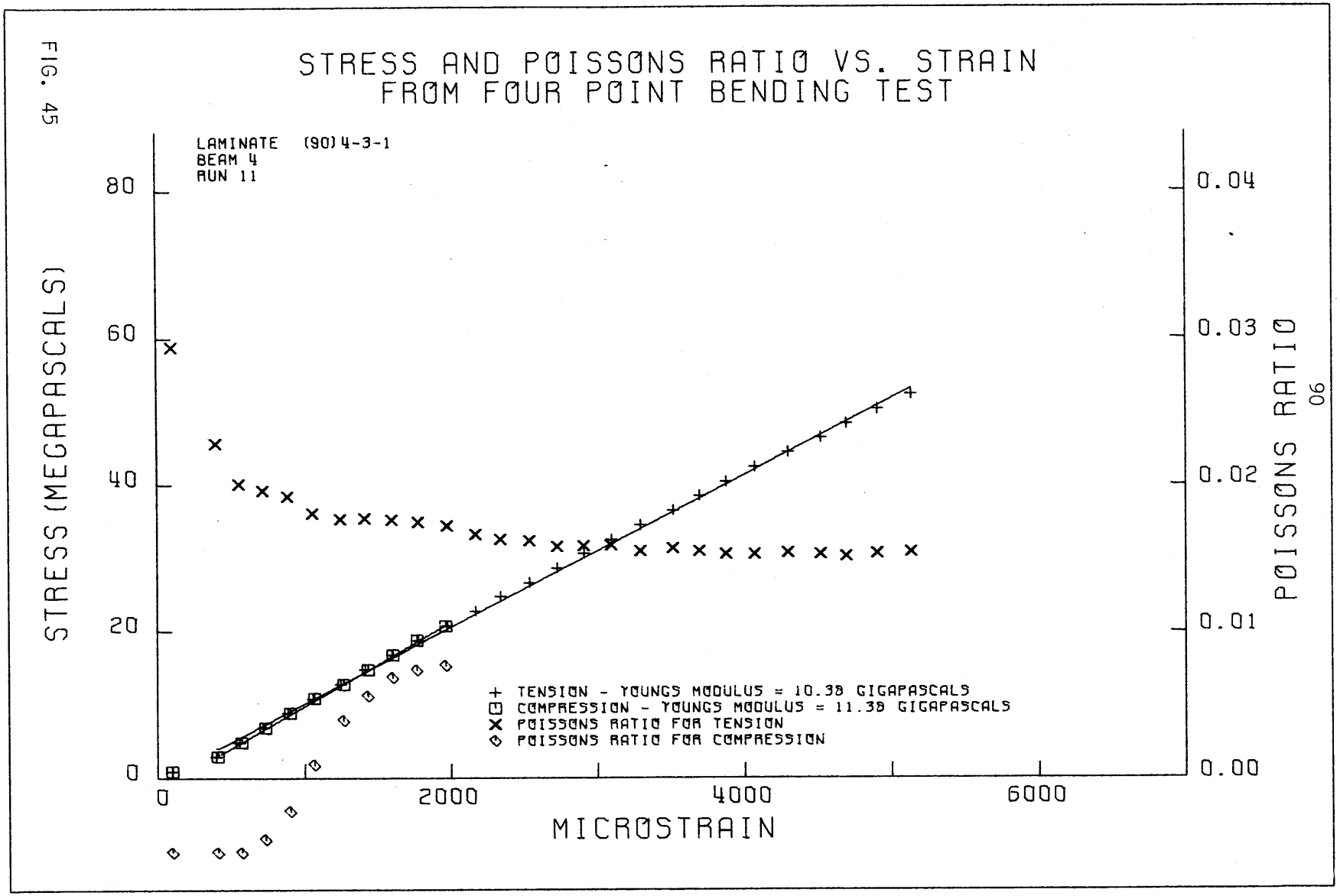
STRESS AND POISSONS RATIO VS. STRAIN
FROM FOUR POINT BENDING TEST
LAMINATE (90)4-3-1
BEAM 4
RUN 11
STRESS (MEGAPASCALS)
80
60
40
20
0
0
2000
4000
6000
MICROSTRAIN
0.04
0.03
0.02
0.01
0.00
POISSONS RATIO
90
+ TENSION - YOUNGS MODULUS = 10.38 GIGAPASCALS
⊡ COMPRESSION - YOUNGS MODULUS = 11.38 GIGAPASCALS
× POISSONS RATIO FOR TENSION
◇ POISSONS RATIO FOR COMPRESSION

FIG. 46

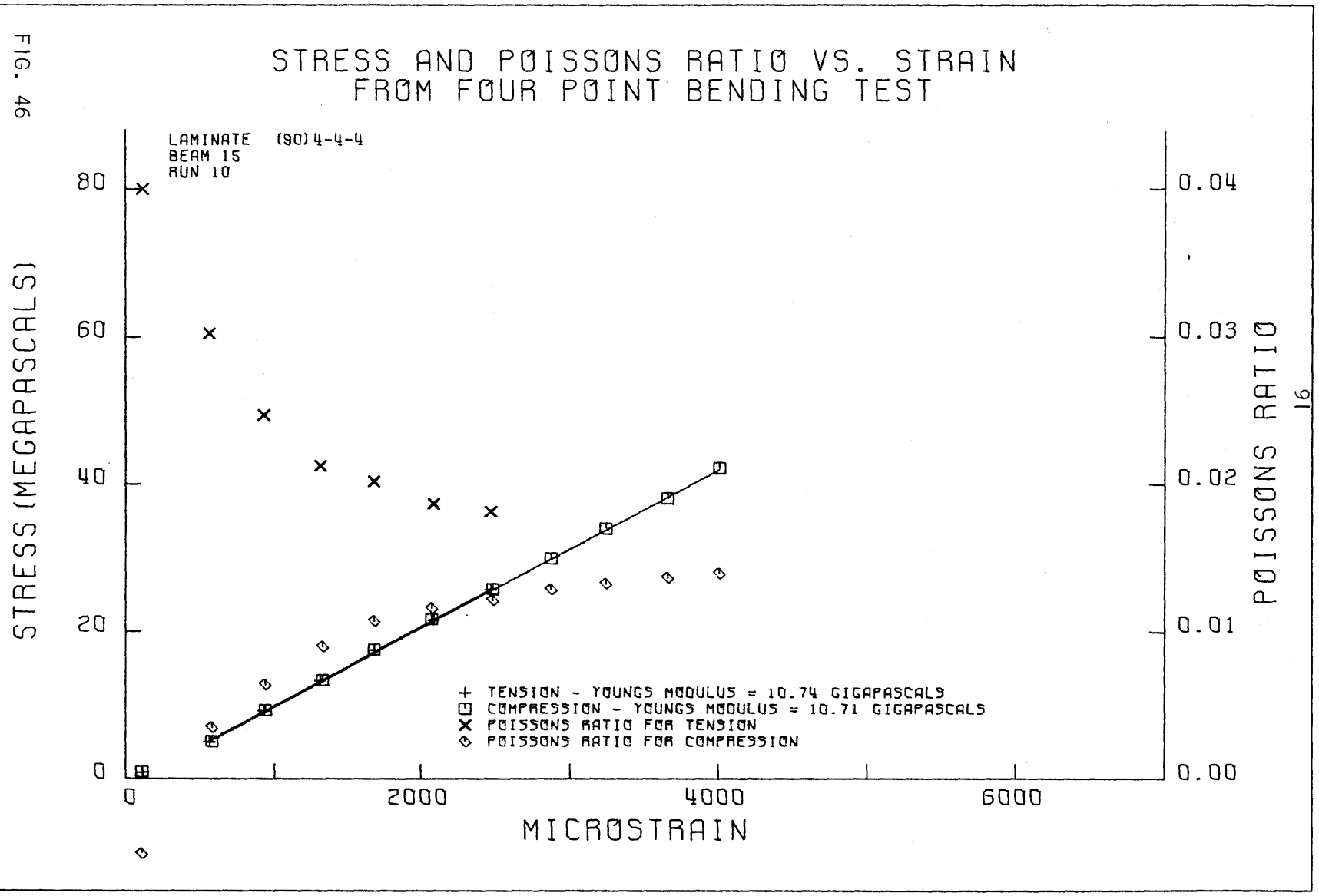
STRESS AND POISSONS RATIO VS. STRAIN
FROM FOUR POINT BENDING TEST
LAMINATE (90)4-4-4
BEAM 15
RUN 10
STRESS (MEGAPASCALS)
80
60
40
20
0
0
2000
4000
6000
MICROSTRAIN
0.04
0.03
0.02
0.01
0.00
POISSONS RATIO
+ TENSION - YOUNGS MODULUS = 10.74 GIGAPASCALS
□ COMPRESSION - YOUNGS MODULUS = 10.71 GIGAPASCALS
× POISSONS RATIO FOR TENSION
◇ POISSONS RATIO FOR COMPRESSION

FIG. 47

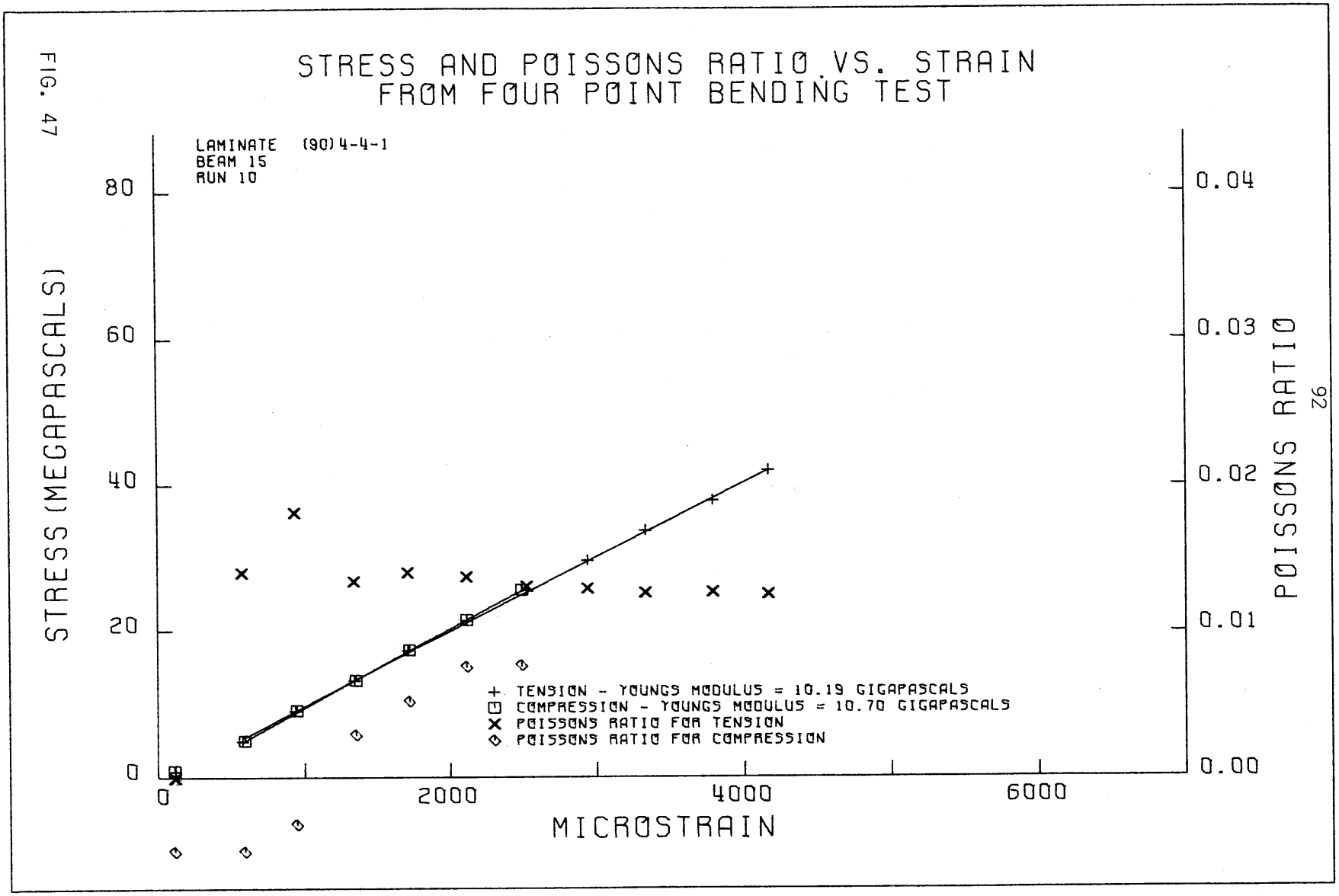
STRESS AND POISSONS RATIO VS. STRAIN
FROM FOUR POINT BENDING TEST
LAMINATE (90)4-4-1
BEAM 15
RUN 10
STRESS (MEGAPASCALS)
80
60
40
20
0
0
2000
4000
6000
MICROSTRAIN
0.04
0.03
0.02
0.01
0.00
POISSONS RATIO
+ TENSION - YOUNGS MODULUS = 10.19 GIGAPASCALS
□ COMPRESSION - YOUNGS MODULUS = 10.70 GIGAPASCALS
× POISSONS RATIO FOR TENSION
◇ POISSONS RATIO FOR COMPRESSION

FIG. 48

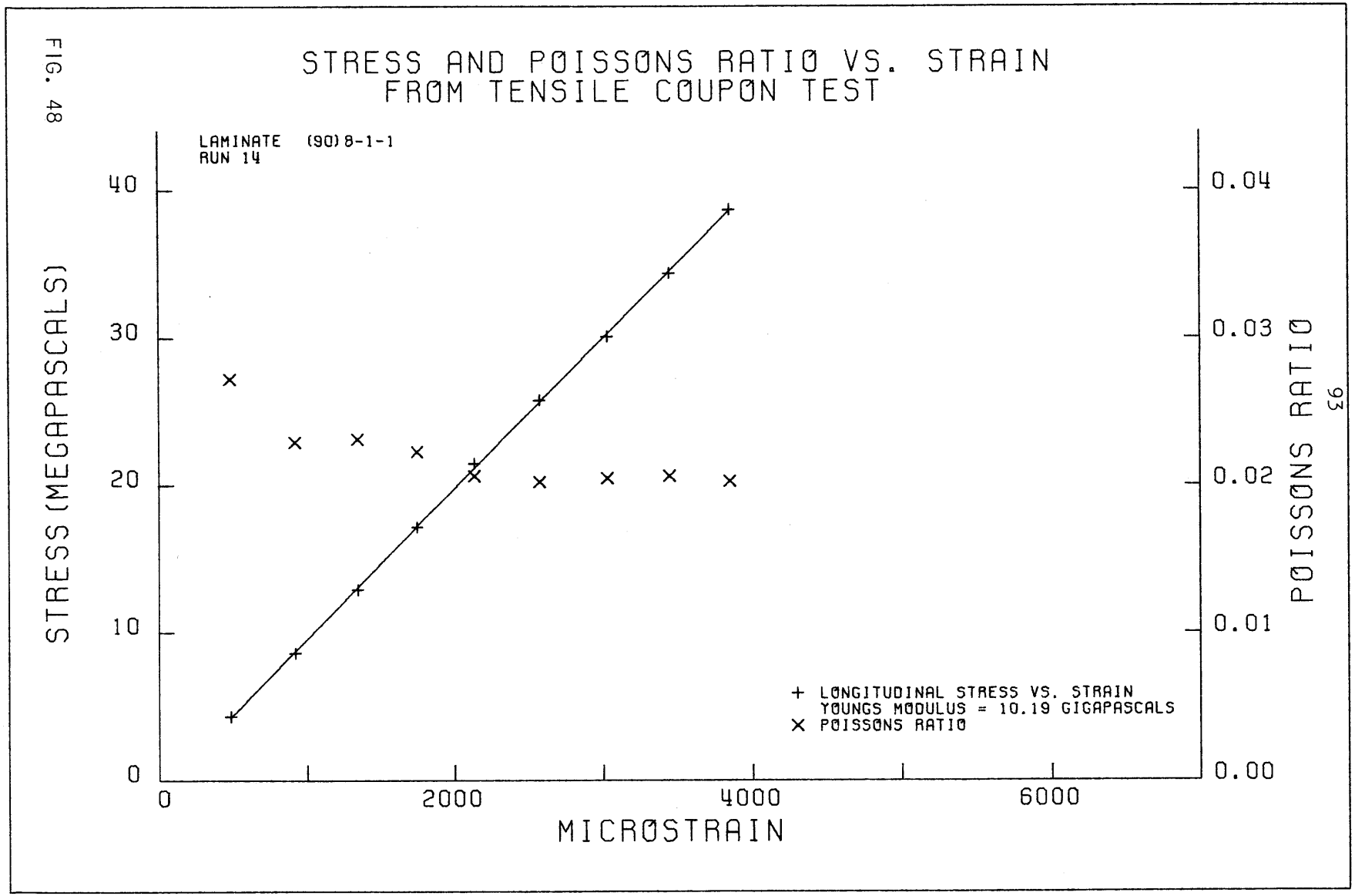
STRESS AND POISSONS RATIO VS. STRAIN
FROM TENSILE COUPON TEST
LAMINATE (90)8-1-1
RUN 14
STRESS (MEGAPASCALS)
40
30
20
10
0
0
2000
4000
6000
MICROSTRAIN
0.04
0.03
0.02
0.01
0.00
POISSONS RATIO
+ LONGITUDINAL STRESS VS. STRAIN
YOUNGS MODULUS = 10.19 GIGAPASCALS
× POISSONS RATIO

FIG. 49

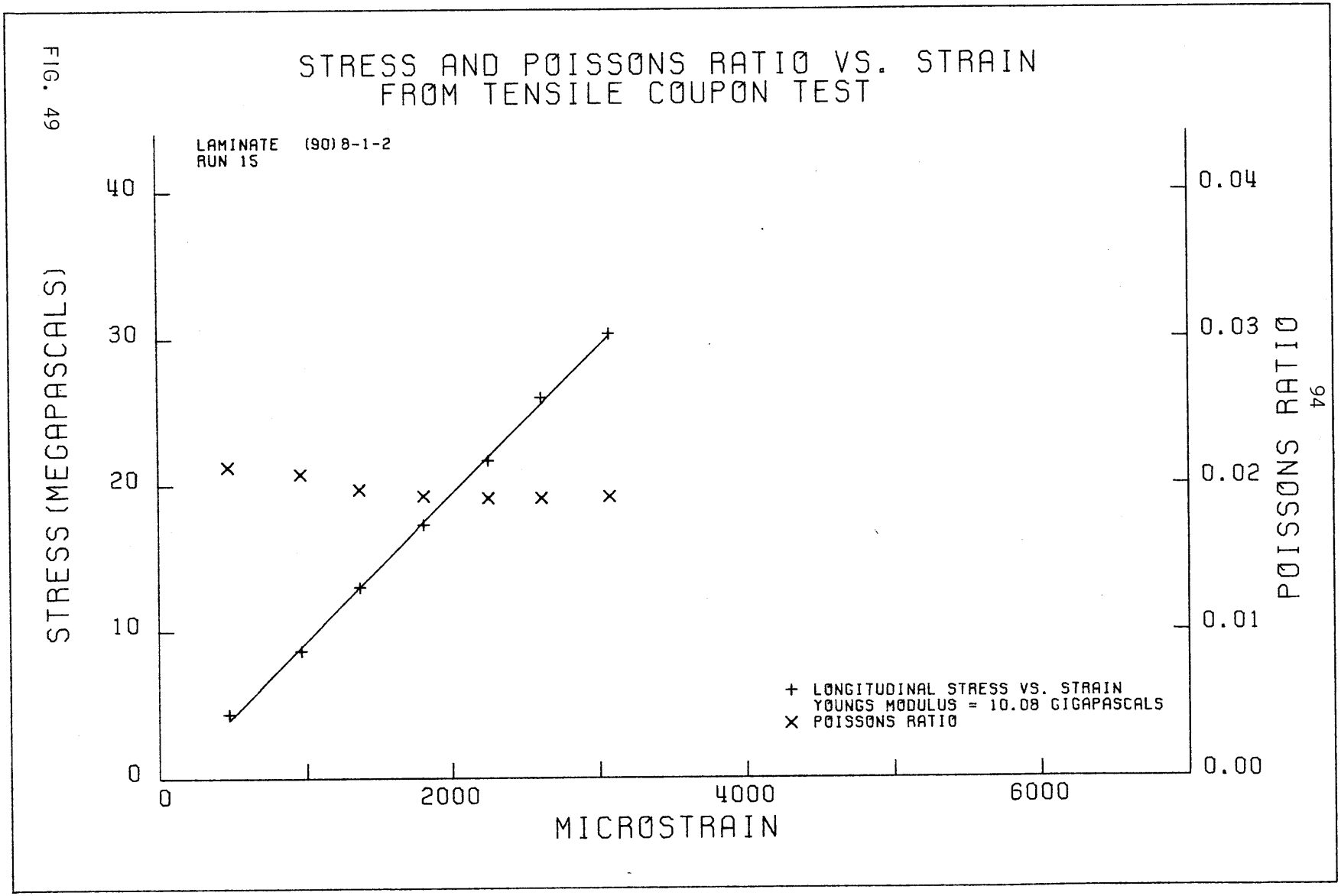
STRESS AND POISSONS RATIO VS. STRAIN
FROM TENSILE COUPON TEST
LAMINATE (90)8-1-2
RUN 1S
STRESS (MEGAPASCALS)
40
30
20
10
0
0
2000
4000
6000
MICROSTRAIN
0.04
0.03
0.02
0.01
0.00
POISSONS RATIO
+ LONGITUDINAL STRESS VS. STRAIN
YOUNGS MODULUS = 10.08 GIGAPASCALS
× POISSONS RATIO

FIG. 50

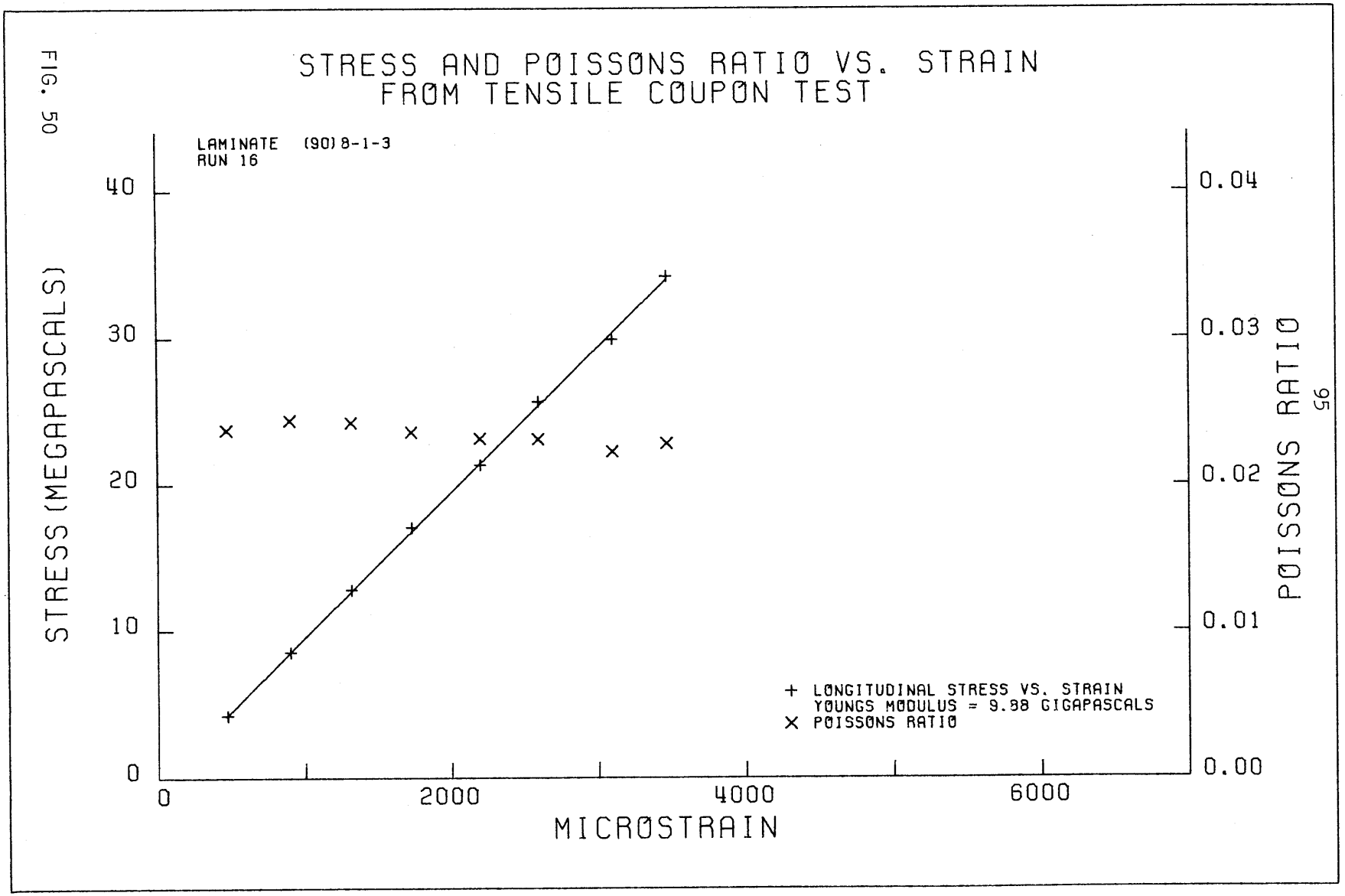
STRESS AND POISSONS RATIO VS. STRAIN
FROM TENSILE COUPON TEST
LAMINATE (90)8-1-3
RUN 16
STRESS (MEGAPASCALS)
40
30
20
10
0
0
2000
4000
6000
MICROSTRAIN
0.04
0.03
0.02
0.01
0.00
POISSONS RATIO
+ LONGITUDINAL STRESS VS. STRAIN
YOUNGS MODULUS = 9.88 GIGAPASCALS
× POISSONS RATIO

FIG. 51

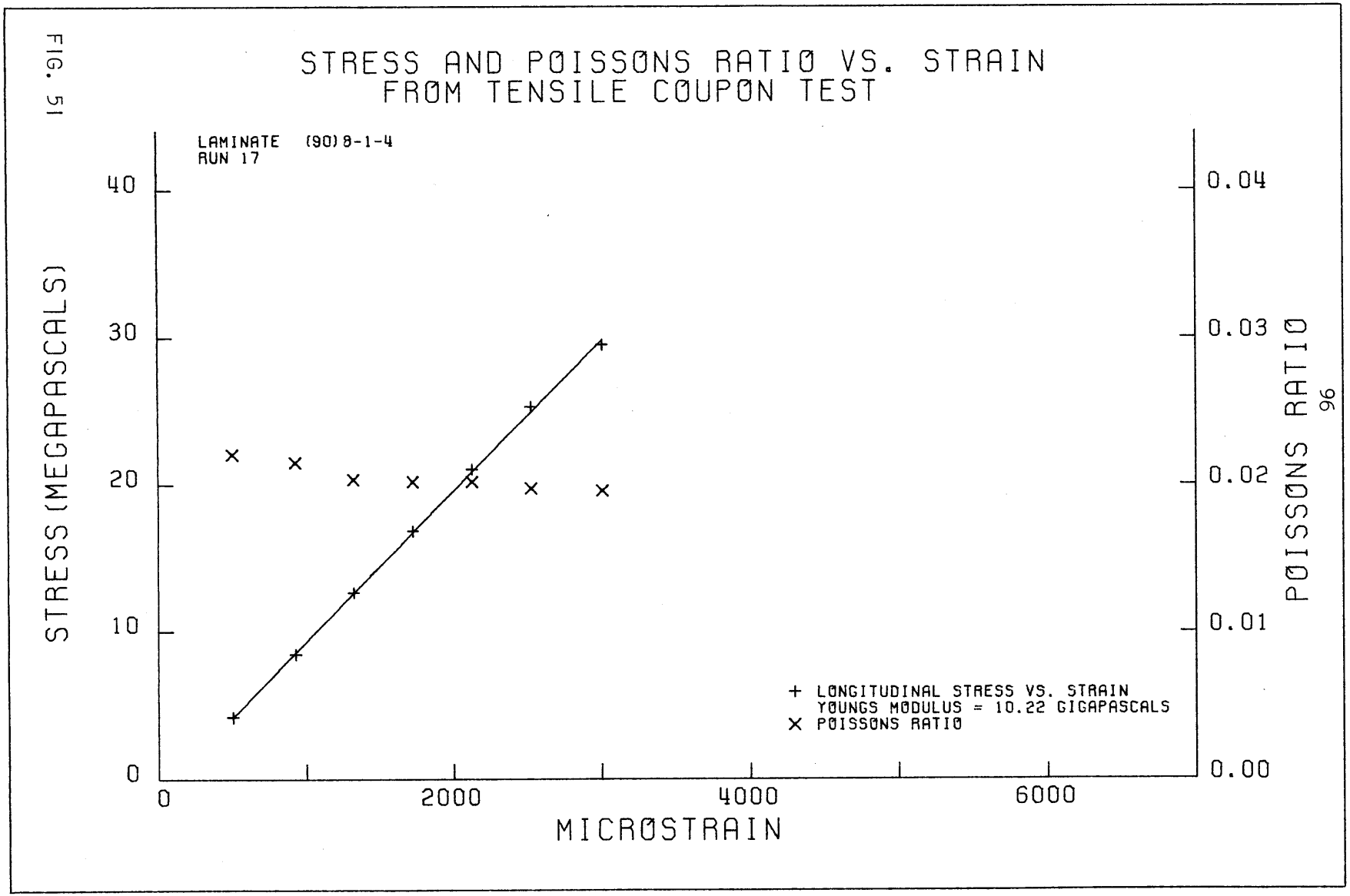
STRESS AND POISSONS RATIO VS. STRAIN
FROM TENSILE COUPON TEST
LAMINATE (90)8-1-4
RUN 17
STRESS (MEGAPASCALS)
40
30
20
10
0
0
2000
4000
6000
MICROSTRAIN
0.04
0.03
0.02
0.01
0.00
POISSONS RATIO
+ LONGITUDINAL STRESS VS. STRAIN
YOUNGS MODULUS = 10.22 GIGAPASCALS
× POISSONS RATIO

FIG. 52

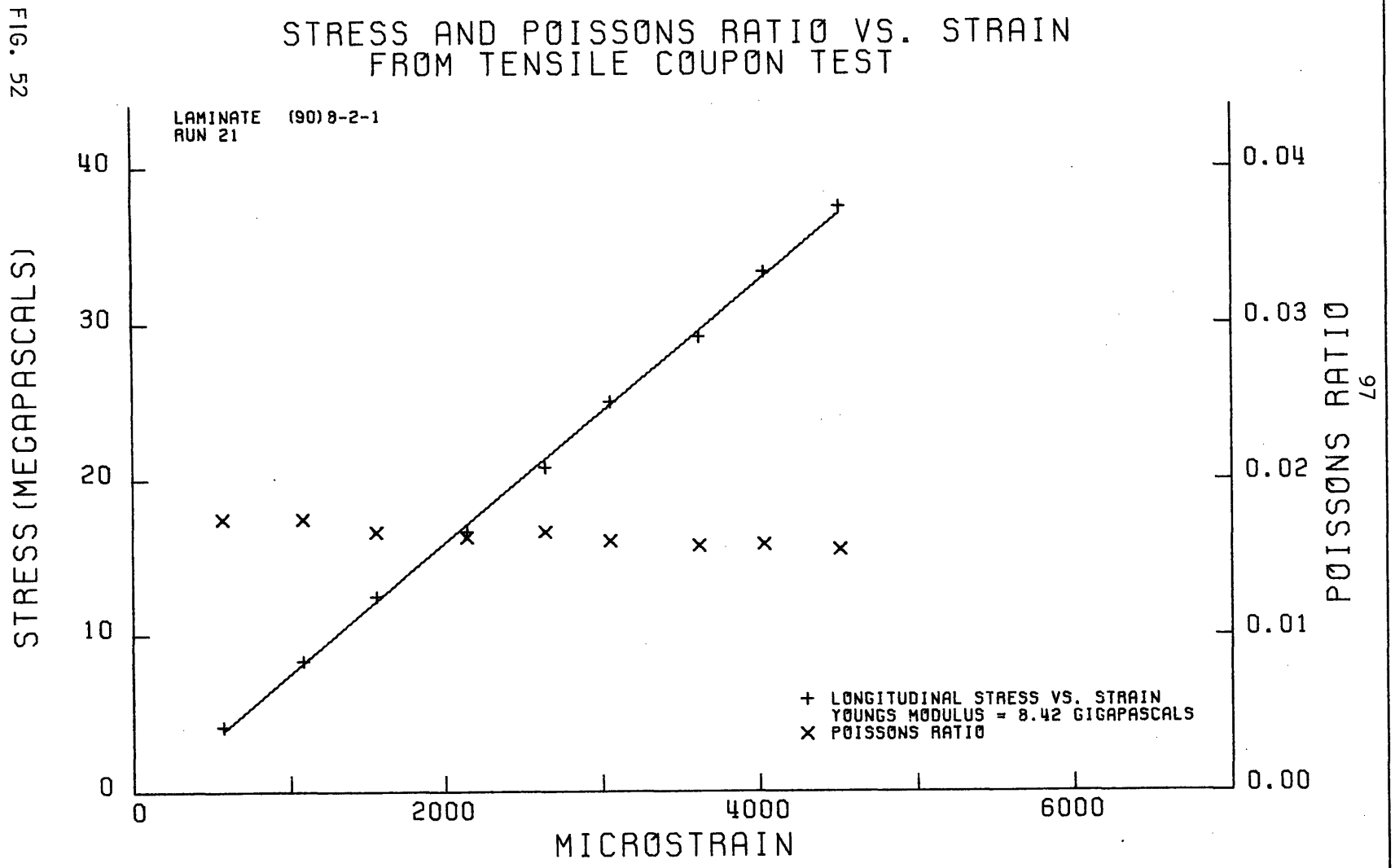
STRESS AND POISSONS RATIO VS. STRAIN
FROM TENSILE COUPON TEST
LAMINATE (90)8-2-1
RUN 21
STRESS (MEGAPASCALS)
0
10
20
30
40
0
2000
4000
6000
MICROSTRAIN
0.00
0.01
0.02
0.03
0.04
POISSONS RATIO
+ LONGITUDINAL STRESS VS. STRAIN
YOUNGS MODULUS = 8.42 GIGAPASCALS
× POISSONS RATIO

FIG. 53

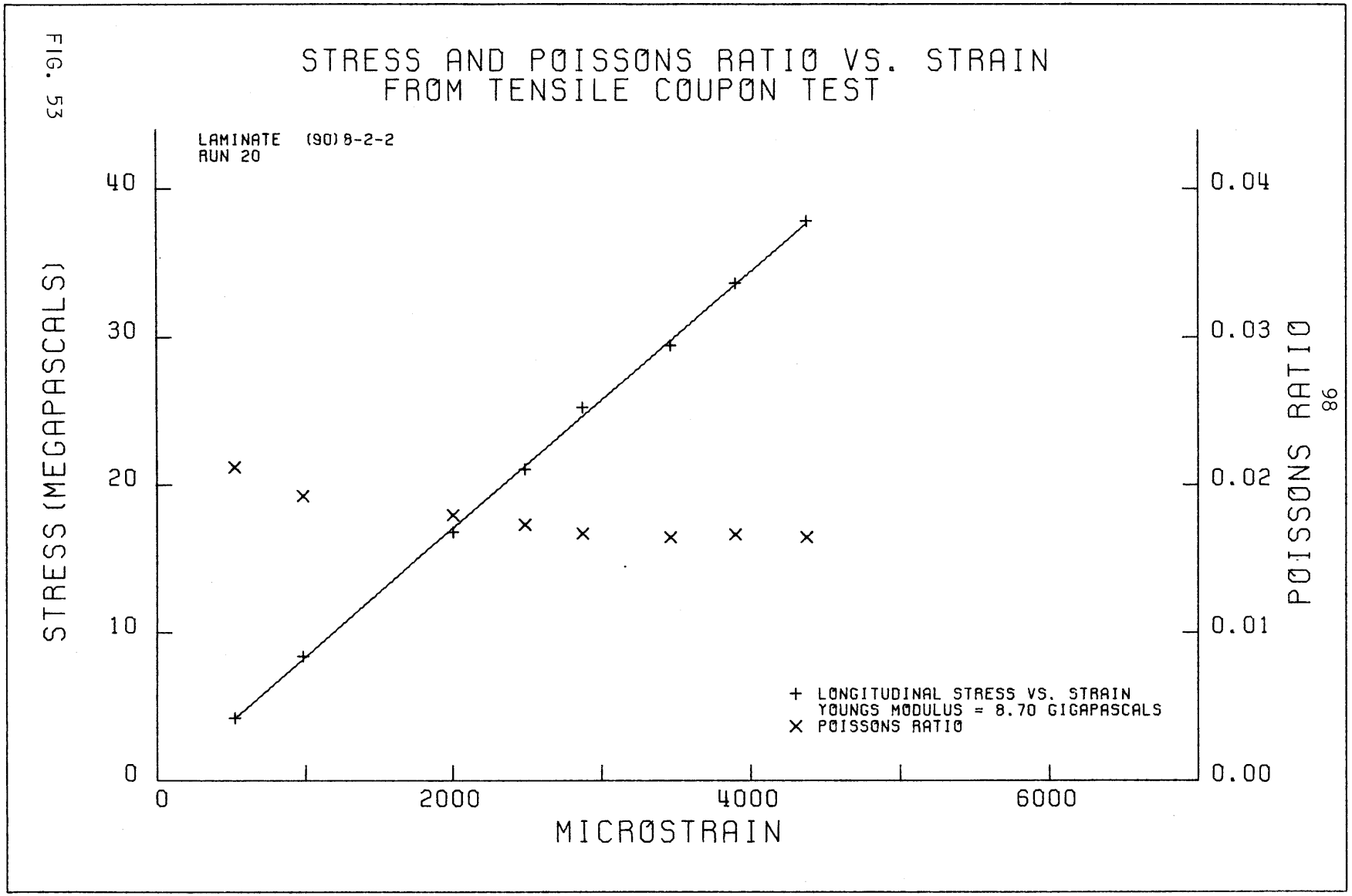
STRESS AND POISSONS RATIO VS. STRAIN
FROM TENSILE COUPON TEST
LAMINATE (90)8-2-2
RUN 20
STRESS (MEGAPASCALS)
0
10
20
30
40
0
2000
4000
6000
MICROSTRAIN
0.00
0.01
0.02
0.03
0.04
POISSONS RATIO
+ LONGITUDINAL STRESS VS. STRAIN
YOUNGS MODULUS = 8.70 GIGAPASCALS
× POISSONS RATIO

FIG. 54

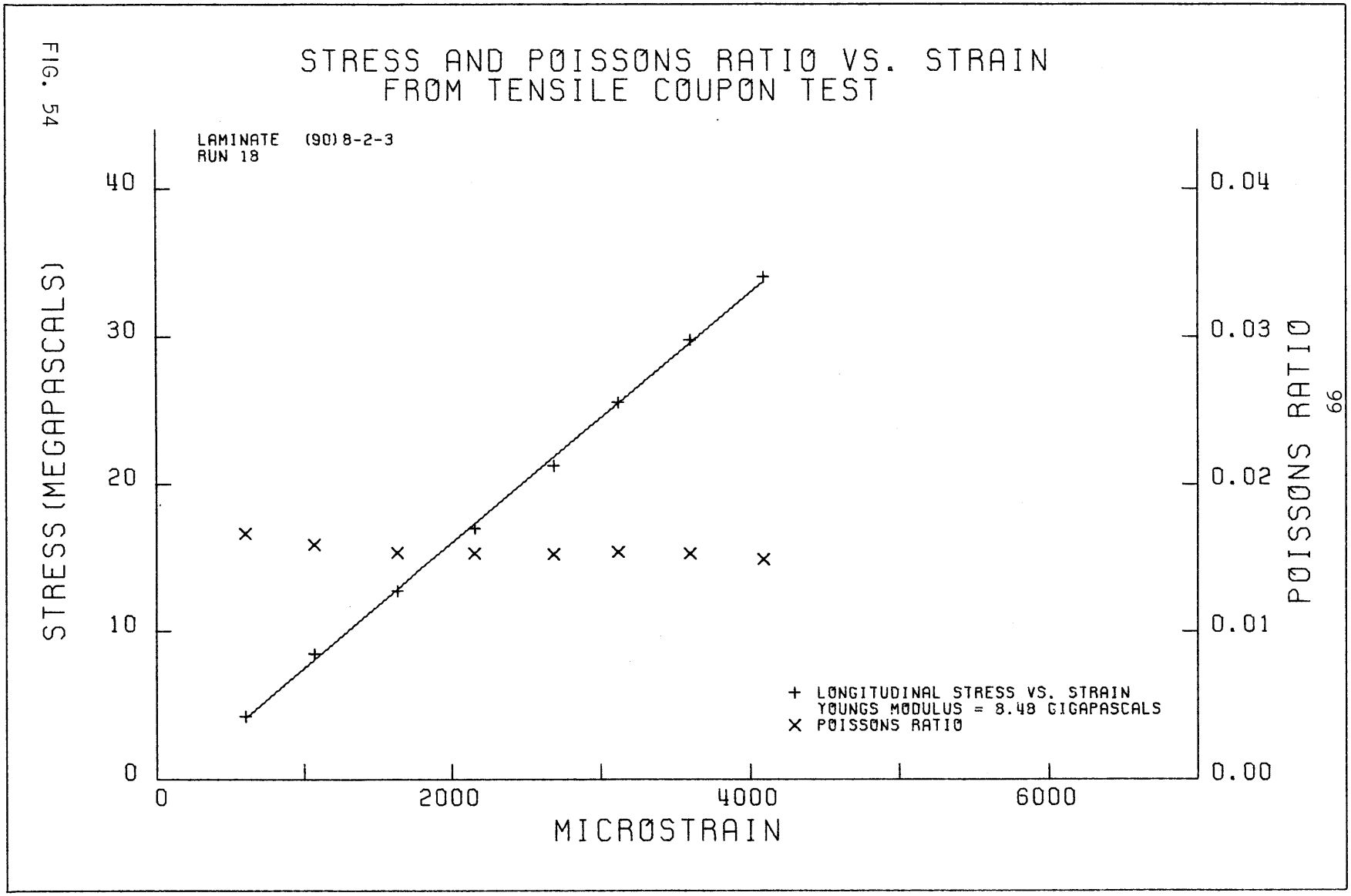
STRESS AND POISSONS RATIO VS. STRAIN
FROM TENSILE COUPON TEST
LAMINATE (90)8-2-3
RUN 18
STRESS (MEGAPASCALS)
40
30
20
10
0
0
2000
4000
6000
MICROSTRAIN
0.04
0.03
0.02
0.01
0.00
POISSONS RATIO
+ LONGITUDINAL STRESS VS. STRAIN
YOUNGS MODULUS = 8.48 GIGAPASCALS
× POISSONS RATIO

FIG. 55

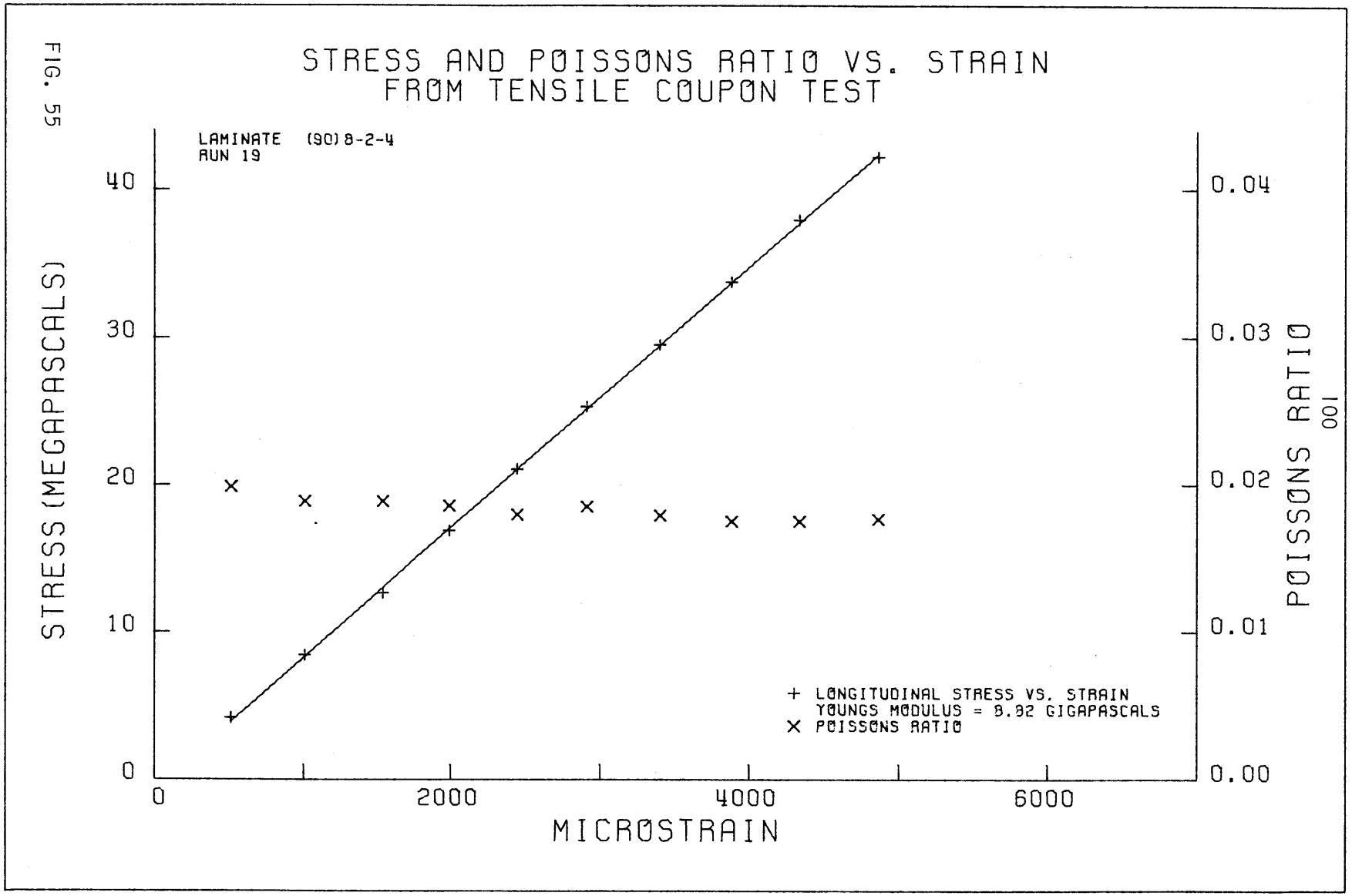
STRESS AND POISSONS RATIO VS. STRAIN
FROM TENSILE COUPON TEST
LAMINATE (90)8-2-4
RUN 19
STRESS (MEGAPASCALS)
40
30
20
10
0
0
2000
4000
6000
MICROSTRAIN
0.04
0.03
0.02
0.01
0.00
POISSONS RATIO
100
+ LONGITUDINAL STRESS VS. STRAIN
YOUNGS MODULUS = 8.82 GIGAPASCALS
× POISSONS RATIO

FIG. 56

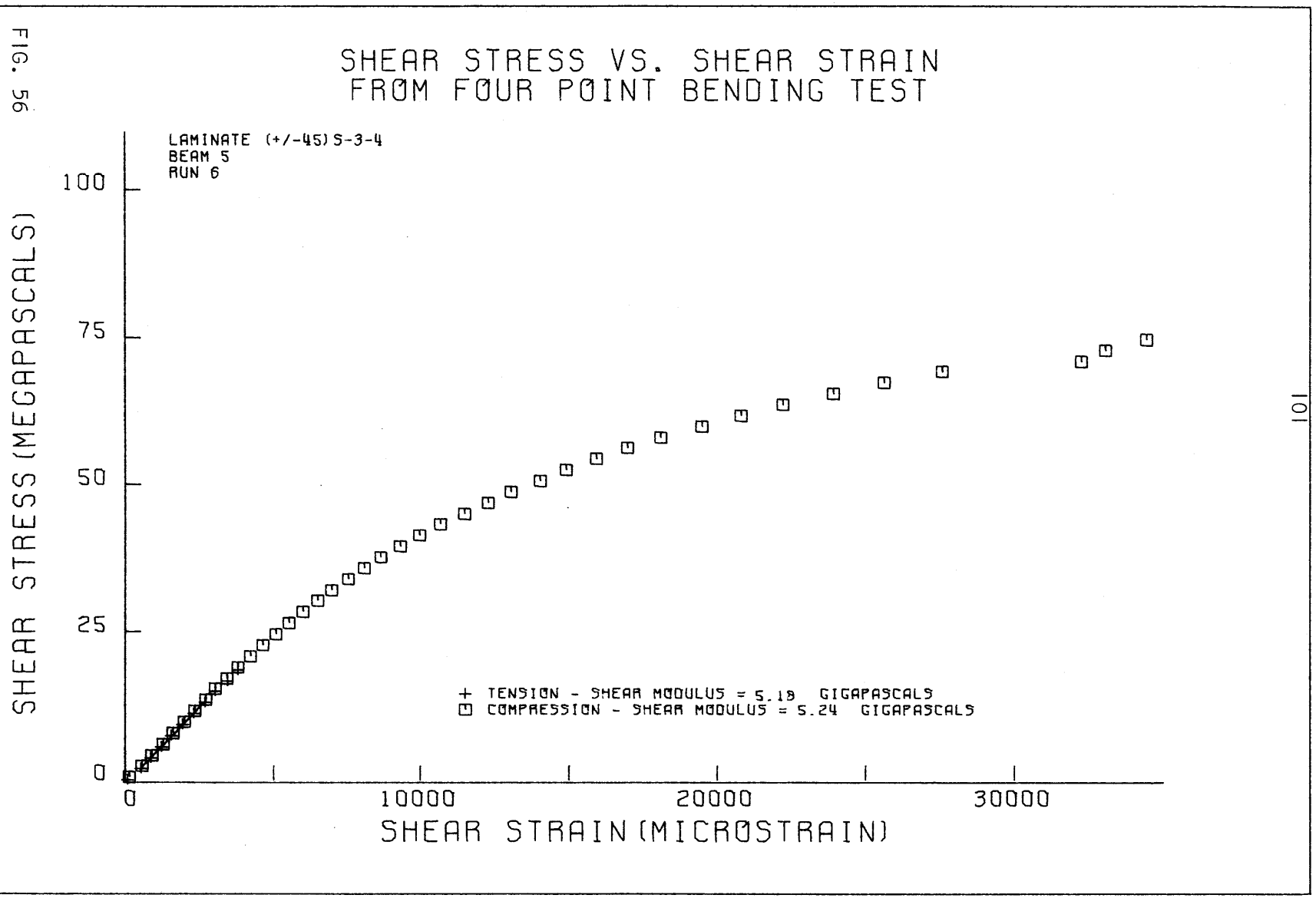
SHEAR STRESS VS. SHEAR STRAIN
FROM FOUR POINT BENDING TEST
LAMINATE (+/-45)S-3-4
BEAM 5
RUN 6
SHEAR STRESS (MEGAPASCALS)
100
75
50
25
0
0
10000
20000
30000
SHEAR STRAIN (MICROSTRAIN)
+ TENSION - SHEAR MODULUS = 5.18 GIGAPASCALS
□ COMPRESSION - SHEAR MODULUS = 5.24 GIGAPASCALS

FIG. 57

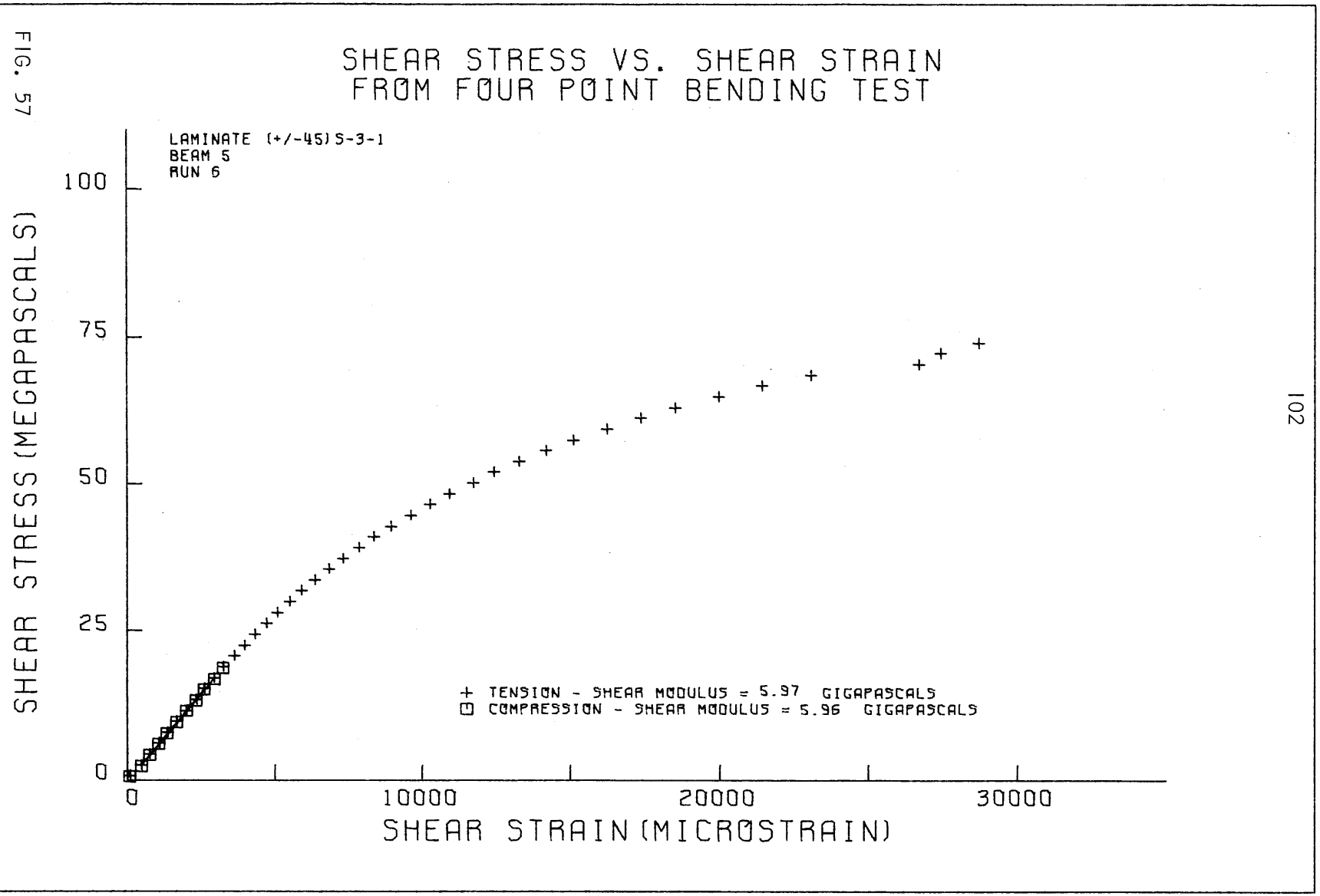
SHEAR STRESS VS. SHEAR STRAIN
FROM FOUR POINT BENDING TEST
LAMINATE (+/-45)S-3-1
BEAM 5
RUN 6
100
75
50
25
0
SHEAR STRESS (MEGAPASCALS)
+ TENSION - SHEAR MODULUS = 5.97 GIGAPASCALS
⊡ COMPRESSION - SHEAR MODULUS = 5.96 GIGAPASCALS
0
10000
20000
30000
SHEAR STRAIN (MICROSTRAIN)

FIG. 58

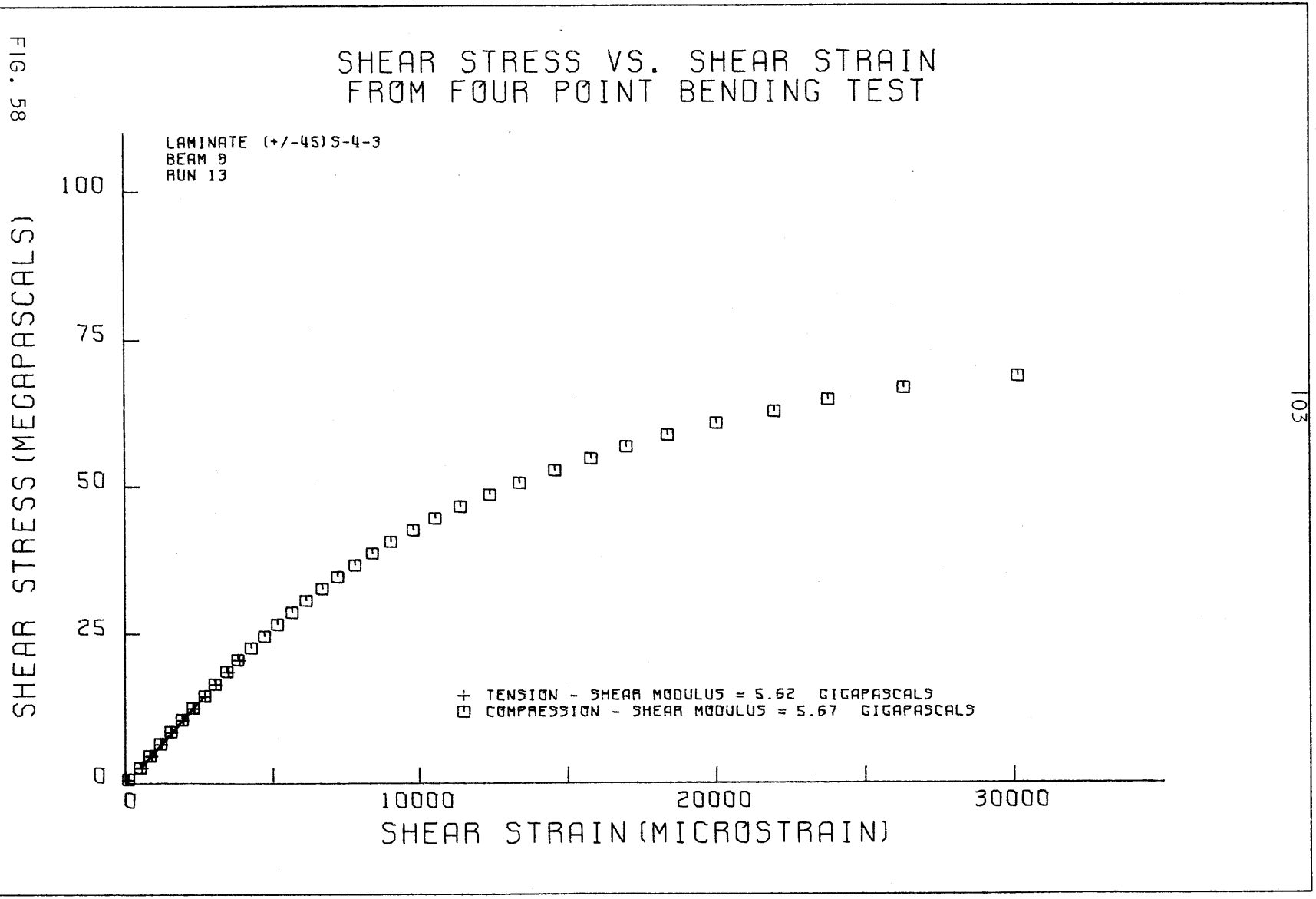
SHEAR STRESS VS. SHEAR STRAIN
FROM FOUR POINT BENDING TEST
LAMINATE (+/-45)S-4-3
BEAM 9
RUN 13
100
75
50
25
0
SHEAR STRESS (MEGAPASCALS)
0
10000
20000
30000
SHEAR STRAIN (MICROSTRAIN)
+ TENSION - SHEAR MODULUS = 5.62 GIGAPASCALS
□ COMPRESSION - SHEAR MODULUS = 5.67 GIGAPASCALS

FIG. 59

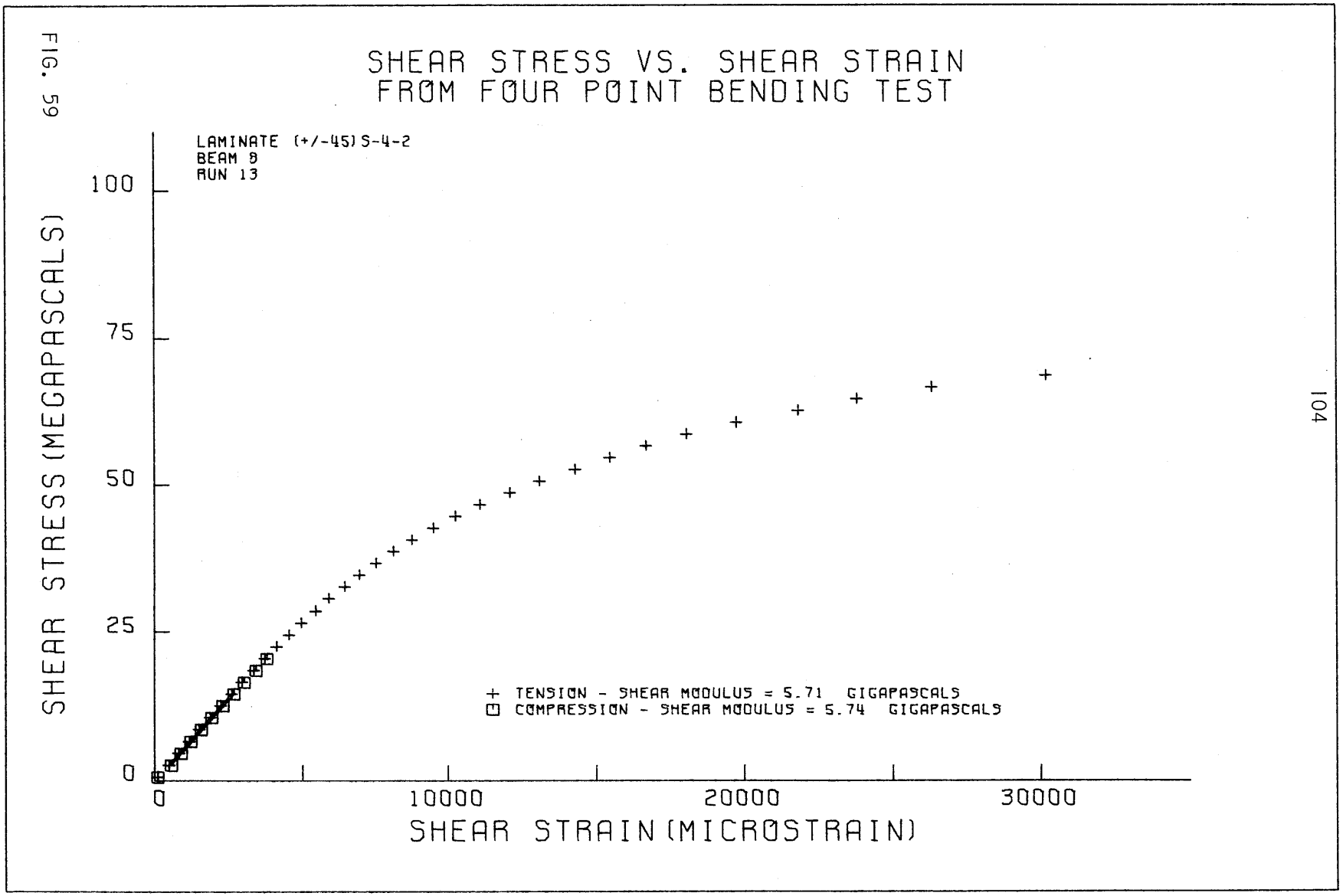
SHEAR STRESS VS. SHEAR STRAIN
FROM FOUR POINT BENDING TEST
LAMINATE (+/-45)S-4-2
BEAM 8
RUN 13
SHEAR STRESS (MEGAPASCALS)
100
75
50
25
0
0
10000
20000
30000
SHEAR STRAIN (MICROSTRAIN)
+ TENSION - SHEAR MODULUS = 5.71 GIGAPASCALS
□ COMPRESSION - SHEAR MODULUS = 5.74 GIGAPASCALS

FIG. 60

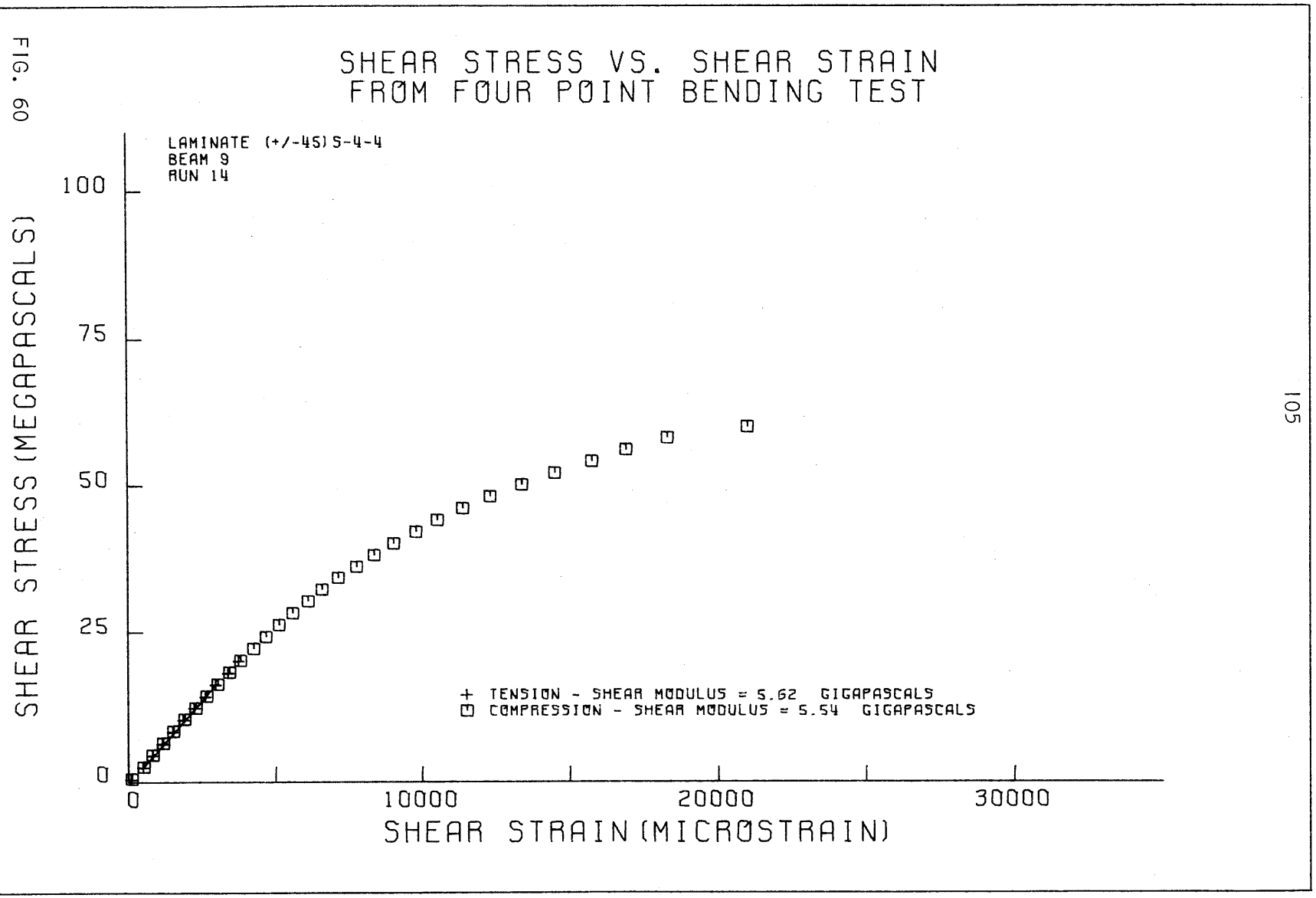
SHEAR STRESS VS. SHEAR STRAIN
FROM FOUR POINT BENDING TEST
LAMINATE (+/-45)S-4-4
BEAM 9
RUN 14
SHEAR STRESS (MEGAPASCALS)
100
75
50
25
0
0
10000
20000
30000
SHEAR STRAIN (MICROSTRAIN)
+ TENSION - SHEAR MODULUS = 5.62 GIGAPASCALS
□ COMPRESSION - SHEAR MODULUS = 5.54 GIGAPASCALS

FIG. 61

SHEAR STRESS VS. SHEAR STRAIN FROM FOUR POINT BENDING TEST

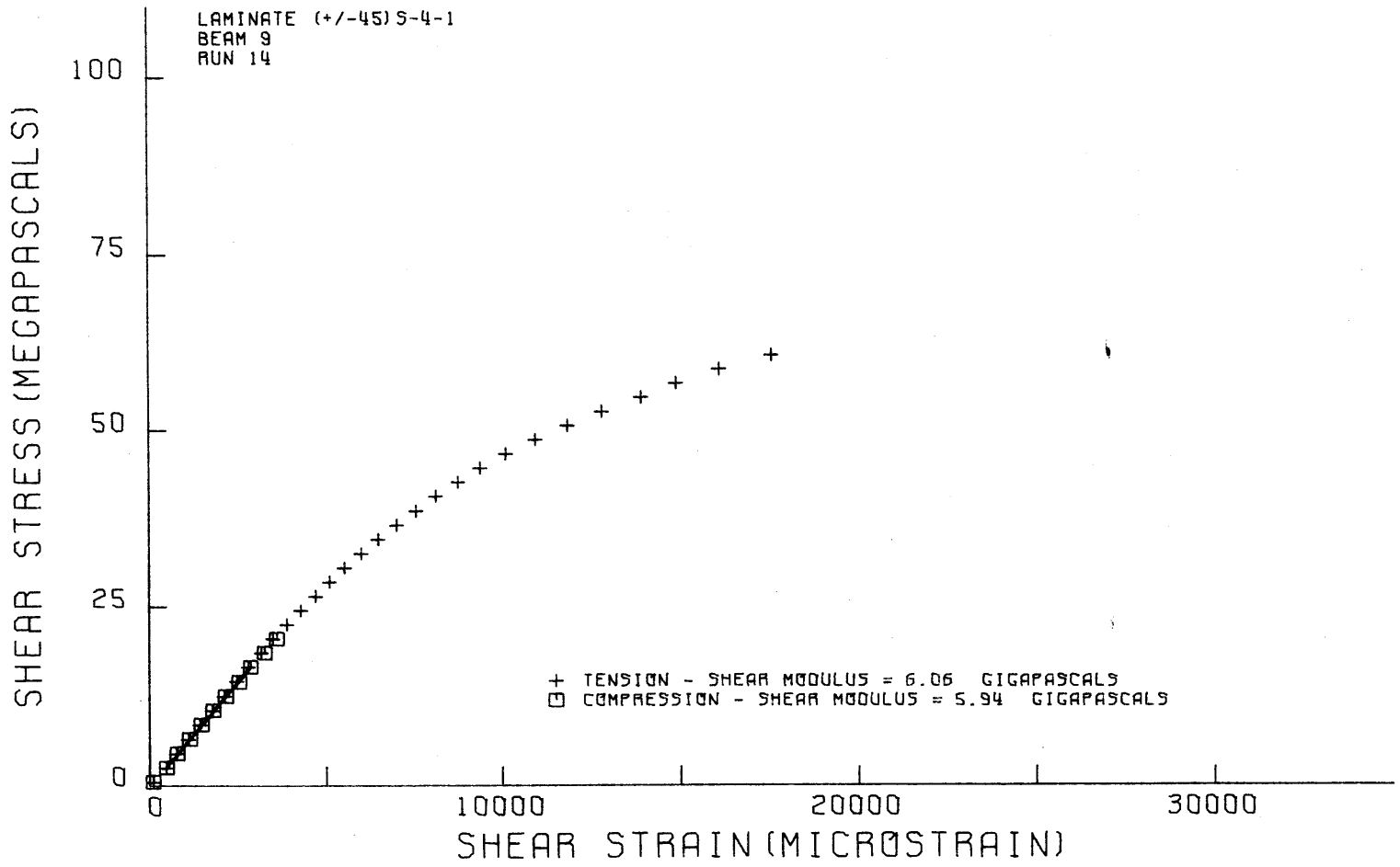

FIG. 62

SHEAR STRESS VS. SHEAR STRAIN FROM FOUR POINT BENDING TEST

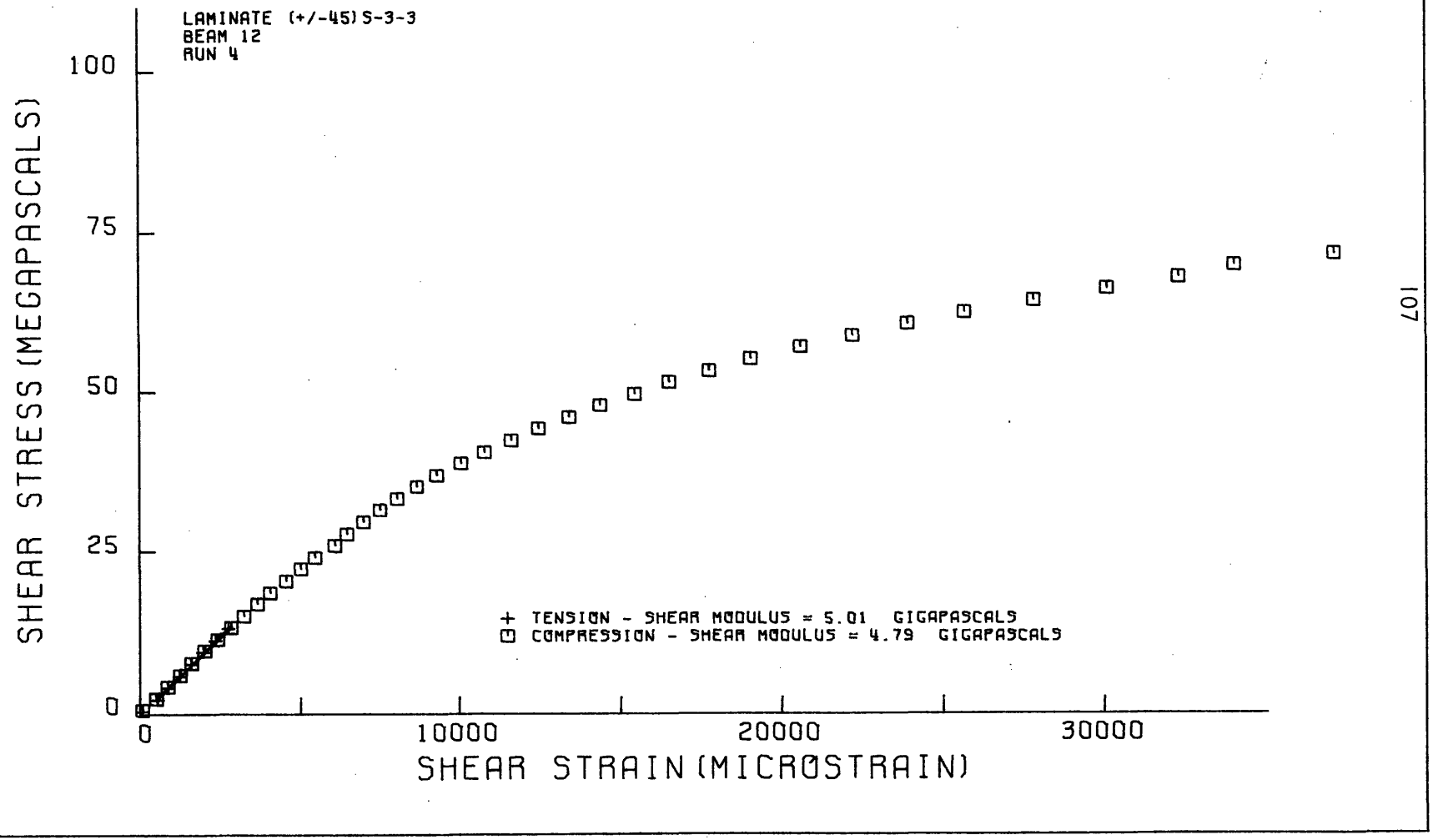

FIG. 63

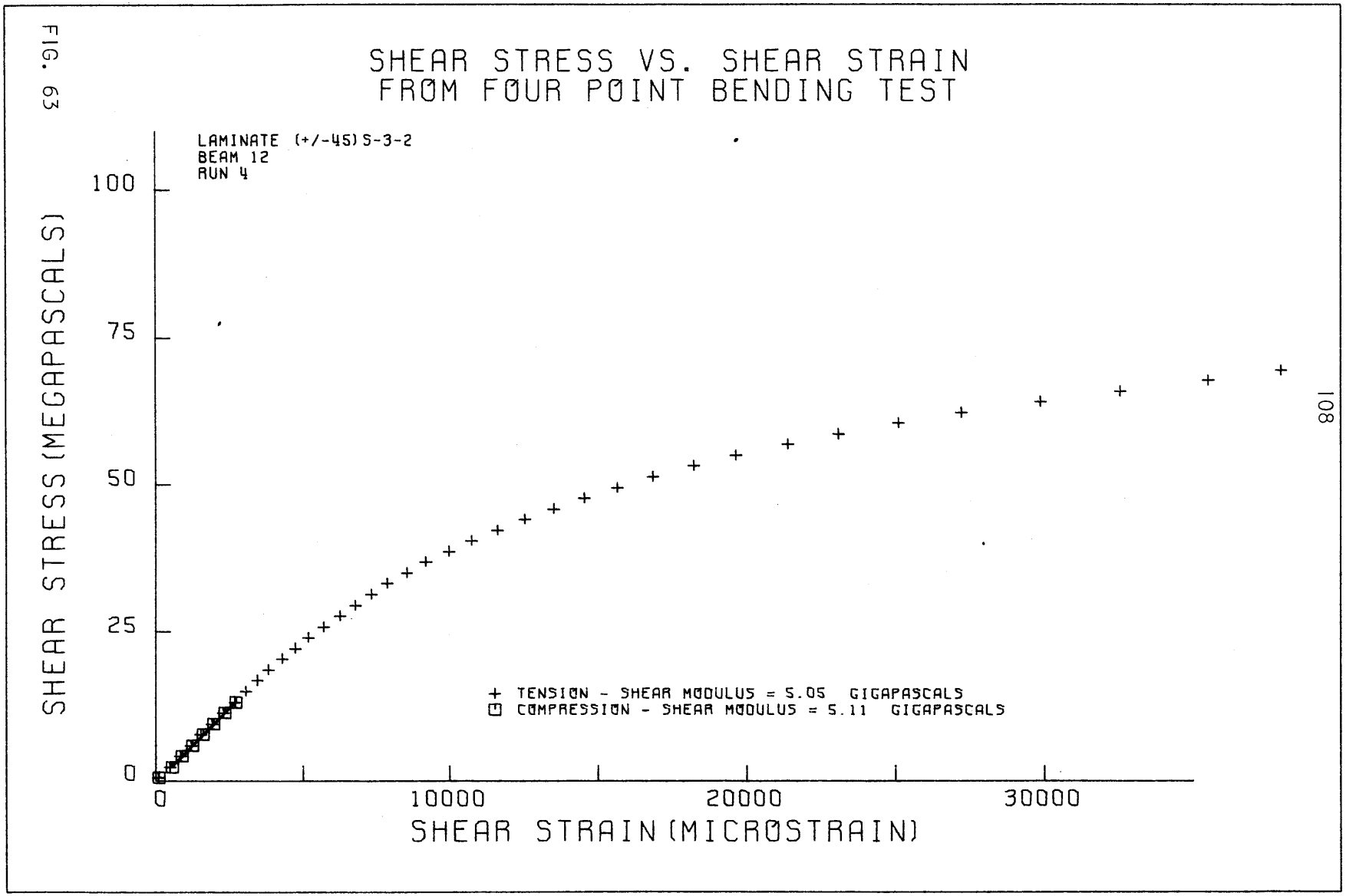
SHEAR STRESS VS. SHEAR STRAIN
FROM FOUR POINT BENDING TEST
LAMINATE (+/-45)S-3-2
BEAM 12
RUN 4
100
75
50
25
0
SHEAR STRESS (MEGAPASCALS)
0
10000
20000
30000
SHEAR STRAIN (MICROSTRAIN)
+ TENSION - SHEAR MODULUS = 5.05 GIGAPASCALS
□ COMPRESSION - SHEAR MODULUS = 5.11 GIGAPASCALS
108

FIG. 64

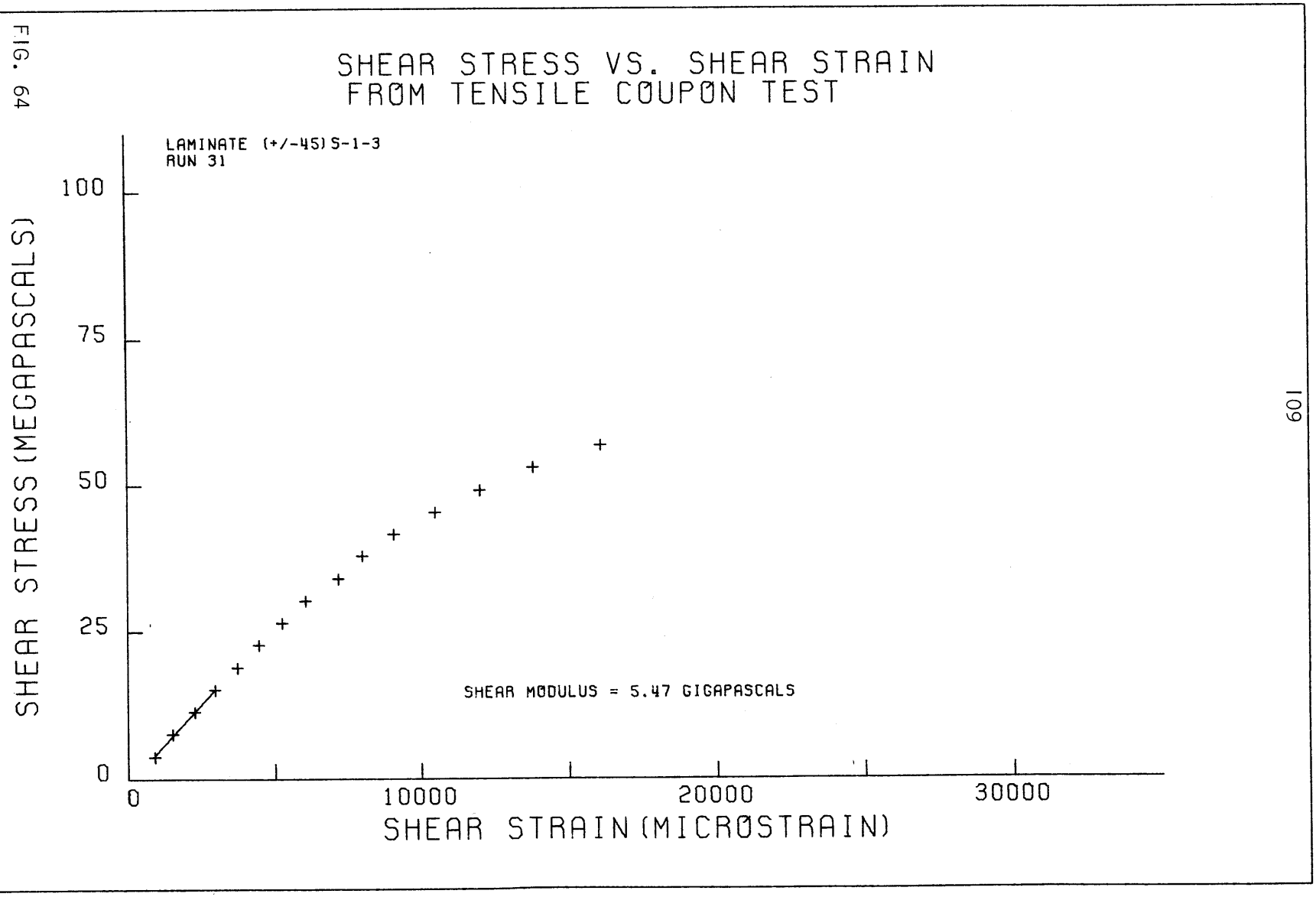
SHEAR STRESS VS. SHEAR STRAIN
FROM TENSILE COUPON TEST
LAMINATE (+/-45)S-1-3
RUN 31
SHEAR MODULUS = 5.47 GIGAPASCALS
SHEAR STRESS (MEGAPASCALS)
100
75
50
25
0
0
10000
20000
30000
SHEAR STRAIN (MICROSTRAIN)

FIG. 65

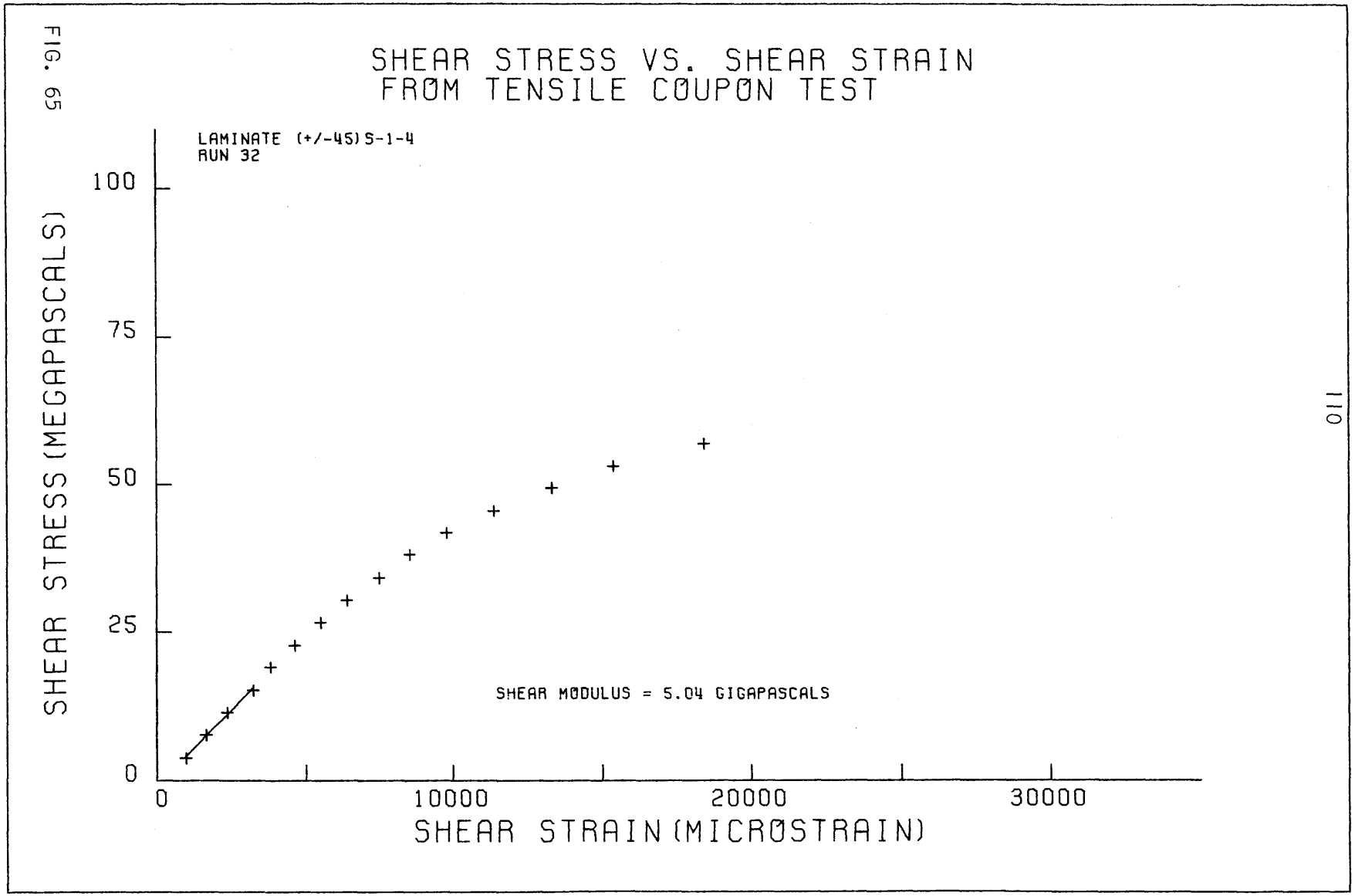
SHEAR STRESS VS. SHEAR STRAIN
FROM TENSILE COUPON TEST
LAMINATE (+/-45)S-1-4
RUN 32
SHEAR MODULUS = 5.04 GIGAPASCALS
SHEAR STRESS (MEGAPASCALS)
100
75
50
25
0
0
10000
20000
30000
SHEAR STRAIN (MICROSTRAIN)

FIG. 66

SHEAR STRESS VS. SHEAR STRAIN FROM TENSILE COUPON TEST

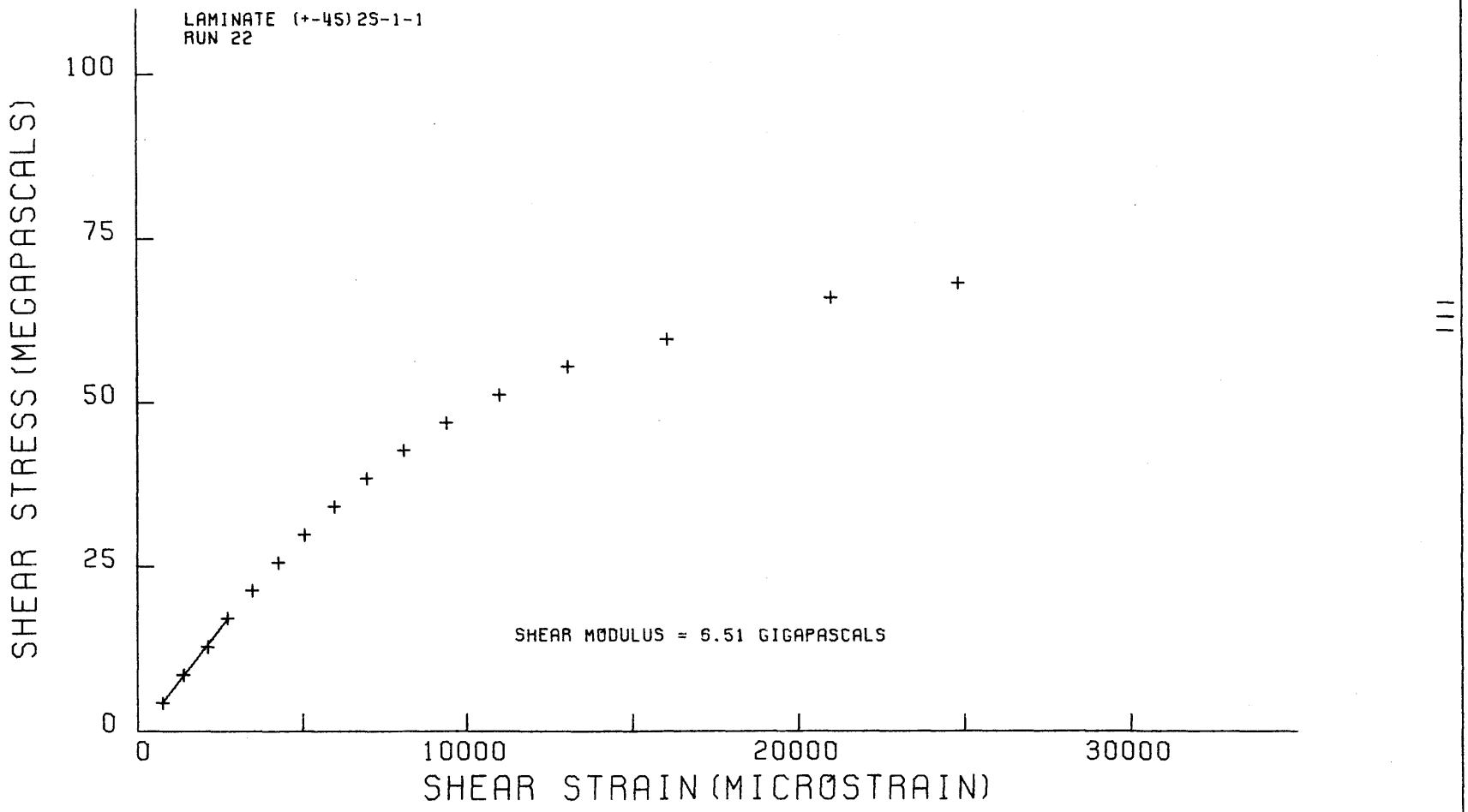

FIG. 67

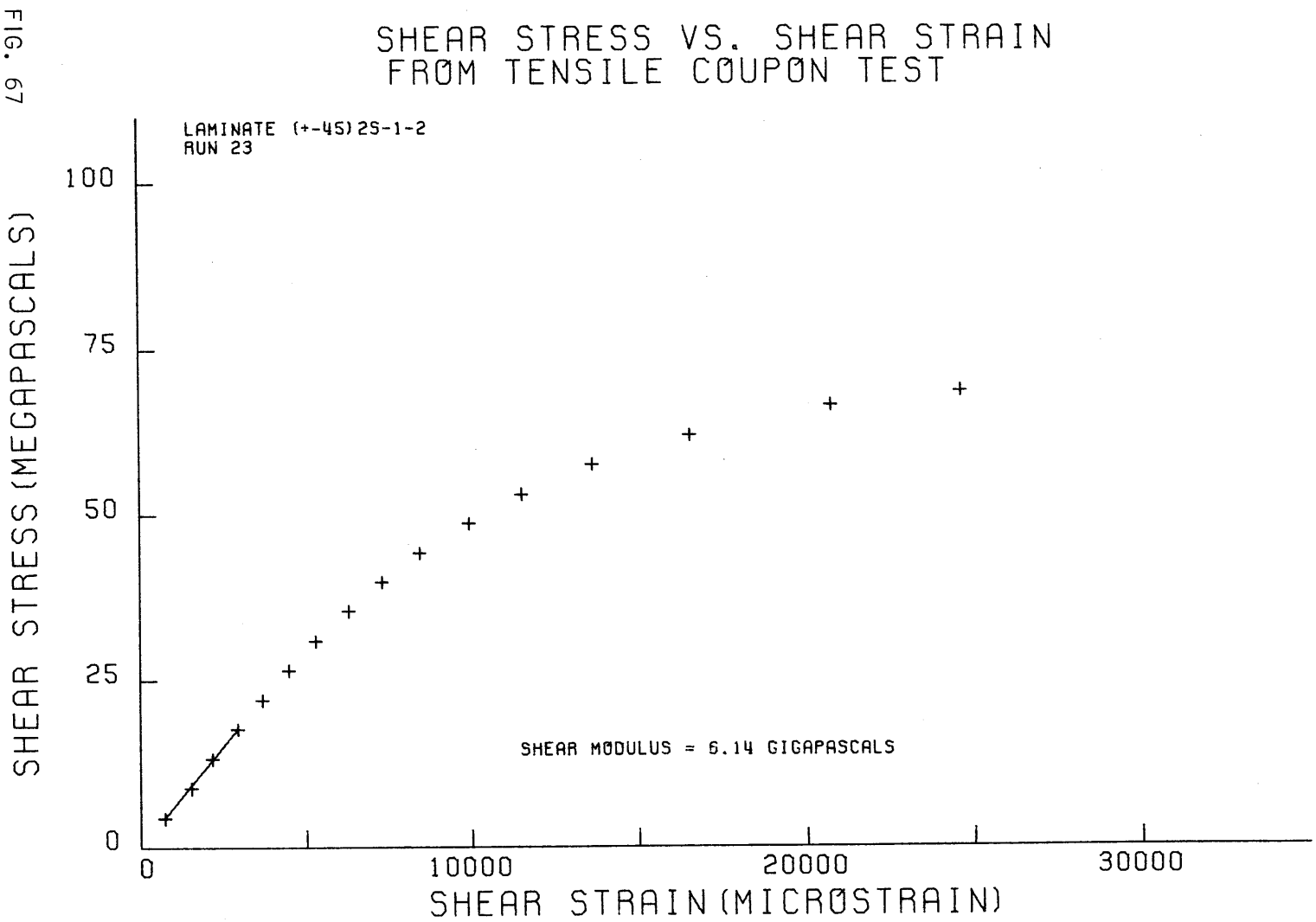
SHEAR STRESS VS. SHEAR STRAIN
FROM TENSILE COUPON TEST
LAMINATE (+-45)2S-1-2
RUN 23
SHEAR STRESS (MEGAPASCALS)
100
75
50
25
0
0
10000
20000
30000
SHEAR STRAIN (MICROSTRAIN)
SHEAR MODULUS = 6.14 GIGAPASCALS

FIG. 68

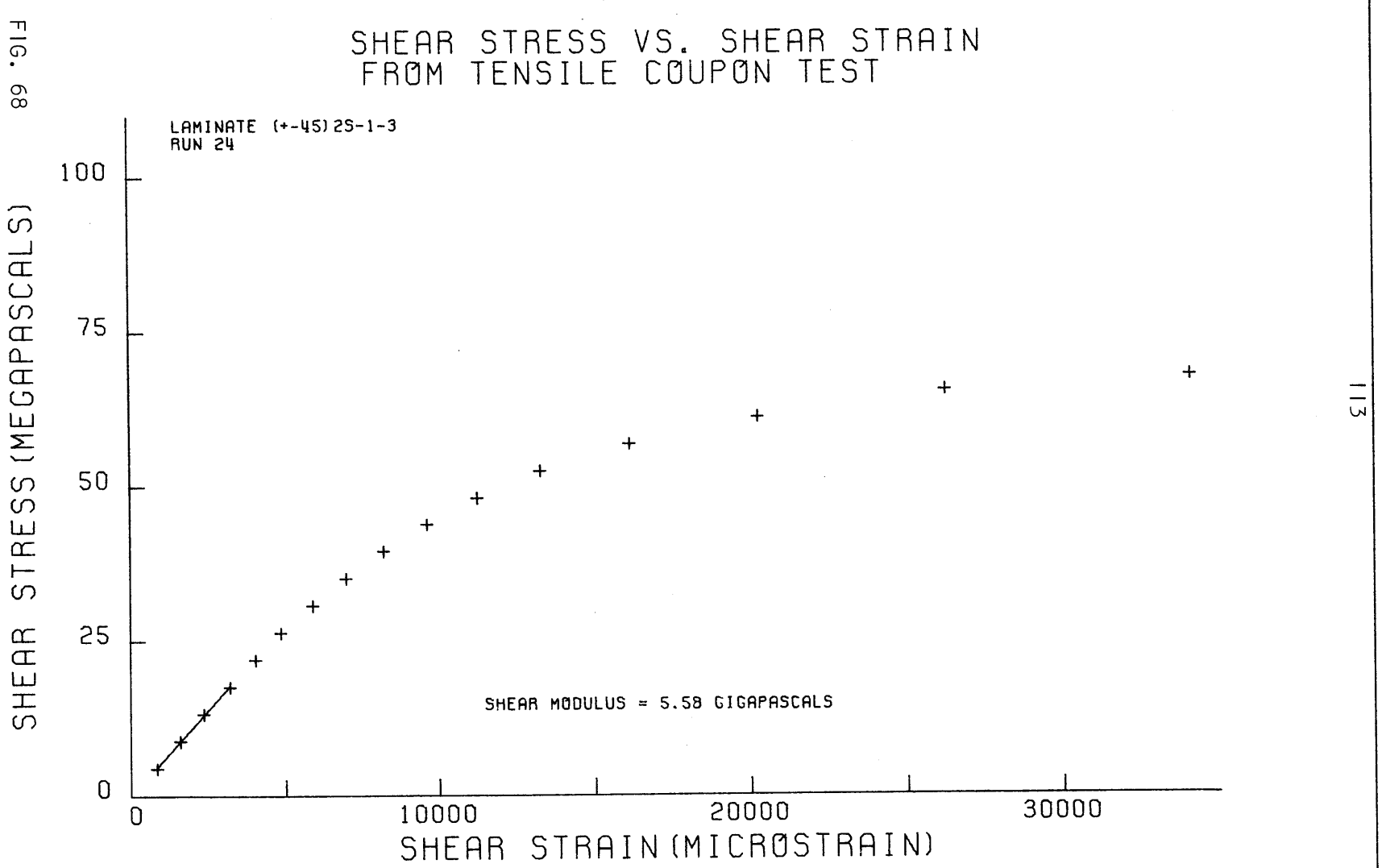
SHEAR STRESS VS. SHEAR STRAIN
FROM TENSILE COUPON TEST
LAMINATE (+-45)2S-1-3
RUN 24
SHEAR MODULUS = 5.58 GIGAPASCALS
SHEAR STRESS (MEGAPASCALS)
100
75
50
25
0
0
10000
20000
30000
SHEAR STRAIN (MICROSTRAIN)

FIG. 69

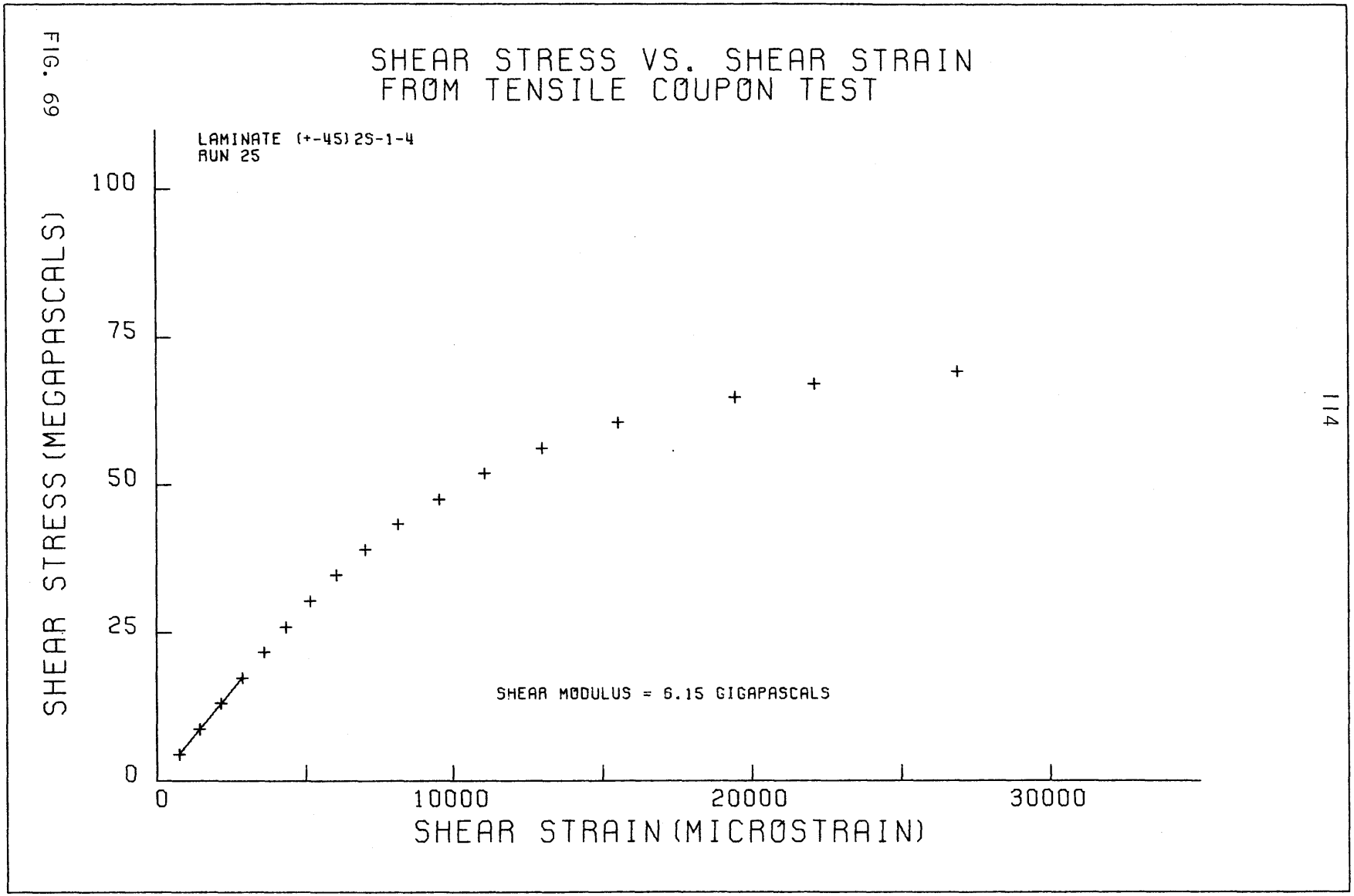
SHEAR STRESS VS. SHEAR STRAIN
FROM TENSILE COUPON TEST
LAMINATE (+-45)2S-1-4
RUN 25
SHEAR MODULUS = 6.15 GIGAPASCALS
SHEAR STRESS (MEGAPASCALS)
100
75
50
25
0
0
10000
20000
30000
SHEAR STRAIN (MICROSTRAIN)

FIG. 70

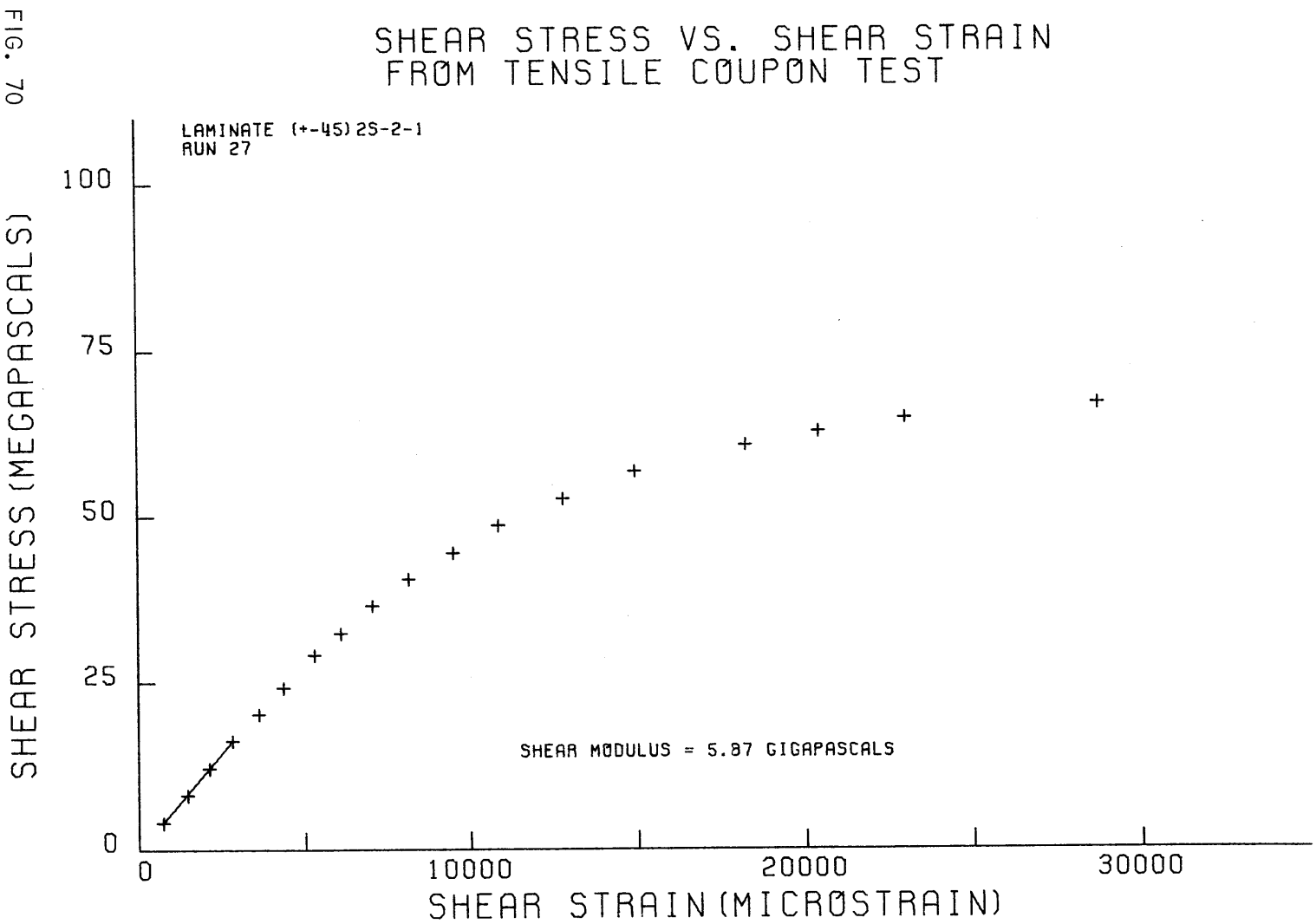
SHEAR STRESS VS. SHEAR STRAIN
FROM TENSILE COUPON TEST
LAMINATE (+-45)2S-2-1
RUN 27
SHEAR MODULUS = 5.87 GIGAPASCALS
SHEAR STRESS (MEGAPASCALS)
100
75
50
25
0
0
10000
20000
30000
SHEAR STRAIN (MICROSTRAIN)

FIG. 71

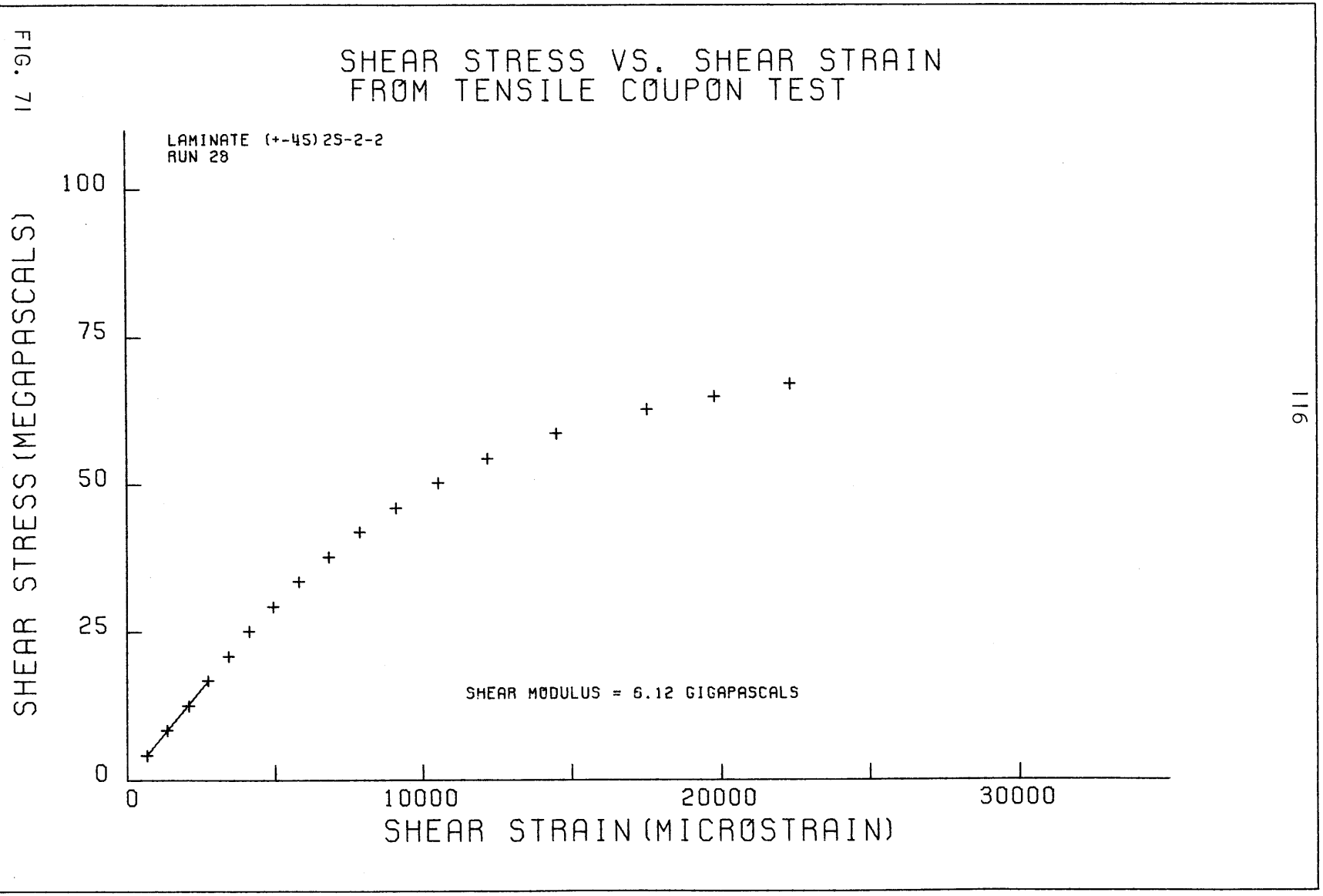
SHEAR STRESS VS. SHEAR STRAIN
FROM TENSILE COUPON TEST
LAMINATE (+-45)2S-2-2
RUN 28
SHEAR STRESS (MEGAPASCALS)
100
75
50
25
0
0
10000
20000
30000
SHEAR STRAIN (MICROSTRAIN)
SHEAR MODULUS = 6.12 GIGAPASCALS

FIG. 72

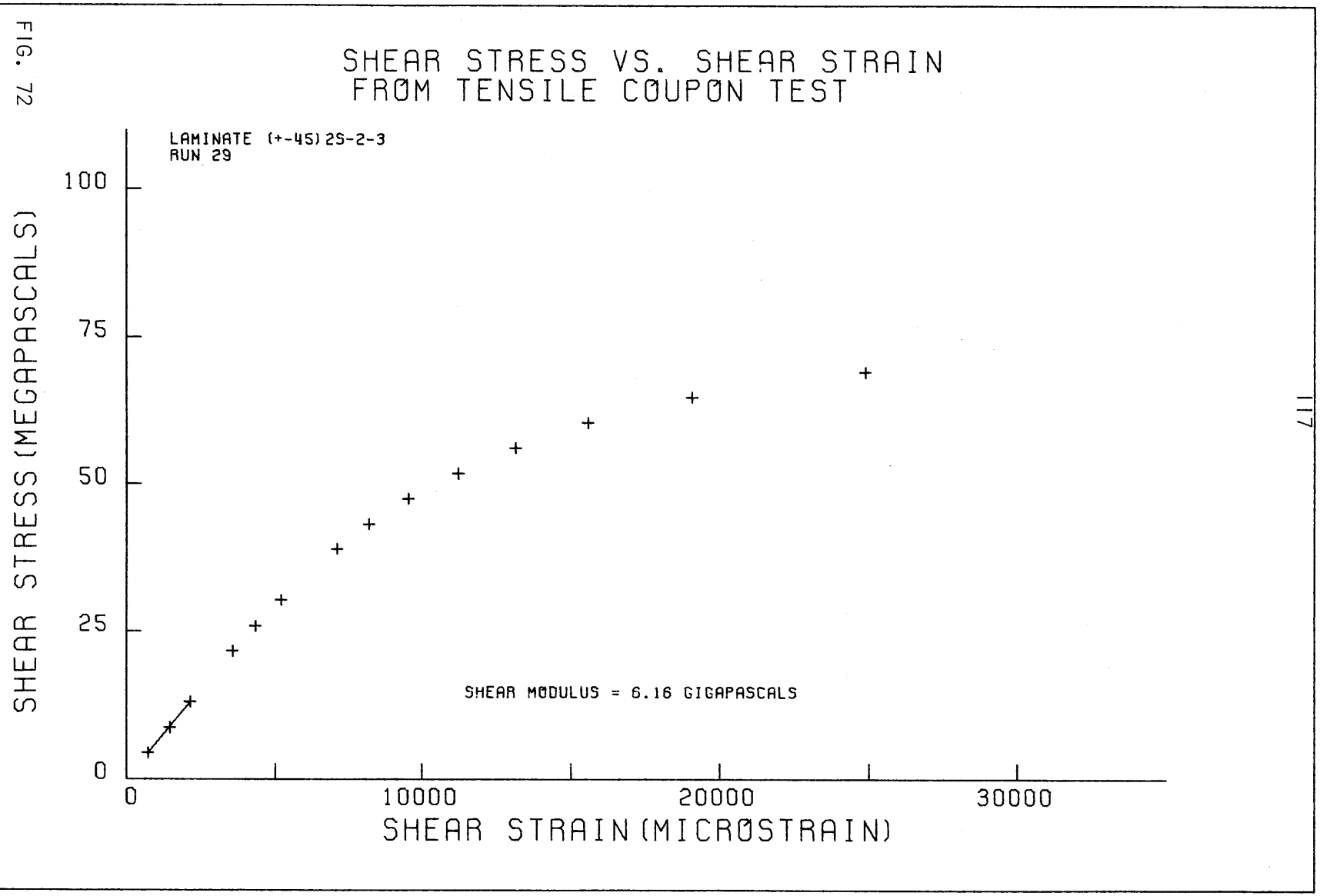
SHEAR STRESS VS. SHEAR STRAIN
FROM TENSILE COUPON TEST
LAMINATE (+-45)2S-2-3
RUN 29
SHEAR MODULUS = 6.16 GIGAPASCALS
SHEAR STRESS (MEGAPASCALS)
100
75
50
25
0
0
10000
20000
30000
SHEAR STRAIN (MICROSTRAIN)

FIG. 73

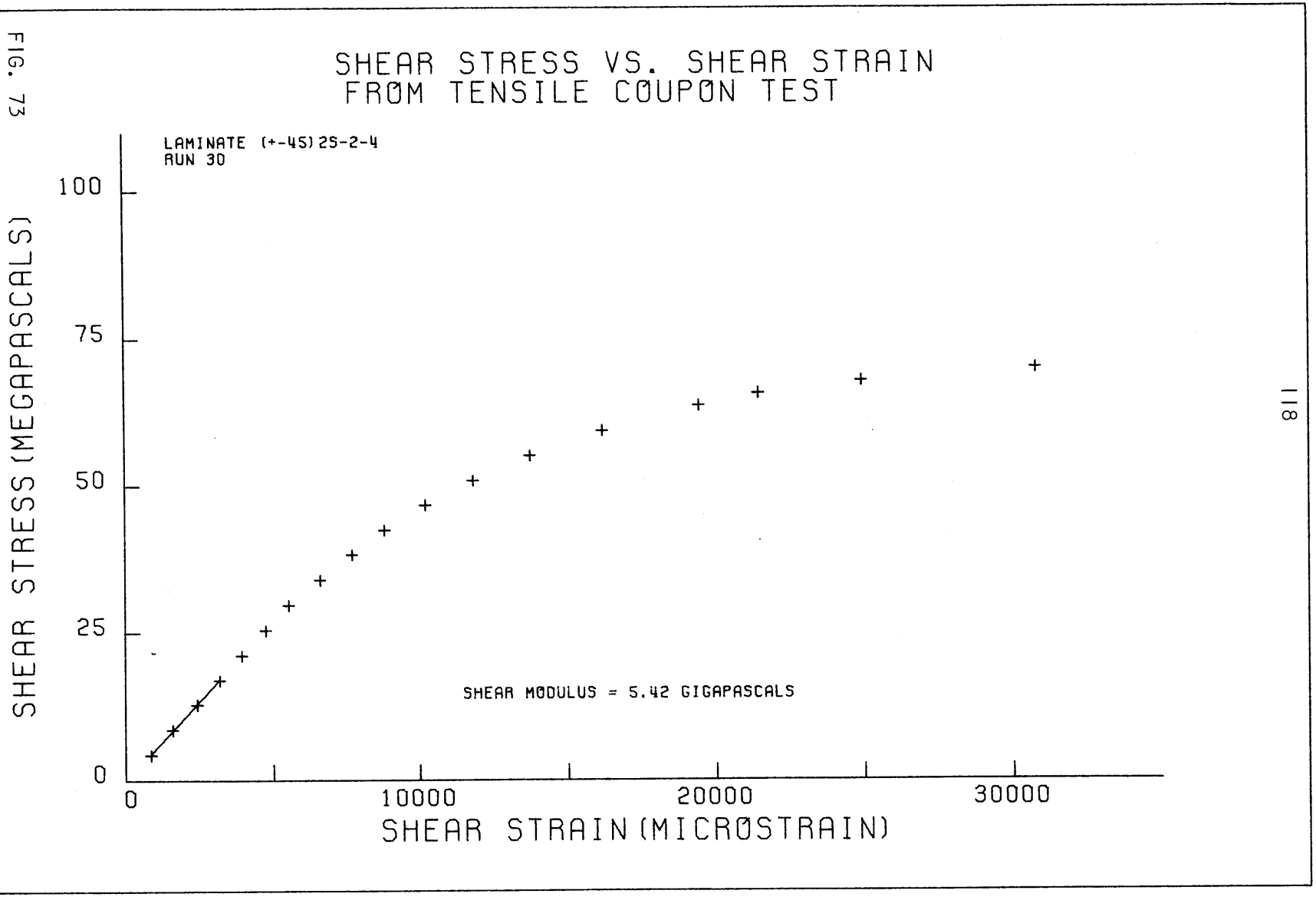
SHEAR STRESS VS. SHEAR STRAIN
FROM TENSILE COUPON TEST
LAMINATE (+-45)2S-2-4
RUN 30
SHEAR STRESS (MEGAPASCALS)
100
75
50
25
0
0
10000
20000
30000
SHEAR STRAIN (MICROSTRAIN)
SHEAR MODULUS = 5.42 GIGAPASCALS

FIG. 74

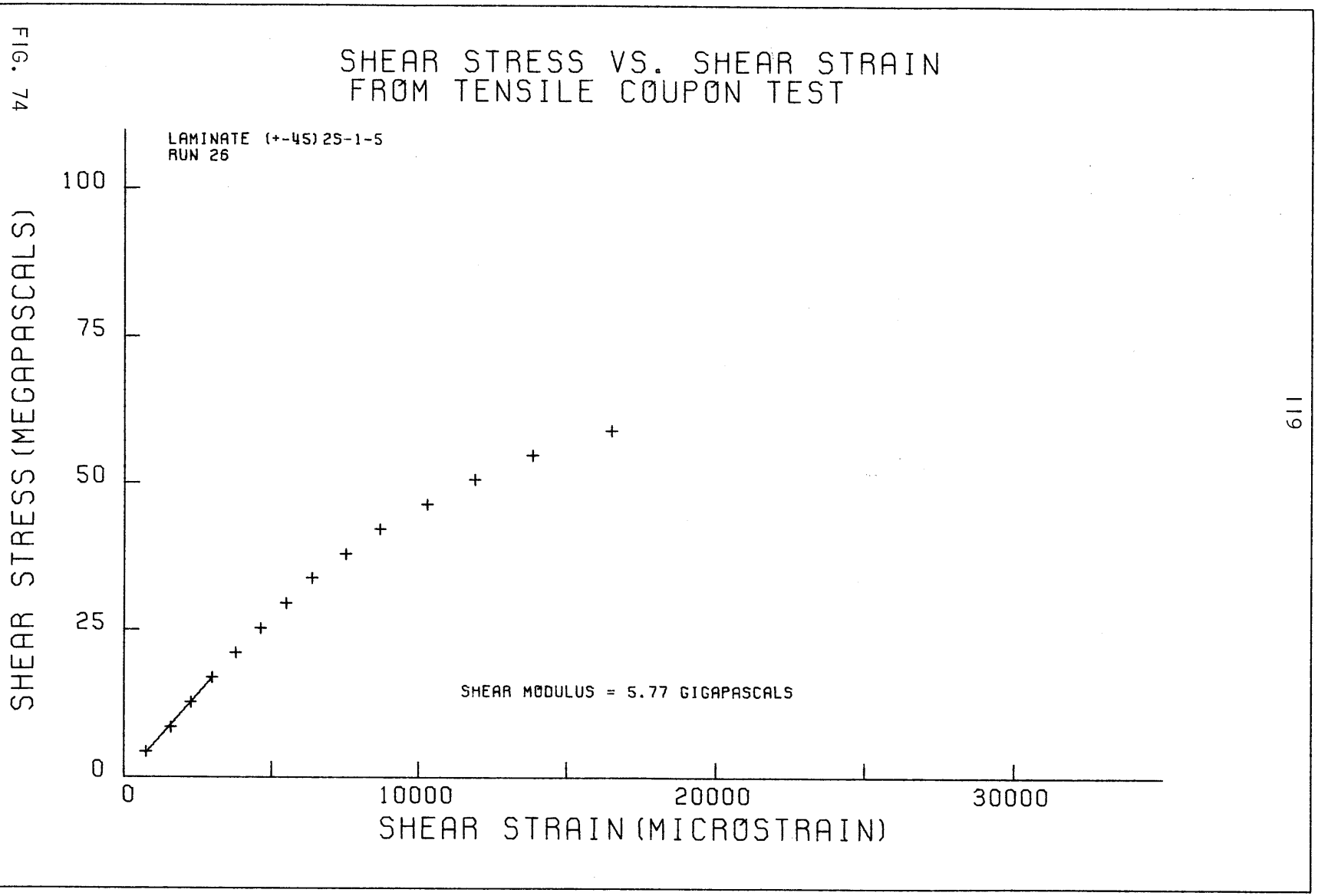
SHEAR STRESS VS. SHEAR STRAIN
FROM TENSILE COUPON TEST
LAMINATE (+-45)2S-1-5
RUN 26
SHEAR STRESS (MEGAPASCALS)
100
75
50
25
0
0
10000
20000
30000
SHEAR STRAIN (MICROSTRAIN)
SHEAR MODULUS = 5.77 GIGAPASCALS

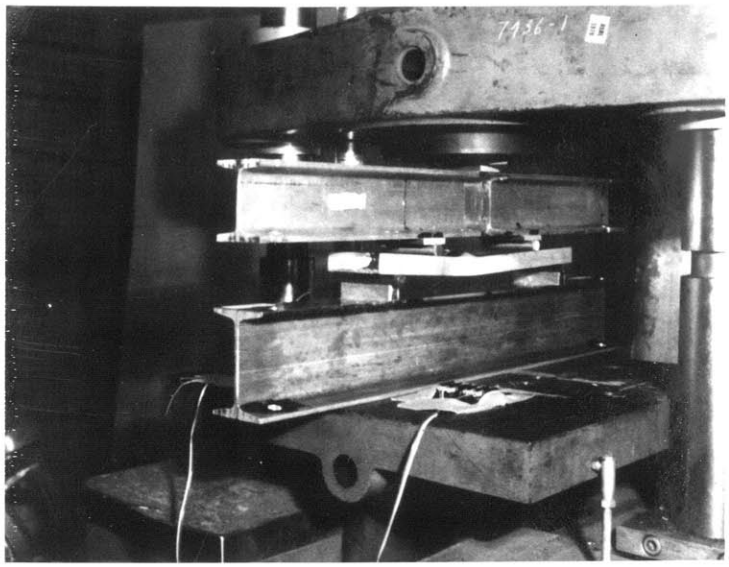

FIG. 8: SANDWICH BEAM 3 IN TEST JIG AFTER FAILURE

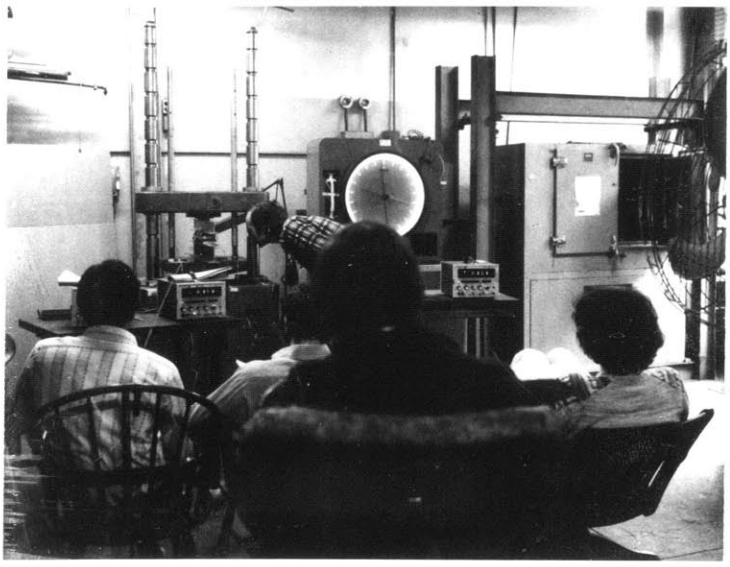

FIG. 9: SANDWICH BEAM TEST SETUP

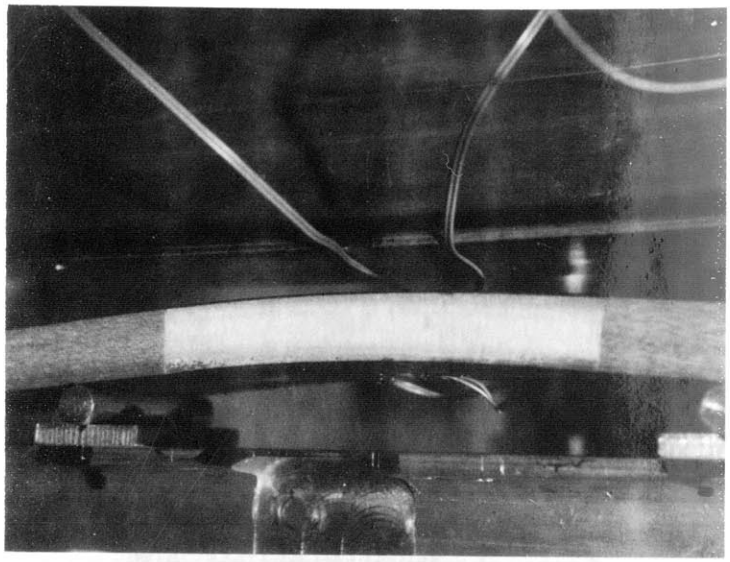

FIG. 11: BEAM 5 BEING TESTED AT A LOAD OF 740 POUNDS